

SYNTHESIS AND RHEOLOGY OF PH-RESPONSIVE
PARTICLES WITH SHAPE ANISOTROPY

BY

TIANYING JIANG

THESIS

Submitted in partial fulfillment of the requirements
for the degree of Master of Science in Chemical Engineering
in the Graduate College of the
University of Illinois at Urbana-Champaign, 2010

Urbana, Illinois

Adviser:

Professor Charles F. Zukoski

ABSTRACT

Seeded emulsion polymerization is used to produce large quantities of shape anisotropic, amphoteric particles in a size range of about 1 μm . Two different kinds of shape anisotropic particles are prepared for comparison to study the effects of incorporating pH-responsive groups on the properties of suspensions containing shape anisotropic colloidal particles. Copolymer dicolloids (CDC) containing pyridine groups are synthesized by swelling spherical, lightly cross linked polystyrene seeds with mixture of styrene and 2-vinyl pyridine (2VP) followed by secondary polymerization. Homopolymer dicolloids (HDC) are made in a similar procedure with only pure styrene swollen into seeds. To investigate the effects of weak attractions, the particles are coated with the nonionic surfactant hexaethylene glycol monododecyl ether (C_{12}E_6). As confirmed by electrophoretic mobility measurements as a function of pH, the CDC particles continue to show amphoteric properties. States of aggregation of dilute suspensions are mapped as functions of ionic strength and pH. The CDC particles show amphoteric behavior with strong attractions in medium pH range, while HDC remain stable at all pH's studied ($3 < \text{pH} < 9$) unless ionic strength is increased to 5M showing that the C_{12}E_6 protects against aggregation into a primary van der Waals minimum as would be seen for bare polymer particles. The flow properties of glassy and gelled suspensions of CDC and HDC are studied as a function of volume fraction and pH. HDC particles display a high kinetic arrest volume fraction ($\phi_g > 0.5$) with small linear elastic modulus (G_0^*) above ϕ_g at different pH conditions and ionic strengths up to 0.5M proving again that the particles experience repulsive or weakly-attractive conditions. The CDC particles behave in a similar manner at high or low pH at an ionic strength, [I] of 0.001M, but gel at a volume fraction of $\phi_g < 0.3$ and display anomalously large G_0^* at the gel transition at intermediate pH or at pH=9 and I=0.5M. The modulus and yielding behavior of these

suspensions indicate that even at $\text{pH}=9$ or $\text{pH}= 3.7$ and $I=0.001$ the CDC particles experience weak attractions that cannot be explained as arising from isotropic repulsions as experienced by the HDC particles. At $\text{pH}=9$ and $I=0.5\text{M}$ or $\text{pH}=4.6$ and $I=0.001\text{M}$, these anomalous attractions are accentuated. These anomalous attractions are understood as arising from the chemical anisotropy of the CDC particles where the protrusion created in the second polymerization step is rich in poly-2VP while the seed is rich in negatively charged sulfate groups. These chemical differences can give rise to directional interactions due to differences in charge or due to differences in hydrophobicity. A key conclusion drawn from this work is that the signature of directional interactions comes in the way gels and glasses yield when stressed. Gel points are shifted by anisotropic interactions but the same gel points can be generated with isotropic interactions if the attractions are strong enough. Instead, gel composed of particles experiencing anisotropic chemical interactions yield with multiple constraints under conditions where this is not seen for particles with isotropic interactions.

Acknowledgements

I would like to express my deepest gratitude to my advisor, Prof. Charles Zukoski, for his patience and enthusiasm in guiding me to make progress in my work. His devotion and effort in science and engineering, inspired me to work excitedly in this area and enjoy the experience a lot. Then I would like to thank all the members in Zukoski group, who help me to go on with my graduate study efficiently and make it a great pleasure to work in the lab. I also want to thank Prof. Charles Schroeder and his group members in supplying help in optical microscopy. Thanks also go to my parents who have been consistently supporting me no matter what difficulties I encountered in life or in work.

This material is based on work supported by the U.S. Department of Energy, Division of Materials Science under Award No.DE-FG02-07ER46471, through the Frederick Seitz Materials Research Laboratory at the University of Illinois Urbana-Champaign. Research in this work was carried out in part in the Frederick Seitz Materials Research Laboratory Central Facilities, University of Illinois University, which are partially supported by the U.S. Department of Energy under grants DE-FG02-07ER46453 and DE-FG02-07ER46471.

Contents

Chapter 1	Introduction.....	1
1.1	Overview	1
1.2	References	9
Chapter 2	Particles Synthesis and System Characterization	14
2.1	Introduction	14
2.2	Particle Synthesis	18
2.3	Characterization of Size and Shape Anisotropy.....	21
2.4	Cleaning Particles and Selection of Stabilizer	23
2.5	Surface Potential Measurement and Tuning Interaction Potential.....	27
2.6	Images of Dilute Suspensions and State Diagram	31
2.7	Tables and Figures	36
2.8	References	48
Chapter 3	Effect of PH-Response on Rheology of Shape Anisotropic Particles	51
3.1	Introduction	51
3.2	Experimental	58
3.3	Results and Discussion.....	62
3.4	Conclusion.....	75
3.5	Tables and Figures	78
3.6	References	100
Chapter 4	Conclusion	104
4.1	Summary	104
4.2	Future Studies.....	107
4.3	References	108

Chapter 1 Introduction

1.1 Overview

Suspensions formed by colloids with shape and chemical anisotropy are widely used in industry. The most common example is clays, which are typically plate shaped with positive edges and negatively charged surfaces. However, most fundamental studies of suspension behavior are based on spherical colloids experiencing isotropic pair interaction potentials. Recently interest has been triggered in systematically exploring the behavior of suspensions containing shape and chemically anisotropic colloids both theoretically and experimentally. Quite novel phase behavior has been predicted by simulation and theory with anisotropic particles compared to spherical particles with isotropic interaction.

Spherical particles experiencing volume exclusion interactions undergo crystallization to face centered cubic (FCC) structure when at volume fractions above 0.50. When the volume fraction of shape anisotropic hard particles is increased, suspensions undergo a series of equilibrium phase transitions that depend on the degree of anisotropy. For spherocylinders and interpenetrating spheres, simulations predict that with an aspect ratio less than 1.4, the particles first enter into a plastic crystal with only center of mass ordered and then gain also rotational order with increasing particle number density¹. For larger aspect ratios, novel crystal phases including nematic phase, Smectic A phase are observed with hard particles with aspect ratio equals to 5². More universally wider phase diagram with novel crystallization behavior has been developed by studying larger range of shape anisotropy degree ($0 < \text{aspect ratio} < \infty$), and more kinds of shapes including ellipsoids with shape changed by different principles and spherocylinders³⁻⁷. When short range attraction introduced, transitions and relative stability in

crystal phases can be varied by controlling width and depth (or temperature) of the attractive well^{8,9}.

The state of random close packing is also of a great interest in theoretical and simulation work with hard shape anisotropic particles¹⁰⁻¹³, which can be obtained experimentally by either rapid increases in volume fraction or size polydispersity. The approach to random close packing goes through a glassy phase where the suspensions stress relaxation time exceeds the measurement time. This state is observed with hard spheres in the volume fraction range $0.58 < \phi < 0.63$ ¹⁴. By introducing modest anisotropy, glass transition of hard dumbbells, triplets and spherocylinders has been explored. The ideal glass transition volume fraction is predicted to be a nonmonotonic function of aspect ratio with a maximum value at $L/D=1.4$ and an increasing linear function up to $L/D=1.22$ for hard dumbbells, where L is the length along the revolution axis and D is the diameter for the two overlapped spheres¹⁰. These studies show that breaking particle symmetry but retaining a symmetric pair potential alters the dynamics of suspensions and their equilibrium phase behavior.

In another aspect, anisotropic interaction potentials are predicted to fundamentally alter phase behavior of colloidal suspensions. In simulations, small spots with square well attraction have been incorporated onto hard spheres to produce directional attractions, and the effect of number of attractive spots on the liquid-gas phase separation boundary (with phase consisting of a concentrated colloidal suspension and the other of a dilute colloidal suspension) has been studied¹⁵⁻²⁰. The results shows that the critical temperature or critical volume fraction for phase separation decreases with decreasing number of spots or valence of bonds each patchy particles can form¹⁵⁻¹⁷. For particles which can form only two bonds, no liquid-phase separation is predicted¹⁸. These simulations do not explore fluid crystal phase boundaries which may render

the liquid-gas phase separation metastable (i.e., if the strength of attraction is fixed and volume fraction increased, at equilibrium one may see crystals form prior to seeing liquid-gas phase separation). In addition, novel assembled structures have been obtained by integrating small attractive patches and by varying the number and positions of patches on particle surfaces, with a variety of equilibrium phases are predicted to occur including chains, sheets, icosahedra^{19, 21} and diamond²⁰.

A distinct type of anisotropic particle interaction is that of Janus particles where the surface is divided into two halves with different natures of interaction. Recent simulation results show a quite novel behavior of negatively sloped liquid-gas phase separation boundary in temperature-density phase diagram for Janus particles with one half hard and the other square well attractive²². More work has been done with Janus particles having dipolar interactions. Molecular dynamics simulation has been used to explore the phase diagram of dipolar particles which show cluster phases, gelation and crystallization, including but not limited to string fluids, body-centered-tetragonal (BCT) crystals and low density gel states²³. More complexity is built by working with a binary mixture of two dipolar particles²⁴. Self-assembled structures formed by particles with dipolar interaction are widely explored with chains²⁵ and rings²⁶ being the most common structures predicted by simulation. At the same time, dipolar interactions also yield sheets, tubular and icosahedral structures²⁶. Other than the equilibrium structures formed, dipolar interactions also result in percolated disordered networks or gels at low volume fraction²⁷.

Some simulation has been developed by incorporating both shape anisotropy and dipolar interactions, predicting liquid-vapor phase separation boundary can be changed by increasing the shape anisotropy of hard dipolar dumbbells²⁸. There is a very obvious transition in the characteristics of condensation. For large aspect ratio ($L/D > 1.3$), side-by-side conformations are

preferred to nose-to-tail conformations. This forces the particles to form dense clusters. The opposite is seen when $L/D < 1.3$ where chains form in the vapor phase, with $L/D = 1.1$ very similar to results with dipolar spheres^{25, 26}. Similar structures are seen in dipolar fluids consisting of particles with magnetic moments²⁹.

Compared to rapid production of results from simulations on the states of aggregation of particles experiencing anisotropic potentials, progress is relatively slow experimentally due to the difficulty in particle synthesis. Current synthesis technologies either results in small yields which makes it impractical to study dense state or produces polydispersed particles. Nevertheless, techniques for making chemically anisotropic particles have been recently reported. Microfluidics is used to make Janus particles with two different matrix materials or similar matrix materials different in additives³⁰⁻³² or shape anisotropic particles with Janus droplet produced first³³. This method is convenient considering the flexibility in selecting and using almost any two different kinds of matrix, but it is usually difficult to control the size and shape monodispersed and also the large size (usually $> 10 \mu\text{m}$) is not applicable in studying dynamics of colloidal dispersions which is one aim in this thesis.

Templating is a widely used method to produce Janus spheres these days providing very nice monodispersed particles. Usually in this method, particles are partially embedded on a solid surface^{34, 35} (or liquid³⁶) with one halves facing to the surface and the other halves exposed to a liquid phase. The exposed fractions of the particle surfaces are reacted with reagents such that the properties of the reacted surfaces differ from those of the embedded surfaces. The particles are released from the template and contain one hemisphere that is non-reacted and the other that is functionalized. Monodispersed particles are obtained and are observed to aggregate into interesting clusters, but even when some modification is made to improve yield by sacrificing

monodispersity³⁷ the quantity is still not applicable for our interests in studying dynamics of high volume fraction suspensions. A similar method termed glancing-angle deposition³⁸ is used to produce patchy particles which needs colloids to order into a monolayer at solid surface and each particle has its member particles as shields. Vapor deposition at different angles can produce different sized patches. Another method is particle lithography³⁹ which again produces small volumes of particles making this method inappropriate for studying structure and dynamics in concentrated suspension.

To make monodispersed shape anisotropic particles, assembling of spheres is an efficient method with an advantage in producing a variety of controllable non-spherical shapes. In an early reported study, negatively charged polystyrene microspheres are adsorbed onto the surface of oil droplets when oil-in-water emulsion formed and assembled into clusters with different sizes after the oil droplet has evaporated. Clusters containing the same number of particles have uniform optimal polyhedral configurations and centrifugation in a density gradient is used to separate clusters with different sizes, yielding different monodispersed non-spherical particles⁴⁰. Programmed microfluidic device is also used to assemble microspheres into chains with configurable anisotropy⁴¹. Although monodispersity is guaranteed by controlled assembly and various shapes can be produced, low yields make this technique not applicable in studying behaviors of dense suspension.

Seeded emulsion polymerization is a method widely used to produce large quantities of weakly shape anisotropic particles⁴²⁻⁴⁴. Cross-linked seed latices are synthesized and swollen with monomer at low temperature. When temperature is increased, the incompatibility between network and monomer (or oligomer) results in phase separation and formation of protrusion at

the surface of seed particle. This method has advantage in producing large quantities of weakly shape anisotropic particles with narrow size distribution.

Recently attempts have been made to incorporate chemical anisotropy into shape anisotropic particles by seeded emulsion polymerization⁴⁴⁻⁴⁶. Two basic ideas are used to produce chemically and shape anisotropic particles by modifying the seeded emulsion polymerization technique. One idea is modifying surface with function groups in a certain step during the synthesis to introduce chemical anisotropy at certain conditions⁴⁵. Another is swelling the cross-linked seeds with another kind of monomer which can form a protrusion with different properties from the seed part during the secondary polymerization step as the source of chemical anisotropy⁴⁴⁻⁴⁶. The basic motivation for both methods is to generate shape anisotropic particles with uniform surface properties during the synthesis steps at certain pH or temperature conditions to make sure that the particles are stable, then chemical anisotropy can be produced and tuned by changing pH or temperature. For the first method, an amphoteric polystyrene seed is used with positively charged protrusion formed to gain pH-sensitive anisotropy⁴⁵. Compared to the first method, swelling seeds with another monomer has two advantages. First, incompatibility of the seed and a different monomer is even larger than swelling with the original monomer. This ensures phase separation and shape anisotropy. Secondly, chemical anisotropy based on the difference in bulk properties of the seed and protrusion is much easier to tune than that based on functional group anisotropic distribution as it is hard to control the amount and distribution of functional groups incorporated during the seeded emulsion polymerization. In previous work the new polymer used to produce the protrusion is either generally physically similar to seed⁴⁶ or chemical differences produce greater colloidal instability during the second polymerization step. There is some work using temperature-sensitive poly(N-isopropyl

acrylamide) (NiPAM) which is quite different from polystyrene seed⁴⁵ but the protrusion does not appear to be cross-linked at the particle surface such that it is not clear that the chemical anisotropy lasts over long periods of time. In another approach, weak acid and basic groups nonuniformly distributed on the particle surface will result in particles where charge differences can be controlled by changes in solution pH. There have been many studies of amphoteric (pH-responsive) particles and pH-responsive polymer microgels where the weak acid and base groups are uniformly distributed supplying basic ideas on potential polymer materials and the fundamental physics of the pH-response.

Some interest has been triggered in making pH-responsive polymer microgels the pH effect of which is introduced by either incorporation of a novel monomer resulting in a pH-sensitive copolymer matrix when it is copolymerized with other monomers⁴⁷ or pH-sensitive homopolymer matrix if it is polymerized by itself⁴⁸⁻⁵⁰. Also the effect of choosing a steric stabilizer is discussed for pH-responsive microgels⁵¹. For these microgel systems, the basic idea is to stabilize cross-linked particles with grafted polymer chains. Those particles are dispersed into suspension at certain pH conditions, but swollen and forming gel when pH is changed. These studies supply ideas that are incorporated here in the synthesis of chemically anisotropic particles⁵².

In addition to attention for making pH-responsive microgels by introducing a functional monomer, there have been quite a few studies published covering the synthesis and stability characterization of pH-responsive amphoteric particles⁵³⁻⁵⁵. Amphoteric particles with different iso-electric points (i.e.p.) have been synthesized just by varying ratio of permanently bound carboxyl and amine groups, and maps have been generated characterizing the degree of coagulation at different pH's, ionic strength's and mixing ratio's of different particles⁵⁴.

Coagulation studies carried out in dilute suspensions have been reported by varying pH values and salt concentration for different types of salts⁵³. It is found that for low salt concentration, particles aggregate in a narrow pH range near the particle i.e.p. This pH range is expanded when the supporting electrolyte is for CsNO₃, which does not have a special effect in enhancement of interfacial structure by introducing a steric hydration barrier as does KNO₃ and LiNO₃. This expanded pH-range effect can be understood in terms of classical colloid stability theories where van der Waals attractions gradually overwhelm electrostatic repulsions as surface charge is decreased.

In addition to pH and ionic strength sensitivity of aggregation, the strength of attraction can also be characterized through the rheological behavior is searched to quantitatively characterize the strength of attraction. In previously published work⁵⁵, yield stresses of concentrated flocculated samples are characterized as functions of pH and volume fraction. The results of yield stress as a function of pH showing a parabolic curve with a maximum value at i.e.p. Generally yield stress is monotonically decreased when the square of zeta-potential is increased with finally the sample became liquid-like when volume fraction is fixed. This effect is understood as a balanced consequence of electrostatic repulsion and van der Waals attraction. Also the addition of adsorbates shifts the position of peak for yield stress and decreases the height of the peak due to a steric effect. There is also some recently published similar study with rheology, from which effect of organic adsorbates on stability of amphoteric colloids is understood⁵⁶ and Hamaker constant is estimated for amphoteric particles⁵⁷.

These previous studies with rheological behaviors of amphoteric particles show the possibility to understand the stability of particles in dense suspension and underlying interaction potentials which can be modified by varying surface charge, strength of van der Waals attraction

(Hamaker constant) and steric effects. More generally, rheological properties of a dense colloidal suspension are controlled by both crowding and interaction potential effects. Specifically, for colloidal gels formed by particles with attractive interaction, yield stress τ_y and linear elastic modulus G_0' are both functions of volume fractions and minimum interaction potential W_{\min} , which is predicted theoretically⁵⁸. Considering this relationship between interaction potential and rheological properties, we are motivated to ask questions such as-“Can we alter the interaction potential by synthesizing a novel kind of particle?”, “What differences can be introduced in the transition volume fraction, linear elastic moduli and yield stresses for jammed states formed by particles with altered interaction potential?”, and “Will different non-linear flow properties be observed due to altered pair potentials?”

In this thesis, synthesis technology of shape and chemically anisotropic particles are searched with seeded emulsion polymerization by incorporating a functional monomer in the secondary polymerization step to introduce concentrated cationic groups on the protrusion and keep seed part negatively charged. Characterization techniques are searched to show the pH-responsive behavior of these shape anisotropic particles and understand the interaction potential. And rheological properties are studied with these novel synthesized particles to understand the underlying mechanism better. In Chapter 2, the synthesis techniques and characterization results of these particles will be discussed. In Chapter 3 the rheology experiment result will be discussed. And a conclusion will be given in Chapter 4.

1.2 References

1. Vega, C.; Monson, P. A., *Journal of Chemical Physics* **1997**, *107* (7), 2696-2697.
2. Avendano, C.; Gil-Villegas, A.; Gonzalez-Tovar, E., *Journal of Chemical Physics* **2008**, *128* (4).

3. De Michele, C.; Schilling, R.; Sciortino, F., *Physical Review Letters* **2007**, 98 (26).
4. Pfleiderer, P.; Schilling, T., *Physical Review E* **2007**, 75 (2).
5. McGrother, S. C.; Williamson, D. C.; Jackson, G., *Journal of Chemical Physics* **1996**, 104 (17), 6755-6771.
6. Donev, A.; Stillinger, F. H.; Chaikin, P. M.; Torquato, S., *Physical Review Letters* **2004**, 92 (25).
7. Bolhuis, P.; Frenkel, D., *Journal of Chemical Physics* **1997**, 106 (2), 666-687.
8. del Rio, E. M.; de Miguel, E., *Physical Review E* **2005**, 71 (5).
9. de Miguel, E.; del Rio, E. M., *Physical Review Letters* **2005**, 95 (21).
10. Yatsenko, G.; Schweizer, K. S., *Physical Review E* **2007**, 76 (4).
11. Yatsenko, G.; Schweizer, K. S., *Journal of Chemical Physics* **2007**, 126 (1).
12. Chong, S. H.; Moreno, A. J.; Sciortino, F.; Kob, W., *Physical Review Letters* **2005**, 94 (21).
13. Moreno, A. J.; Chong, S. H.; Kob, W.; Sciortino, F., *Journal of Chemical Physics* **2005**, 123 (20).
14. Cheng, Z.; Chaikin, P. M.; Russel, W. B.; Meyer, W. V.; Zhu, J.; Rogers, R. B.; Ottewill, R. H., *Materials & Design* **2001**, 22 (7), 529-534.
15. Bianchi, E.; Tartaglia, P.; Zaccarelli, E.; Sciortino, F., *Journal of Chemical Physics* **2008**, 128 (14).
16. Zaccarelli, E.; Buldyrev, S. V.; La Nave, E.; Moreno, A. J.; Saika-Voivod, I.; Sciortino, F.; Tartaglia, P., *Physical Review Letters* **2005**, 94 (21).
17. Zaccarelli, E.; Saika-Voivod, I.; Moreno, A. J.; La Nave, E.; Buldyrev, S. V.; Sciortino, F.; Tartaglia, P., *Journal of Physics-Condensed Matter* **2006**, 18 (36), S2373-S2382.

18. Bianchi, E.; Largo, J.; Tartaglia, P.; Zaccarelli, E.; Sciortino, F., *Phys Rev Lett* **2006**, *97* (16), 168301.
19. Zhang, Z. L.; Glotzer, S. C., *Nano Letters* **2004**, *4* (8), 1407-1413.
20. Zhang, Z. L.; Keys, A. S.; Chen, T.; Glotzer, S. C., *Langmuir* **2005**, *21* (25), 11547-11551.
21. Wilber, A. W.; Doye, J. P. K.; Louis, A. A., *Journal of Chemical Physics* **2009**, *131* (17).
22. Sciortino, F.; Giacometti, A.; Pastore, G., *Physical Review Letters* **2009**, *103* (23).
23. Goyal, A.; Hall, C. K.; Velev, O. D., *Physical Review E* **2008**, *77* (3).
24. Goyal, A.; Hall, C. K.; Velev, O. D., *Soft Matter* **2010**, *6* (3), 480-484.
25. Weis, J. J.; Levesque, D., *Physical Review Letters* **1993**, *71* (17), 2729-2732.
26. Van Workum, K.; Douglas, J. F., *Physical Review E* **2006**, *73* (3).
27. Miller, M. A.; Blaak, R.; Lumb, C. N.; Hansen, J. P., *Journal of Chemical Physics* **2009**, *130* (11).
28. Ganzenmuller, G.; Camp, P. J., *Journal of Chemical Physics* **2007**, *126* (19).
29. Tlusty, T.; Safran, S. A., *Science* **2000**, *290* (5495), 1328-1331.
30. Chen, C. H.; Shah, R. K.; Abate, A. R.; Weitz, D. A., *Langmuir* **2009**, *25* (8), 4320-4323.
31. Seiffert, S.; Romanowsky, M. B.; Weitz, D. A., *Langmuir* **2010**, *26* (18), 14842-14847.
32. Yuet, K. P.; Hwang, D. K.; Haghgooeie, R.; Doyle, P. S., *Langmuir* **2010**, *26* (6), 4281-4287.
33. Nisisako, T.; Hatsuzawa, T., *Microfluidics and Nanofluidics* **2010**, *9* (2-3), 427-437.
34. Hong, L.; Cacciuto, A.; Luijten, E.; Granick, S., *Nano Letters* **2006**, *6* (11), 2510-2514.
35. Hong, L.; Cacciuto, A.; Luijten, E.; Granick, S., *Langmuir* **2008**, *24* (3), 621-625.
36. Jiang, S.; Granick, S., *Langmuir* **2008**, *24* (6), 2438-2445.

37. Hong, L.; Jiang, S.; Granick, S., *Langmuir* **2006**, 22 (23), 9495-9499.
38. Pawar, A. B.; Kretzschmar, I., *Langmuir* **2008**, 24 (2), 355-358.
39. Snyder, C. E.; Yake, A. M.; Feick, J. D.; Velegol, D., *Langmuir* **2005**, 21 (11), 4813-4815.
40. Manoharan, V. N.; Elsesser, M. T.; Pine, D. J., *Science* **2003**, 301 (5632), 483-487.
41. Sung, K. E.; Vanapalli, S. A.; Mukhija, D.; McKay, H. A.; Millunchick, J. M.; Burns, M. A.; Solomon, M. J., *Journal of the American Chemical Society* **2008**, 130 (4), 1335-1340.
42. Sheu, H. R.; Elaasser, M. S.; Vanderhoff, J. W., *Journal of Polymer Science Part a-Polymer Chemistry* **1990**, 28 (3), 629-651.
43. Mock, E. B.; De Bruyn, H.; Hawket, B. S.; Gilbert, R. G.; Zukoski, C. F., *Langmuir* **2006**, 22 (9), 4037-4043.
44. Kim, J. W.; Larsen, R. J.; Weitz, D. A., *Journal of the American Chemical Society* **2006**, 128 (44), 14374-14377.
45. Mock, E. B.; Zukoski, C. F., *Langmuir* **2010**, 26 (17), 13747-13750.
46. Tang, C.; Zhang, C. L.; Liu, J. G.; Qu, X. Z.; Li, J. L.; Yang, Z. Z., *Macromolecules* **2010**, 43 (11), 5114-5120.
47. Hoare, T.; Pelton, R., *Macromolecules* **2004**, 37 (7), 2544-2550.
48. Dupin, D.; Fujii, S.; Armes, S. P.; Reeve, P.; Baxter, S. M., *Langmuir* **2006**, 22 (7), 3381-3387.
49. Howard, S. C.; Craig, V. S. J.; FitzGerald, P. A.; Wanless, E. J., *Langmuir* **2010**, 26 (18), 14615-14623.
50. Amalvy, J. I.; Wanless, E. J.; Li, Y.; Michailidou, V.; Armes, S. P.; Duccini, Y., *Langmuir* **2004**, 20 (21), 8992-8999.

51. Dupin, D.; Armes, S. P.; Connan, C.; Reeve, P.; Baxter, S. M., *Langmuir* **2007**, *23* (13), 6903-6910.
52. Bradley, M.; Rowe, J., *Soft Matter* **2009**, *5* (16), 3114-3119.
53. Healy, T. W.; Homola, A.; James, R. O.; Hunter, R. J., *Faraday Discussions* **1978**, *65*, 156-163.
54. James, R. O.; Homola, A.; Healy, T. W., *Journal of the Chemical Society-Faraday Transactions I* **1977**, *73*, 1436-1445.
55. Leong, Y. K.; Scales, P. J.; Healy, T. W.; Boger, D. V.; Buscall, R., *Journal of the Chemical Society-Faraday Transactions* **1993**, *89* (14), 2473-2478.
56. Johnson, S. B.; Brown, G. E.; Healy, T. W.; Scales, P. J., *Langmuir* **2005**, *21* (14), 6356-6365.
57. Teh, E. J.; Leong, Y. K.; Liu, Y.; Ong, B. C.; Berndt, C. C.; Chen, S. B., *Powder Technology* **2010**, *198* (1), 114-119.
58. Larson, R. G., The structure and rheology of complex fluids. In *Topics in Chemical Engineering*, Gubbins, K., Ed. Oxford University: New York, 1999; pp 342-353.

Chapter 2 Particles Synthesis and System Characterization

2.1 Introduction

By introducing and controlling anisotropic interaction potential, simulations have shown that it is possible to introduce complicated phase behavior and novel structures in colloidal suspensions above and beyond that seen in suspensions of spherical colloidal experiencing asymmetric interactions¹⁻⁸. However, current technologies for manufacturing chemically anisotropic particles⁹⁻¹⁵ have limitations in low yields, making it difficult to experimentally study novel behavior other than clustering in dilute suspension^{16,17}.

Seeded emulsion polymerization has been used to make large quantities of weakly shape anisotropic particles with a wide size range¹⁸⁻²⁰ and recently been applied in attempts of incorporating chemical anisotropy to non-spherical particles^{21, 22}. In this method, cross-linked spherical seeds are first made by emulsion polymerization with uniform surface charge distribution, either negative or positive depending on the function groups of initiator and the ionic surfactant used to stabilize the particles in synthesis. The seed particles are then swollen with monomer at room temperature. The temperature is then increased, resulting in an incompatibility between polymer network and monomer swollen into the seed that leads to formation of a liquid monomer protrusion on the surface of the seeds. This liquid protrusion is stabilized by added surfactant and undergoes a secondary polymerization to form a solid protrusion after completion of reaction.

Previous work has been carried out to study the thermodynamics of swelling and phase separation in this process^{19, 20}. The free energy change in swelling a polymer network with monomer are composed of three parts, mixing of monomer and polymer network $\Delta\bar{G}_m$, elastic energy change of polymer network $\Delta\bar{G}_{el}$, the interfacial energy change $\Delta\bar{G}_t$.

$$\Delta\bar{G}_{m,p} = \Delta\bar{G}_m + \Delta\bar{G}_{el} + \Delta\bar{G}_t \quad (2.1)$$

According to Flory-Huggins theory²³,

$$\Delta\bar{G}_m = RT[\ln(1 - \nu_p) + \nu_p + \chi_{mp}\nu_p^2] \quad (2.2)$$

According to Flory-Rehner equation²³,

$$\Delta\bar{G}_{el} = RTNV_m \left(\nu_p^{1/3} - \frac{\nu_p}{2} \right) \quad (2.3)$$

And $\Delta\bar{G}_t$ can be expressed by Morton equation²⁴,

$$\Delta\bar{G}_t = \frac{2V_m\gamma}{a} \quad (2.4)$$

Here ν_p is the volume fraction of the polymer in the swollen system, χ_{mp} is the interaction parameter between polymer and monomer, V_m is the volume of monomer, R is gas constant, T is temperature. a is the radius of swollen seed, γ is the interfacial tension between particles and water and N is the effective number of chains in swollen seed per unit volume. Among these three parameters, $\Delta\bar{G}_m$ gives a negative contribution to $\Delta\bar{G}_{m,p}$ making swelling of polymer network favorable, while $\Delta\bar{G}_{el}$ and $\Delta\bar{G}_t$ are positive making phase separation preferred.

In the expression of $\Delta\bar{G}_m$, one thing to notice is that the term $RT\chi_{mp}\nu_p^2 \geq 0$ which makes a positive contribution to the free energy of mixing. In details, interaction potential between species 1 and species 2 (χ_{12}) has the following definition²⁵:

$$\chi_{12} \equiv \frac{z\Delta w}{kT} \quad (2.5)$$

Here z is the number of interacting neighbors per molecule and Δw is the exchange energy which has an expression as following.

$$\Delta w = w_{12} - \frac{1}{2}w_{11} - \frac{1}{2}w_{22} = \frac{1}{2}[\sqrt{|w_{11}|} - \sqrt{|w_{22}|}]^2 \geq 0 \quad (2.6)$$

Here w_{ij} is the interaction potential between molecule i and molecule j. So the greater the difference between the two species, the interaction energy cost grows with the chemical

difference between the two species thus increasing the tendency for phase separation. It is found out that in the initial step of swelling when the swelling ratio (monomer: polymer) is small, contribution of $\Delta\bar{G}_m$ overwhelms the other two terms¹⁹. So the tendency of seeds swelling will be decreased when a monomer different from the one used to synthesis seeds is introduced in the swelling step.

However, once the swelling step reaches an equilibrium state $\Delta\bar{G}_{m,p}=0$, in the secondary polymerization, this incompatibility will also give a positive contribution to phase separation once a new monomer is introduced. This tendency makes it possible to form prospective shape anisotropy and chemical anisotropy.

In this study, synthesis technology based on above principles to control seeded emulsion polymerization was searched to make pH-sensitive amphoteric particles with shape anisotropy. The basic idea is to first make seed particles with a certain kind of charge from the initiator, with a protrusion formed by another monomer during the subsequent secondary polymerization. This protrusion has the same charge as seed part in a certain pH range during the synthesis, but has charge sign reversed when pH is changed without charge change on seed part. Therefore, this strategy can supply us with amphoteric shape anisotropic particles with dipolar interaction at certain pH. Specifically this was done by making negatively charged seeds, swelling them with 2-vinyl pyridine (2VP) and carrying out the second polymerization under high pH where both seed and protrusion will have negative charges. The P2VP formed protrusion has the capability to be protonated as the pH is lowered. The protrusion is expected to have on its surface only P2VP, and the seed is expected to contain both the original negative charges bonded in place by crosslink and some amount of P2VP at the surface. The concept is that although the exact

distribution of P2VP is unknown, negative charges can be expected to reside only on the seed particle. Thus as pH is varied, a charge dipole should develop in the anisotropic particle.

In this study, an earlier reported soap-free emulsion polymerization recipe was used to make negatively charged seed particles with diameter~800nm²⁶. In this recipe, a solvent mixture of methanol and water in absence of surfactant results in large seed size. Large seeds and resulting anisotropic particles (~1 μm) are sought in order to make it practical to image particle in suspension with optical microscopy but keep particles still sufficiently small to obtain Brownian motion to study dynamics of suspension. To find an appropriate balanced point in the dilemma brought by incompatibility described above, attempts were made with three different monomers to swell polystyrene seeds. To optimize chemical differences and to achieve desired chemical and shape anisotropies, 2-vinyl pyridine (2VP) was chosen and mixed with styrene before being used to swell the seeds. By using the monomer mixture, an appropriate balanced point in the dilemma brought by incompatibility described above was found.

This mixture of monomer underwent a secondary polymerization at high pH and formed a copolymer protrusion when the reaction was finished to give a copolymer dicolloid (CDC). 2VP was chosen not only because of good phase separation but also due to its pH-responsive behavior without further modification. Once the reaction was completed, shape anisotropic particles were obtained with the seed part negatively charged and protrusion containing concentrated pyridine groups. When pH is decreased, the poly-2VP (P2VP) becomes protonated which is the mechanism to generate pH-responsive particles with shape anisotropy. Scheme 2.1 shows basic mechanism of this process. For further control experiment, a similar procedure was used to make only shape anisotropic without pH-response with only styrene used to swell seeds and give homopolymer dicolloids (HDC).

In the following sections, details will be given regarding the particle synthesis and system characterization. Reaction procedures will be introduced in section 2.2 and characterization result of shape anisotropy and particle size will be given in section 2.3. And the cleaning procedure is introduced in section 2.4, with selection of stabilizer for further study discussed. Surface potential characterization and state behavior of dilute suspension will be talked about in section 2.5 and section 2.6 separately. Related figures and tables will be given in section 2.7.

2.2 Particle Synthesis

Anionic polystyrene seeds cross-linked by 2wt% divinyl benzene (DVB) with diameter ~800nm were first made based on a soap-free emulsion polymerization recipe²⁶. All the materials were used as received without further purification.

A 500mL round bottom flask fitted with a glass impeller with a poly-tetrafluorethylene (PTFE) blade was immersed into a water bath with constant temperature ~80°C. And the impeller was connected to a Glas-Col 099D G31 stirrer system which would run at ~220 rpm during the reaction. 52mL deionized water (DIW) and 68mL methanol (Fisher Scientific, certified A.C.S.) was added into the flask, allowing 15 minutes for heating up of the materials. Then 60mL of styrene (Sigma-Aldrich, 99%) was added into the reactor and allowed for 15 minutes to be heated, with stirring started once the styrene was added. Once it was at temperature, 0.55g potassium persulfate (KPS) (Fisher scientific, 99.5%) dissolved in 20mL DIW was discharged into the reactor to initiate the polymerization. After 2 hours, 1.088g DVB (Aldrich, 55% mixture of isomers tech, grade) was added. The reaction was allowed to proceed for 22 hours. Once the reaction was completed, the volume fraction of the seed suspension was determined, by placing ~0.5mL suspension into 20mL glass vial, drying the suspension in ~110°C oven and calculating the volume loss with measured weight loss based on a polystyrene

density of $1.055\text{g}\cdot\text{cm}^{-3}$. The accurate diameter of the seed was determined by scanning electron microscopy (SEM) which will be described in detail in the next section.

A previously developed procedure²⁰ was followed to coat the seeds with hydrophilic layer to make sure of the stability of the seeds and possible better phase separation, by initiating polymerization of vinyl acetate (VA). The required amount of VA was calculated as $\sigma A_p V_t \phi / V_p$, where A_p and V_p are surface area and volume of a single seed calculated with the result of particle diameter in SEM. V_t and ϕ are the total volume and volume fraction of suspension used in this reaction with 200mL and 0.08 chosen separately. σ is the desired mass of VA coated on particle surface per unit area which is $3.56 \times 10^{-21} \text{g}\cdot\text{nm}^{-2}$ in this study. The amount of KPS used is 25% of the mass of the VA used. 10^{-3}M sodium hydroxide (NaOH) (Fisher Scientific, 98.6%) solution is used to dilute the seed particle suspension and dissolve KPS (the amount of solution to dissolve KPS was usually 20mL in this study), making sure the final volume fraction and total volume in this reaction are 0.08 and 200mL separately.

A 500mL round bottom flask with a PTFE-coated stir bar was filled with diluted seed suspension, and put into an oil bath with constant temperature $\sim 80^\circ\text{C}$. After 20 minutes to allow thermal equilibrium, all the KPS dissolved in 20mL 10^{-3}M NaOH solution and 1/4 of the desired VA (Aldrich, 99.9+%) were added to start the reaction. The remaining VA was added into the system in the following 45 minutes with 1/4 every 15 minutes. The reaction was allowed to proceed for 24 hours. The resulting coated seed particle suspension was placed into SpectraPor 4 dialysis tubing (molecular weight cut-off 12,000-14,000) and dialyzed against DIW for 2 days with DIW changed for about four times. Then the volume fraction was determined by weight loss after drying $\sim 0.5\text{mL}$ suspension based on a polystyrene density of $1.055\text{g}\cdot\text{cm}^{-3}$.

Following this step, dicolloids were made by swelling the coated seeds (based on a total swelling ratio: $\text{mass}(\text{monomer}):\text{mass}(\text{polymer})=2:1$) and a secondary polymerization reaction. The amount of cross-linker used is 1% of the total mass of monomer in this step to make sure that the network density in the protrusion is high enough to guarantee no obvious dissolve when making P2VP hydrophilic by decreasing pH. A 200mL round bottom glass flask fitted with a glass impeller with a PTFE blade was immersed into a water bath at room temperature. The impeller was connected to a Glas-Col 099D G31 stirrer system that would run at $\sim 220\text{rpm}$ during the reaction. Then 75mL of the coated seed particle suspension at a volume fraction of $\sim 5\%$ made by diluting suspension from above with 10^{-3}M NaOH solution was discharged into the reactor. 0.200g 2,2'-azobisisobutyronitrile (AIBN) (Aldrich, 98%) was dissolved into mixture of 3.970g 2VP (Aldrich, 97%) and 3.970g styrene with 0.0792g DVB followed. This mixture was added into the suspension and stirring was started. The swelling step was kept on for 24 hours including 2.5 hours to increase the temperature of the water bath and reaction system to $70\text{ }^{\circ}\text{C}$. Afterwards 3.00g sodium dodecyl sulfate (SDS) (Bio-Rad, electrophoresis purity reagent purity) dissolved in 30mL 10^{-3}M NaOH solution and 2.20 g hydroquinone (Sigma-Aldrich, ReagentPlus 99%) dissolved in 35mL 10^{-3}M NaOH solution were added. The reaction was allowed to proceed for 24 hours.

The above procedure was used to make CDC. To make HDC, similar steps were followed only with 7.940g styrene used instead of mixture of 2VP and styrene to swell particles and 1.900g hydroquinone used as inhibitor in aqueous phase to make sure of similar final shape of both dicolloids.

To understand the phase separation in this process and prepare for potential control experiment, two similar recipes were used to synthesize homopolymer spheres (HSP) and

copolymer spheres (CSP), the only difference in which was that no DVB was added during the reaction of making seed particles.

2.3 Characterization of Size and Shape Anisotropy

Scanning electron microscope (SEM Hitachi 4700) was used to characterize the size and shape of both seed particles and dicolloids. After the reaction for making seed particles or dicolloids was finished, 1mL pipette was used to transfer a small amount of suspension on to the surface a SEM copper sample grid (SPI supplies) and the suspension was dried quickly. SEM micrographs were used to characterize the particles. The software ImageJ was used to format images and measure important size parameters including diameter of the spheres (D) and average diameter (D) of the two overlapped spheres and the largest length along the line connecting the centers of the two spheres (L) in dicolloids.

The SEM images of CDC particles and HDC particles are presented in Figure 2.1. Generally with similar synthesis recipes and steps, similar size and degree of shape anisotropy were obtained for both HDC particles and CDC particles. However, due to the incompatibility of polystyrene and 2VP, swelling with a mixture of 2VP and styrene was more difficult than swelling with pure styrene. As a result, a larger fraction of the monomer was not incorporated into the seeds when making CDC particles than that for making HDC particles. Therefore, more hydroquinone was required to eliminate small secondary particles in aqueous phase. Also this incompatibility might be the reason for less stability of the reaction system for making CDC particles, so smaller stirring rate was chosen to avoid aggregation observed with large stirring rate.

Diameters of seeds were repeatedly measured for 20 particles and the average was used to calculate the amount of VA desired to coat the seed. The diameter of seed was about 800nm

with standard deviation (SD) $<5\%$ of the size. From the images, in both kinds of dicolloids, the size of the protrusion was slightly smaller than that of the seed particle part. For convenience of further study, average value of the diameters of seed part and protrusion is used as D . And the length of particle along the line connecting two centers of the overlapped spheres L was also measured. 20 repeated measurements at different positions of the sample grid were taken and the average was used with $L\approx 1100\text{nm}$ and $D\approx 850\text{nm}$ and both $SD<5\%$. The aspect ratio L/D was about 1.3 for both particles. These values vary slightly from batch to batch but we do not expect the small variations to dramatically influence the physical properties of the suspensions. Nevertheless, specific measurements were carried out for specific batch once these parameters were desired for some calculation of rheology data which will be discussed in the next chapter.

The images for HSP particles and CSP particles are shown in Figure 2.2. With similar steps of seed expansion and secondary polymerization for uncross-linked seed, particles looked perfectly spherical when the seeds were swollen with pure styrene, but egg-shaped when the seeds were swollen with mixture of styrene and 2VP. This proves again the incompatibility of polystyrene and 2VP and the resulting favorable conditions for phase separation even in absence of the positive contribution of elastic energy change described in Equation 2.3. This preferred phase separation presented in reaction of making dicolloids is desired for guaranteed shape anisotropy and potentially greater chemical anisotropy. However, it is not desirable in making prospective seeds for control experiments to prove charge anisotropy, as the anisotropic charge distribution will be present to different degrees in both CDC particles and CSP particles. Nevertheless, the phase separation seen when the seed are not cross linked supports the notion that the protrusions are dominated by P2VP ensuring that the particles are chemically anisotropic. This

similarity in properties was confirmed with state diagram discussed in section 2.6. So the CSP particles were not synthesized in large scale.

2.4 Cleaning Particles and Selection of Stabilizer

The resulting suspension was cleaned by settling where the supernatant was first replaced with 10^{-3}M NaOH. After the particles settled for several times, it took more than 5 hours for the particles to settle. The suspension was then placed into SpectraPor 4 dialysis tubing (molecular weight cut-off 12,000-14,000) and underwent dialysis against 10^{-3}M NaOH solution for 2-3 days with the solution changed for about four times until conductivity of the solution outside the tubing became constant. This cleaning procedure eliminated the hydroquinone, oligomer and other species which would influence further characterization of the particles. 10^{-3}M NaOH solution was chosen to ensure a high pH and thus guarantee stability of pH-responsive CDC particles. At the end of this procedure the particle volume fraction was determined by weight loss after drying $\sim 0.5\text{mL}$ suspension based on a homopolymer density of $1.055\text{g}\cdot\text{cm}^{-3}$ for HDC particles and a copolymer density of $1.066\text{g}\cdot\text{cm}^{-3}$ for CDC particles.

Three different kinds of stabilizer were tested to introduce weak attractions rather than strong attractions but still keep it possible to detect pH-responsive properties.

The first was poly(ethylene glycol) methyl ether methacrylate (PEGMA) which is a macromolecular monomer with a long hydrophilic chain and a double bond able to undergo a copolymerization with other monomers. It has been used as a stabilizer for pH-responsive microgel formed by P2VP²⁷. This stabilizer was introduced during the secondary polymerization step due to its activity of polymerization. 1.20g PEGMA solution (Aldrich, average Mn $\sim 2,080$, 50wt% in water) was added into the SDS solution before discharged into the reaction, with other procedures exactly the same. Dicolloids with similar shape anisotropy were made. However, the

particles were not amphoteric- no changes in electrophoretic mobility were observed with changes in pH. Also quite a few clusters were observed in SEM images, meaning that addition of PEGMA that we expect to only undergo a copolymerization on the surface of the protrusion might also have some effect in bridging different particles by copolymerization.

Another stabilizer tested in our work was partially hydrolyzed poly-vinyl alcohol (PVA) which can be physically adsorbed on the surface of the particles and used as a stabilizer during the synthesis before²⁸. As a partially hydrolyzed polymer chain, it can be loosely adsorbed on the surface of the particles with hydrophobic part attached and hydrophilic part floating in the aqueous phase to form a steric layer. The details in the experiment are as follows: A 200mL round bottom flask fitted with a glass impeller with a poly-tetrafluorethylene (PTFE) blade was immersed into a water bath with room temperature. And the impeller was connected to a Glas-Col 099D G31 stirrer system which would run at ~200rpm during the process. 85mL cleaned CDC suspension was filled in. The amount of PVA (1wt% in solution) desired was calculated based on the volume fraction of the suspension. Then PVA (Aldrich, 87–89% hydrolyzed, $M_n \sim 13,000\text{--}23,000$) was added and stirring was started. This polymerization was allowed to continue for 24 hours. Again similar as the particles coated with PEGMA, no pH-responsive behavior was observed at different pH conditions. These particles are very stable no matter how pH was changed although we expect some degree of aggregation. We attribute this effect to a large grafted layer on the particle surfaces. PVA with this molecular weight was already the shortest which we found can be commercially purchased, and this M_n is not very large considering the possible loosely adsorbing conformation on the particle surface. Again even assuming that this stability was due to the excessive amount of PVA on the surface, it is difficult to control this parameter as it is physically adsorbed.

In summary, although a loosely coated polymer hair (either chemically bonded or physically adsorbed) on the surface of the particles can produce a steric stabilizing layer, the resulting stability is so large that the particle behavior is no longer sensitive to chemical differences on the particle surface. In addition, the grafted or adsorbed polymers have the effect of masking the underlying changes in pH sensitive groups. As a result, we sought a third stabilizer for further characterization and study of suspension flow properties.

The stabilizer we selected was a nonionic surfactant, hexaethylene monododecyle ether ($C_{12}E_6$) based on previous work on polystyrene colloids^{29, 30}. The chemical structure of this molecule is given in Figure 2.3. This molecule has one hydrophilic part and one hydrophobic part with the total length~4nm. Assuming the surfactant is close packed on the particle surface this will result in a minimum particle surface separation of ~8nm. Fully coverage by the stabilizer will truncate the van der Waals attractions thus avoiding strong aggregation at high ionic strength when surface charge is screened out. At the same time, the surfactant layer will be less penetrable by small ions and thinner than grafted and adsorbed layers such that the pH sensitivity of the particles will be observed.

The amount of surfactant desired for fully coverage was determined by surface tension measurement. The result of surface tension measurement is shown in Figure 2.4. The critical micelle concentration (c.m.c.) was determined by fitting a line to the data of surface tension vs. surfactant concentration in log scale for three conditions, in DIW, in presence of $\phi=0.285$ HSP particles ($D=1150\text{nm}$) and in presence of $\phi =0.054$ CDC particles ($D=850\text{nm}$, $L=1100\text{nm}$).

In DIW, c.m.c of $C_{12}E_6$ was found to be $8 \times 10^{-5}\text{M}$ which was the same as previously reported result²⁹.

To determine the adsorption isotherm of C12E6 on the homopolymer particles, the surface tension of a relatively concentrated suspension of HSP particles was measured as a function of the amount of added surfactant. The particle concentration was adjusted such that, given the low absolute amount of surfactant absorbed per particle, accurate determination of monolayer coverage was possible. Based on the shift in the critical micelle concentration in presence of particles, it was found out that on polystyrene particles surface, the surfactant has a concentration 1.5molecules/nm² at full coverage, meaning 0.67nm² per molecule, which acceptably compares to previous reported 0.62nm²/molecule²⁹ and 0.27nm²/molecule³⁰. Further experiment for homopolymer particles was carried out with particles fully coated based on this data.

To find out surface coverage of the surfactant on copolymer particles, relatively dilute suspension of CDC particles was selected. Low volume fraction was selected for two reasons. First, it is difficult to produce stable copolymer particle suspension at high concentration due to its relatively low surface potential even at high pH as discussed in the next section. Second, the particles adsorb a relatively large amount of surfactant allowing the measurement to be made at low volume fraction. Although spheres are better considering convenience in calculation, CDC particles were still preferred due to the phase separation issue in CSP particles discussed in the last section, as a result of which, we were not able to control the exact fraction of P2VP on the surface of the CSP because of random phase separation and have a reproducible surface coverage result. A little more complicated calculation was carried out based on $A_p = 2\pi DL$, $V_p = \frac{1}{2}\pi L^2 \left(D - \frac{L}{3}\right)$, where A_p and V_p are surface area and volume fraction of a single particle separately. It was found that on the surface of CDC particles, the surfactant has an average concentration of 9.8molecules/nm² at full coverage, meaning 0.10nm² per molecule, which are

quite reasonable results for surfactant adsorption on solid surface. Although we were not sure about the surfactant distribution on CDC particle surface, which might also be anisotropic due to chemical anisotropy, it was reasonable to use this average value and check with surface tension measurement to make sure of full coverage.

After coating the particles an $8 \times 10^{-5} \text{M}$ C_{12}E_6 solution was used to dilute particles in the next sections.

2.5 Surface Potential Measurement and Tuning Interaction Potential

Electrophoretic mobility was studied as a function of ionic strength at high pH and as a function of pH at a fixed medium ionic strength for both CDC particles and HDC particles to obtain information about the surface charge. The surface potentials of the particles were measured using the ZetaSizer in presence of surfactant C_{12}E_6 using samples with volume fraction $< 10^{-5}$. Here in the ionic conditions searched into, $D\kappa > 100$ where D is the particle diameter and κ is the Debye layer parameter, so the Smoluchowski theory was valid to convert electrophoretic mobilities into zeta-potentials in the measurement.

First, the electrophoretic mobility was measured as a function of concentration of sodium chloride (NaCl) (FisherScientific) for these two particles in presence of 10^{-3}M NaOH . This base concentration was a value large enough to ensure that little positive charge from the pyridine groups was introduced to guarantee a comparable measurement taken for both particles. This choice of electrolyte was thus a balance of the desire to characterize the particles as in their synthesized state and need to keep the particles stable. Five different salt concentrations were selected to search the effect of screening surface charge by adding salt, 0M, 0.01M, 0.05M, 0.1M and 0.5M. (Thus the lowest ionic strength probed was 10^{-3}M and the highest was 0.501M when the presence of the base was taken into account.) Electrophoretic mobilities were converted to

zeta potentials using the Smoluchowski theory. Here $D\kappa > 100$ for all systems studied as calculated below. The result of the zeta-potential is shown in Table 2.1. Obviously, the CDC particles have a smaller amount of negative surface charge than HDC particles at all ionic strengths for this high pH, indicating some change introduced by the P2VP. At this pH the pyridine groups are not charged. As a result, we expect some degree of charge anisotropy is present although the particles are treated as uniformly charged. To understand the effect of zeta-potential change on interaction potentials initiated by adding salt or incorporating P2VP, calculation of interaction potential was used below.

For uniformly charged spheres, the interaction potential (U) of this system is composed of three parts shown below (Equation 2.7), electrostatic repulsive potential (U_E), van der Waals attractive potential (U_V) and steric part introduced by addition of surfactant (U_S).

$$U = U_E + U_V + U_S \quad (2.7)$$

And the expression of these three different parts are shown in Equations 2.8, 2.9, 2.10 separately below.

$$U_E = \pi \epsilon \epsilon_r \psi_s^2 D \ln[1 + \exp(-\kappa h)] \quad (2.8)$$

$$U_V = -\frac{A_H}{12} \left(\frac{1}{x^2+2x} + \frac{1}{x^2+2x+1} + 2 \ln \frac{x^2+2x}{x^2+2x+1} \right), \quad (x = \frac{h}{D}) \quad (2.9)$$

$$U_S = \begin{cases} \infty, & h < \delta \\ 0, & h > \delta \end{cases} \quad (2.10)$$

Here, relative dielectric constant $\epsilon_r = 80$ for water, dielectric constant for vacuum $\epsilon = 8.854 \times 10^{-12} C^2/N \cdot m^2$, the diameter of spheres $D=1150\text{nm}$ and the closest surface distance between two spheres $\delta=8\text{nm}$ determined as twice of the surfactant length. And ψ_s is surface potential, h is the surface distance between two particles, κ^{-1} is Debye thickness which is determined as $0.304/[\text{Ionic strength (M)}]^{0.5}$ (nm) for NaCl. For these five ionic strength considering the concentration of NaOH, 0.001M, 0.011M, 0.051M, 0.101M, and 0.501M, κ^{-1} has

the values 9.61nm, 2.90nm, 1.35nm, 0.96nm and 0.43nm separately. Approximately Hamaker constant $A_H = 3.2kT$ for both HDC and CDC particles considering both have polystyrene as the main component although P2VP main has a different value.

In estimating the pair potentials we assume that with the base concentration of $10^{-3}M$, the pH is kept high enough for both particles to have approximately uniform negative charge distributions on their surfaces due to persulfate groups. Based on the zeta-potential data in Table 2.1 and the equations for interaction potentials given above, the interaction potential in units of kT are plotted as a function of surface separation distance for both CDC and HDC particles for different salt concentrations in Figure 2.5. To simplify this calculation aimed for searching only ionic strength effect other than shape anisotropy, it was also assumed that the interaction potentials of these dicolloids are similar to that for spheres with $D=1150nm$ which were produced with similar synthesis procedure.

From these calculations, some basic conclusions can be drawn. For both particles with $[NaCl]=0M$, electrostatic repulsion dominated in a large separation distance range ($h<80nm$), so particles can be treated as hard dicolloids without any overall attractive interactions if particles are treated with charge distributed uniformly. For medium salt concentrations ($[NaCl]=0.01M, 0.05M$ and $0.1M$), van der Waals attraction start to dominate the pair potential at intermediate separations with a local minimum ($-U_{min}<10kT$) formed outside the surfactant layer. At very small separations, the pair potential remains dominated by electrostatic repulsions. For these conditions, CDC particles develop a deeper local minimum in interaction potentials than HDC particles. With higher ionic strength $[NaCl]=0.5M$, HDC particles still had local minimum $U_{min}\approx-13kT$ at a surface separation of about 1nm with electrostatic repulsion becomes important approaching outside of the surfactant layer. However, for the CDC particles, van der Waals

attraction dominates over all the surface separation range with a minimum $U_{\min} < -15kT$ right at the outside surface of the surfactant. Considering the approximate assumption of uniform surface charge distribution and inaccuracy in measuring zeta-potential at high ionic strength, the details of the pair potential at small separations will have a magnified uncertainty. Nevertheless, the weaker average particle surface charge seen with the CDC particles indicates they will be less stable as ionic strength is raised but even when the double layer is fully screened, due to the surfactant coatings, the maximum strength of attraction will be on the order of 10-15kT.

In presence of surfactant and $10^{-2}M$ NaCl, zeta-potential as a function of pH is also plotted in Figure 2.6 for seed particles, CDC particles and HDC particles. This salt concentration was selected as it was high enough to guarantee ionic strength uniformity when concentrated hydrochloride acid or sodium hydroxide was added to adjust pH, but still small to avoid screening out surface charge according to calculation above. HDC particles and seeds had similar pH-responsive behavior with constant high negatively surface potential ($\approx -50mV$) over a wide pH range above pH=3, and underwent a sharp increase when pH was below 3 in surface potential suggesting that at these pH's the sulfate groups were becoming protonated.

For CDC particles, zeta-potential was increased gradually from $\sim -20mV$ to $\sim -30mV$ when pH was decreased, indicating that positive charge introduced by pyridine groups became dominate at low pH. The iso-electric point (i.e.p) was at $pH \approx 4$ meaning average surface charge was about zero at $pH \approx 4$. At this point, negative charges introduced by sulfate groups are mainly located on seed surface should be approximately equal to positive charge introduced by protonated pyridine groups. At high pH, sulfate groups dominated to make CDC particles positively charged and at low pH pyridine groups dominated to make CDC particles positively charged.

These measurements provide a good estimate of an average zeta-potential. Based on the synthesis method, we anticipate that there should be some anisotropy degree of charge distribution at the i.e.p. Based on the data at high pH and remaining stability of HDC particles at pH=4, we can assume that if charge anisotropy is present, at i.e.p the largest absolute surface potential was approximately 20mV at seed surface and protrusion introduced by sulfate group and pyridine groups separately. However, considering possible minor migration of sulfate groups to protrusion and incorporating of P2VP into seed part during the secondary polymerization, this charge anisotropy can be smaller.

To estimate the attractive interaction potential between protrusion and seed part, calculation using two spheres with opposite charge signs was developed for a series of surface potentials with varying degrees of charge anisotropy. Equations 2.7-2.10 were used with a negative sign added to Equation 2.8 as electrostatic interaction is attractive instead of repulsive. The result of calculation is shown in Figure 2.7. The U_{\min} happens at the surface of the surfactant for all the charge anisotropy degrees, which is $-17kT$ with no charge anisotropy ($\Psi_1=-\Psi_2=0mV$), and $-190kT$ for the possible largest charge anisotropy ($\Psi_1=-\Psi_2=20mV$). These calculations suggest the attraction between CDC particles at the i.e.p will be large even in presence of surfactant.

2.6 Images of Dilute Suspensions and State Diagram

Optical microscopy was used to study structure of clusters formed by CDC particles in a pH range covering i.e.p (3-6) and a series of salt concentrations (0M-0.01M). First, cleaned particles coated with surfactant was diluted into solution with fixed salt concentration in presence of $C_{12}E_6$ to gain a volume fraction ~ 0.001 and $pH > 6$. And then concentrated HCl

solution containing same salt concentration was added to adjust pH to a lower value. Then $\sim 5 \mu\text{L}$ suspension was used to take optical microscopy images.

HDC particles were very stable, dispersed individually into suspension at all the conditions. Representative images are shown in Figure 2.8 at different conditions for CDC particles. For the ionic strength searched into ($[\text{NaCl}] \sim 0-0.01\text{M}$), the ionic strength effect was not obvious. Only pH had an important influence on the assembling properties. When $\text{pH} \geq 6.0$ ($\text{pH}=5.0$ was near a transition value where the stability was sensitive to ionic strength and this value can be different from batch to batch) or $\text{pH} \leq 3.0$, particles were stable and mostly dispersed in the suspension as individual particles forming only a few some small clusters. These small clusters were dynamic, which particles can stick to or move off frequently, showing that the particles experience only weak attractions. For $\text{pH}=4.0$, particles aggregated quickly with rigid floccs formed and could not be broken easily by small disturbances. At this condition large dense clusters with random shapes containing more than 100 particles were observed, in which relative positions of particles did not change indicating strong bonding between particles. However, in suspension with these large clusters were also short chains which still had rigid configuration neither growing larger by adsorbing more particles or clusters nor breaking into small parts with small disturbance. Images of these short chains are shown in Figure 2.9. The length of short chains was never longer than 20 particles. Of significance, short chains of this type were not observed in the HDC suspensions under any ionic strength of pH conditions.

Obviously, under these conditions, large dense clusters are more favorable than long aligned chains. Three reasons account for these observations: First, the Debye length is much smaller than the size of the particle ($\kappa^{-1} \ll D$), minimizes the electrostatic repulsions between the protrusions or the seed parts of different particles. As a result, there is not a large energy gain in

to particles forming linear chains. Second as described in previous work, the shape anisotropy might introduce a preferred side-by-side conformation. Simulations demonstrate that this configuration is the lowest free energy configuration for dipolar particles with an aspect ratio $L/D > 1.3^6$. Here we work with particles with $L/D \sim 1.3$. As a result we may be at the edge of the boundary between stable strings and stable clusters. Third, strong attractions estimated in Figure 2.7 will result in a fast aggregation. The strong bonds may trap particles in nonequilibrium configurations. However, the short chains observed with the CDC particles and not in the HDC particles indicates that the synthesis route described here produces a novel interaction potential.

To understand the nature and strength of interaction potentials better in a wider ionic strength and pH range, state diagrams indicating the domains of stability and instability were mapped for both HDC particles and CDC particles. To adjust pH without changing ionic strength and volume fraction at a large extent, suspension with fixed $[\text{NaCl}]$ at volume fraction ~ 0.001 was made first and then pH was adjusted with adding concentrated acid or base containing same $[\text{NaCl}]$. This process was used such that ionic strength was essentially constant in the medium pH range with $[\text{NaCl}]$ fixed. Volume fraction variations during these steps resulted in a change of no more than 5% of the total (~ 0.001 volume fraction units) as not too much concentrated acid was needed. By observing the suspension state to see whether there was strong floccs formed or particle were just dispersed into suspension, the stability was determined for each sample with fixed ionic strength and pH. The state diagram was mapped for HDC particles and CDC particles separately, with different symbols indicating whether the sample was stable at a certain point and the shadow part indicating the area of aggregation in the state diagram. The results are shown in Figure 2.10.

For HDC particles with state diagram mapped in Figure 2.10 (a), almost all the samples are stable very stable until 5M salt was added. Even at this condition, only tiny floccs were observed. This ionic strength condition is far from the range we usually worked in. The stability of the particles at low volume fraction proves that the maximum attractions felt by the particles remains weak and that the surfactant is a superb steric stabilizer. For $[\text{NaCl}]=2\text{M}$ and 5M , particles floated up to the surface after 12 hours due to large density of salt solution. However, no substantial differences in aggregation phenomenon are observed, showing that the state diagram for dilute suspension of PS DB is not concentration-sensitive. As a result we conclude that only weak attractions are present with HDC particles over a wide pH and ionic strength range.

For CDC particles with state diagram mapped in Figure 2.10 (b), at low ionic strength, aggregation was only observed at intermediate pH's near i.e.p, proving again that these particles are pH-responsive amphoteric particles. Here it was necessary to note that, hydrophilicity of CDC particles may change when varying pH. This could result in a change in adsorption isotherm of surfactant thus making condition for full coverage valid for high pH not valid at low pH. It was impossible to measure the adsorption isotherm again due to serious aggregation. At high ionic strength, aggregation was observed at all the pH's, but the transition $[\text{NaCl}]$ was much lower than that for HDC particles. This result confirms the conclusion drawn for interaction strength calculated in Section 2.6 for these two particle types at high pH for different ionic strength. With a smaller average surface charge, it was easier for CDC particles to aggregate when ionic strength was increased to a medium value ($[\text{NaCl}]=0.1\text{M}$).

Although it was reasonable to have particles less stable and more sensitive to ionic strength with smaller surface potential, it is still difficult to understand the underlying

mechanism thoroughly and many other factors might also significantly influence the stability. For HDC particles, aggregation was observed only at $I=5M$ with stable suspension obtained at all the other ionic strengths below that, confirming the result in calculating pair potential that only $\sim -10-15kT$ minimum could be achieved by coating the surfactant. This means even for CDC particles, only the effect of screening out surface charge by increasing ionic strength is not large enough to induce serious aggregation. Some other factor must account for this instability. First, there was already some charge anisotropy even at high pH although pyridine groups were not protonated, according to the electrophoretic mobility data taken for $[NaCl]=0.001M$ for both particles. Secondly, Hamaker constant $A_H=3.2kT$ for polystyrene was used for considering van der Waals attraction for both particles as it was difficult to characterize the surface fraction of P2VP, but in fact Hamaker constant of P2VP which was mainly contained in the protrusion of CDC particles was different. Last but not the least, this different chemical component of the seed part and the protrusion might result in anisotropic adsorption isotherm, making the assumption of full coverage of surfactant debatable. All these potential chemical anisotropies might result in some anisotropic pair interaction and could have accounted for less stability of the CDC particles.

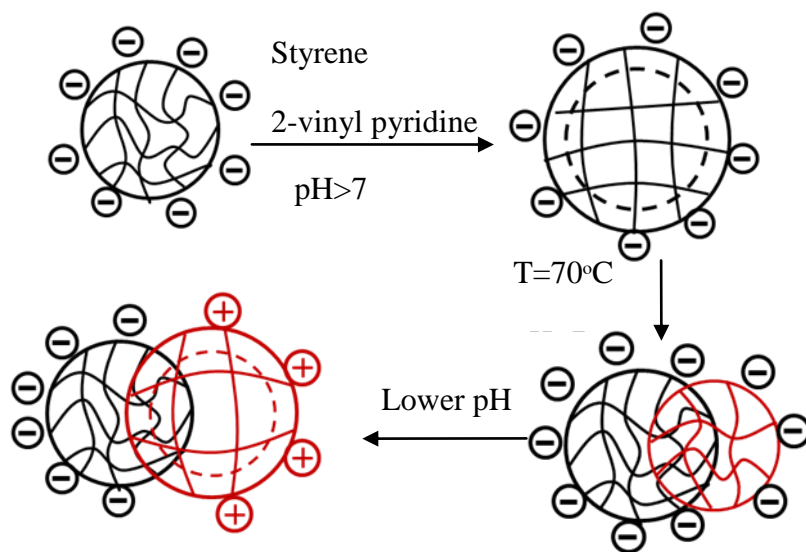
To understand the effect by introducing P2VP better, the phase diagram of CSP particles was also mapped below in Figure 2.10 (c). These particles display very similar behaviors to the CDC particles. At low ionic strength, aggregation was only observed at intermediate pH's proving that these particles were also pH-responsive amphoteric particles and, at high ionic strength ($[NaCl] \geq 1M$) aggregation was obtained over the full pH range. From the SEM images shown in Figure 2.2, CPS particles were also expected to undergo a phase separation during the seeded emulsion polymerization, so there some degree of chemical anisotropy will exist.

However, this anisotropy was not as large as that of CDC particles accounting for two minor differences in the state diagram. First, the intermediate pH range for aggregation at low ionic strength shifted to lower values. Second, transition ionic strength for serious aggregation throughout all the pH range shifts up (For high pH, CDC particles aggregated but CSP particles were stable at $[\text{NaCl}]=0.1\text{M}$). These two differences can be explained by arguing that a smaller phase separation might keep more negatively charge sulfate groups remaining on particle surface, which made it necessary to go to a lower pH condition to get enough protonation for aggregation and to increase to a higher ionic strength to sufficiently screen out highly negative surface charge. Considering the substantial similarity with CDC particles introduced from the uncontrollable phase separation, CSP particles were not made in large quantities to study the flow properties.

Generally, aggregation with strong attraction was presented in CDC suspension in a much wider range compared to HDC particles, which could be explained by both smaller amount of surface charge and potential chemical anisotropy. To better understand the underlying pH and ionic strength dependence of the pair interaction, we moved on to study the flow properties introduced in the next chapter.

2.7 Tables and Figures

Scheme 2.1. Synthesis Strategy by Seeded Emulsion Polymerization^a



^a Negative charge is introduced to the surface of seed particle by incorporating sulfate group from initiator potassium per sulfate. The seed particles are then swollen with a mixture of styrene and 2-vinyl pyridine containing certain amount of divinyl benzene at high pH and undergoing a secondary polymerization to form protrusions concentrated in pyridine groups to introduce high concentration of positive charge when the protrusions are slightly swollen at low pH.

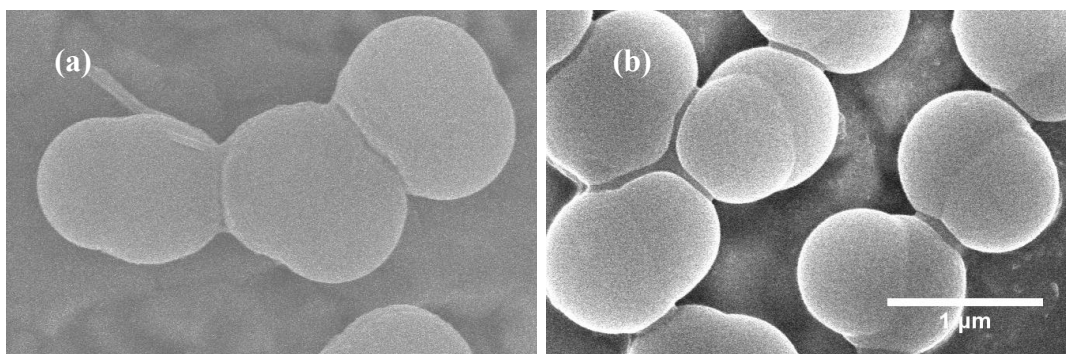


Figure 2.1. (a) Shape anisotropic particles with protrusion formed by PS (HDC) and (b) shape anisotropic particles with protrusion formed by poly(styrene-co-(2-vinyl) pyridine) (CDC).

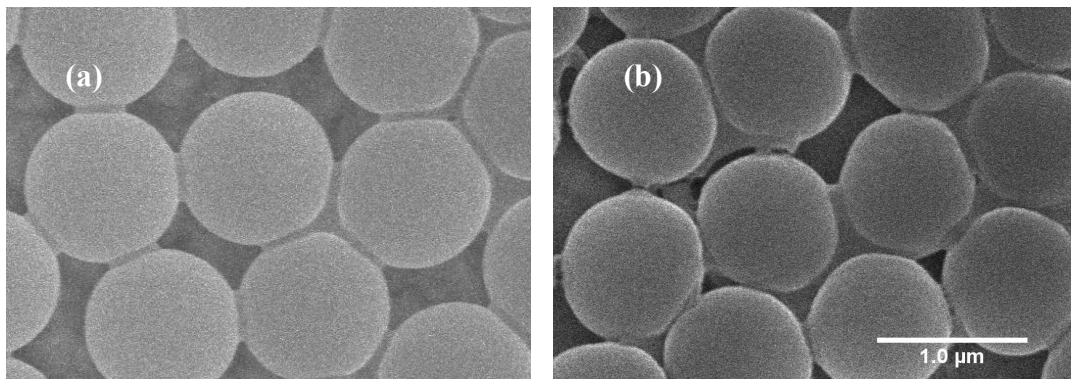


Figure 2.2. (a) Spherical particles formed by PS (HSP) and (b) “spherical” particles with formed by poly (styrene-co-(2-vinyl) pyridine) (CSP).

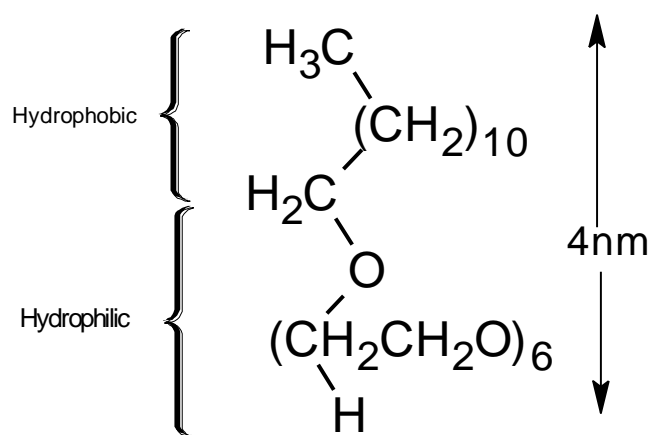


Figure 2.3. Chemical Structure of surfactant C_{12}E_6 . The molecule length determines the separation distance between two particles.

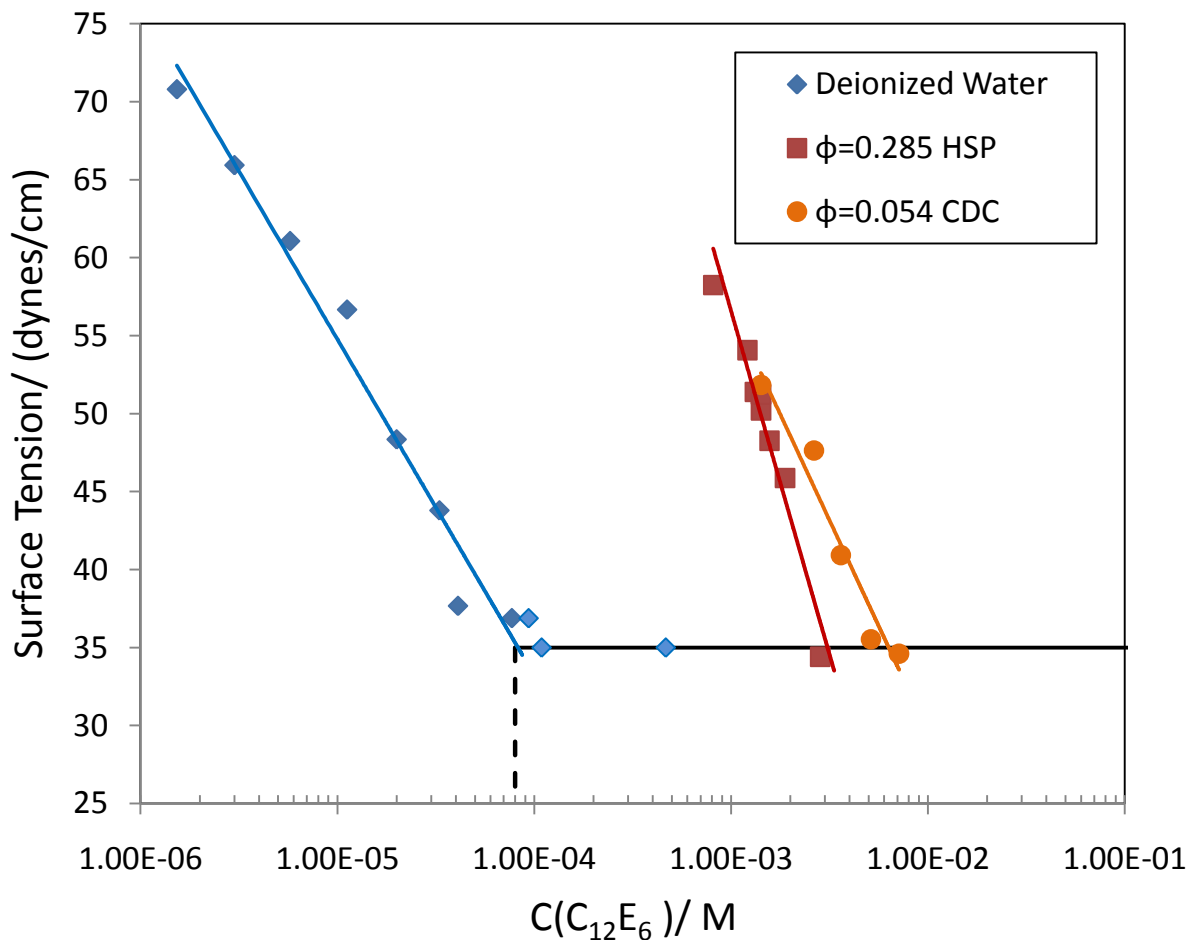


Fig 2.4. Surface tension measurement in deionized water (diamonds), $\phi=0.285$ PS spheres (HSP) made with similar approach by using non-crosslinked seeds (squares), $\phi=0.054$ PS/P2VP DB (CDC) (circles). The critical of micelle concentration in DIW ($8 \times 10^{-5} M$) and surface coverage data on PS are in good agreement with literature reports.

Table 2.1. Zeta-potential measurement in presence of C₁₂E₆ and 10⁻³M NaOH for different salt concentration

CDC particles		
[NaCl]	zeta-potential (mV)	width(mV)
0M	-66	±1.6
0.01M	-27.8	1.6
0.05M	-13.9	1.6
0.1M	-13.4	1.7
0.5M	-1.6	4.8
HDC particles		
[NaCl]	zeta-potential (mV)	width(mV)
0M	-93.1	±1.6
0.01M	-54.1	1.6
0.05M	-31.3	1.6
0.1M	-20.3	1.7
0.5M	-6	5

(a)

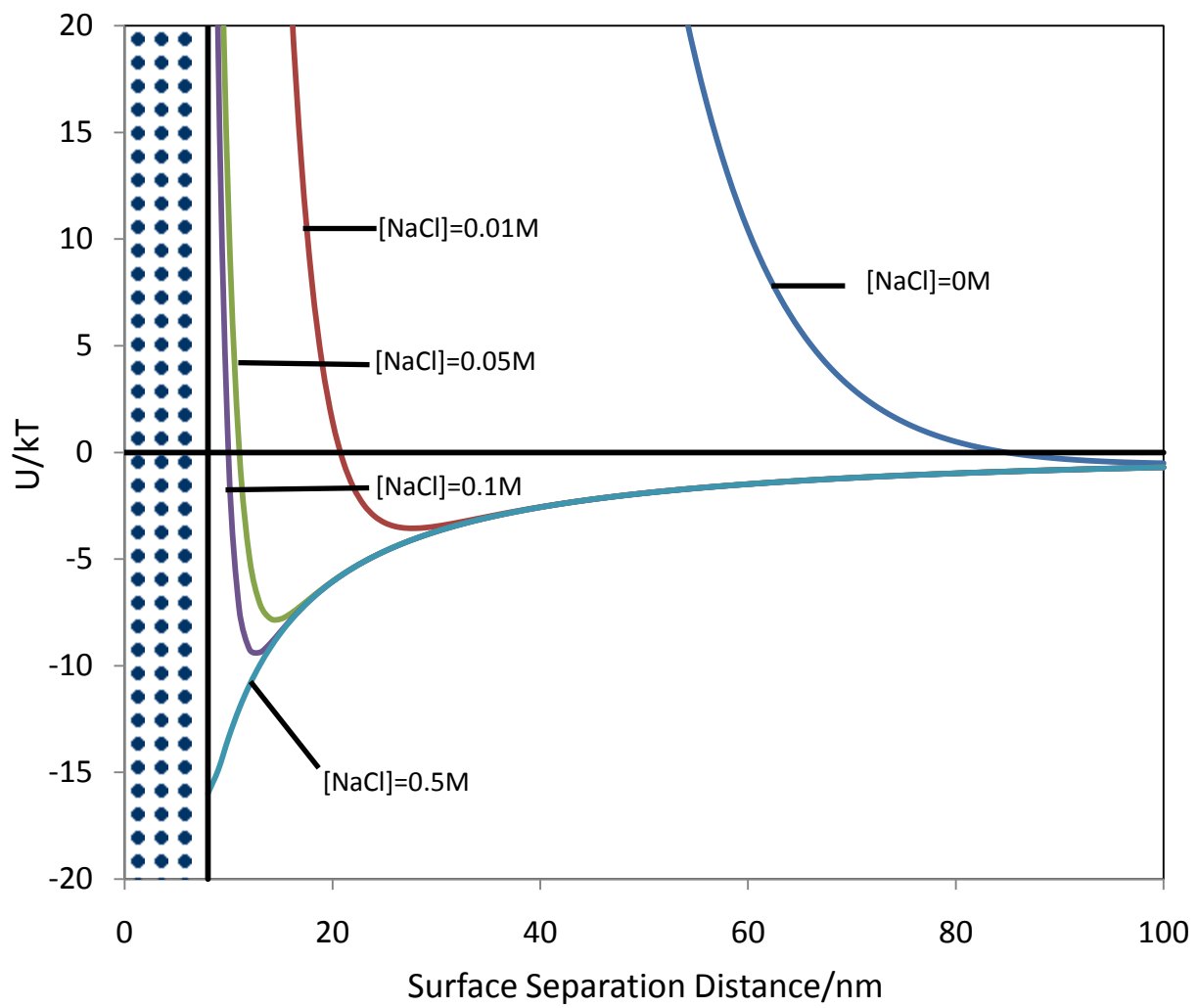


Figure 2.5. (continued on next page)

(b)

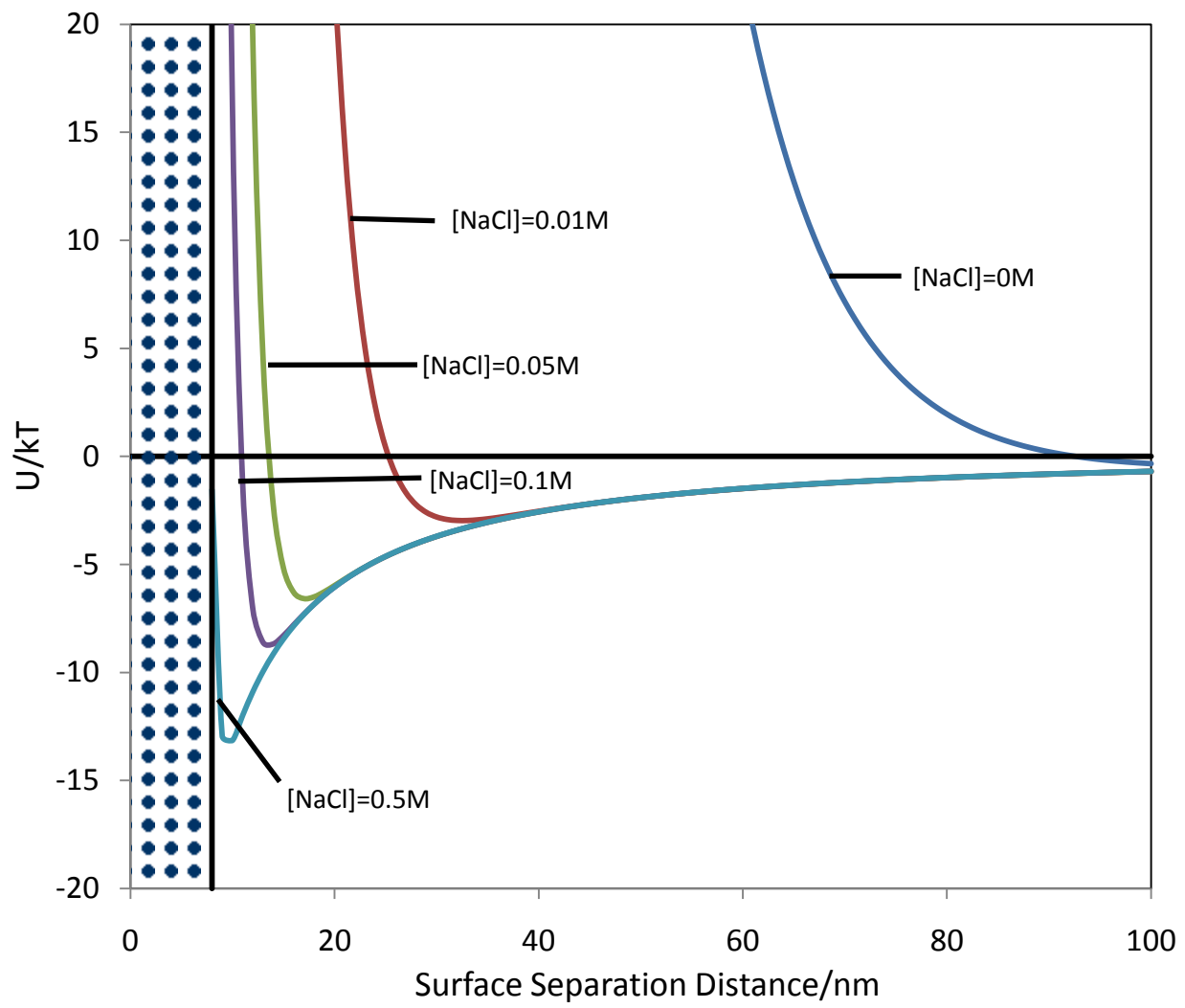


Figure 2.5. Interaction Potential for uniformly charged (a) CDC particles (b) HDC particles in presence of 10^{-3} M NaOH at high pH for [NaCl]=0M, 0.01M, 0.05M, 0.1M, 0.5M.

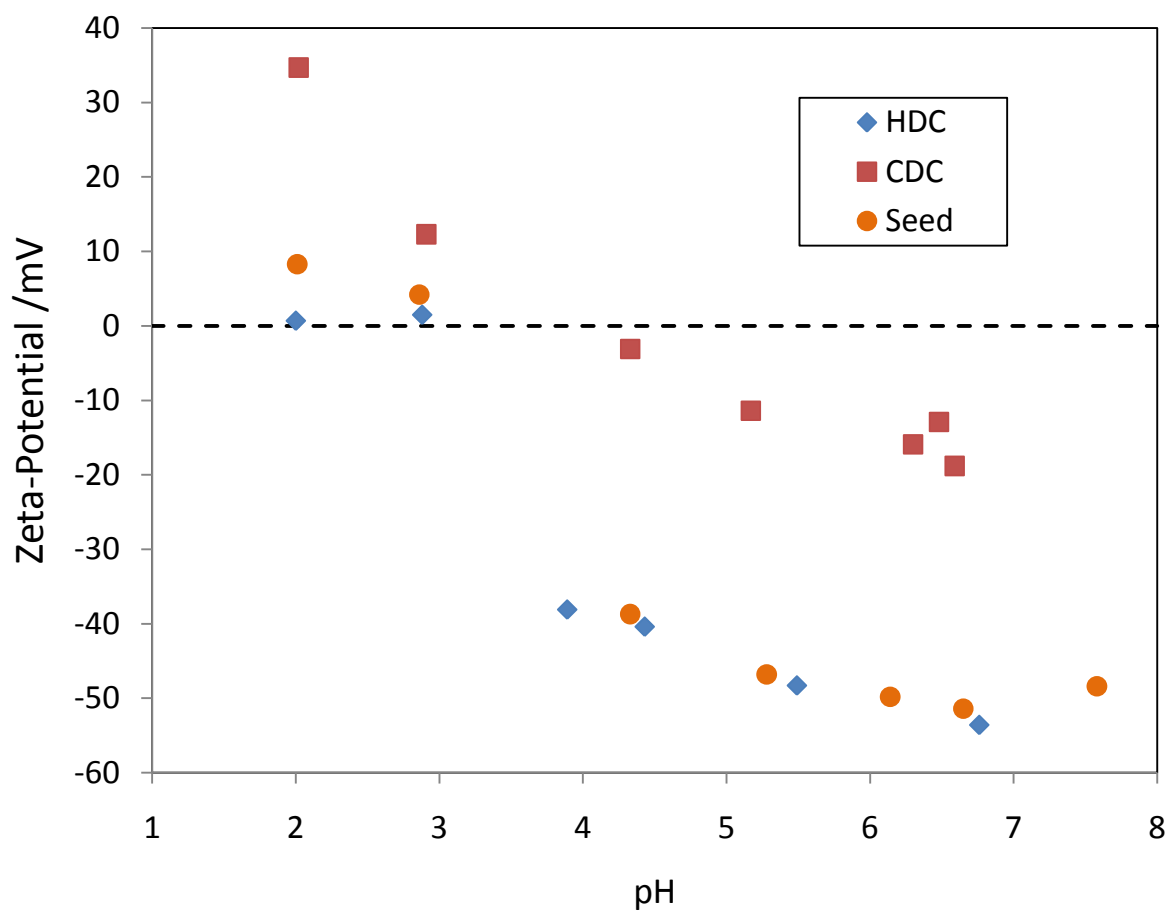


Figure 2.6. Zeta-potential as a function of pH for HDC particles (diamonds), CDC particles (squares) and seed (circles) in presence of $C_{12}E_6$ and $10^{-2}M$ NaCl.

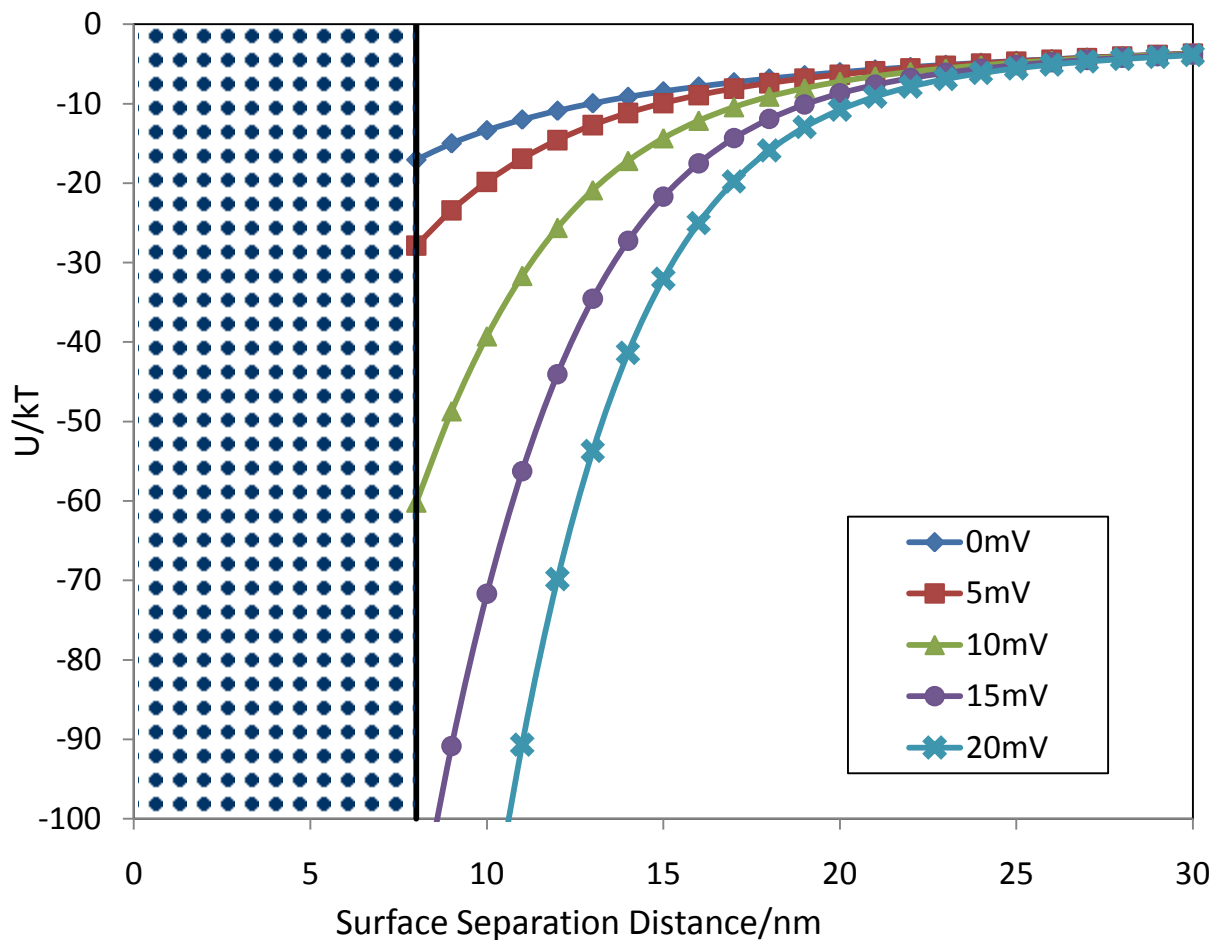


Figure 2.7. Interaction potential as a function of surface separation distance between two spheres with surface potential $\Psi_1 = -\Psi_2 = 0mV$ (diamonds), $5mV$ (squares), $10mV$ (triangles), $15mV$ (circles), $20mV$ (crosses).

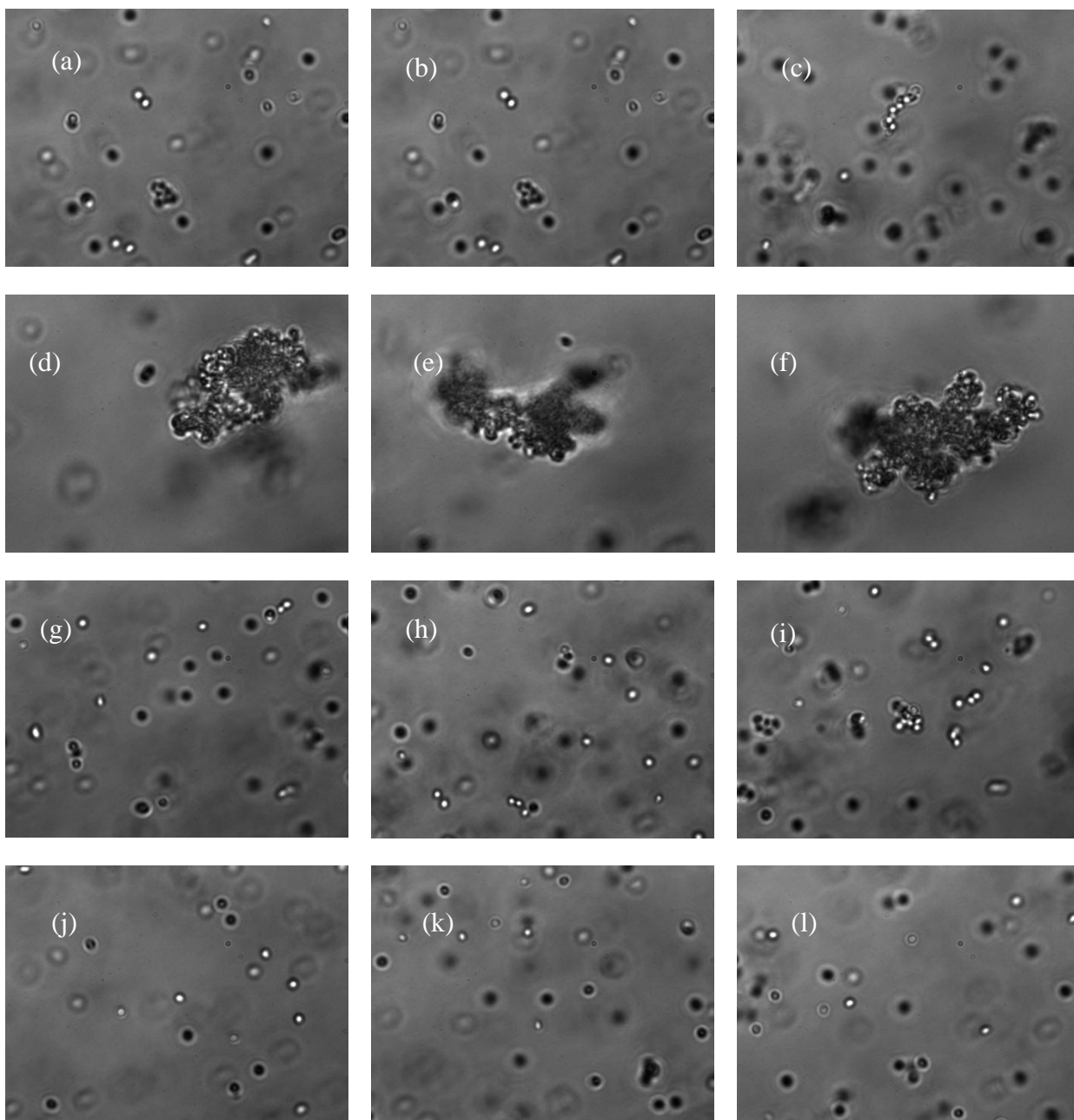


Figure 2.8 Optical microscopy images of CDC particles at a variety of pH's, pH=3.0 (a-c), pH=4.0 (d-f), pH=5.0 (g-i), pH=6.0 (j-l) and a variety of ionic strengths, [NaCl]=0M (a, d, g, j), [NaCl]=0.001M (b, e, h, k), [NaCl]=0.01M (c, f, i, l). The size of the images is $101\ \mu\text{m} \times 76\ \mu\text{m}$.

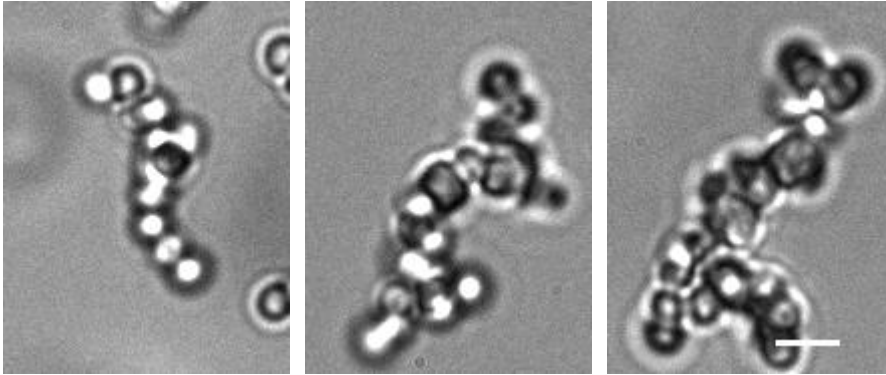


Figure 2.9. Short chain shaped clusters in suspension of CDC particles at pH=4, I=0.01M (Scale bar length is 2 μ m). Most clusters have irregular shape and contain large numbers of particles, but quite a few small clusters have short chain configuration which is not observed with HDC particles.

(a)

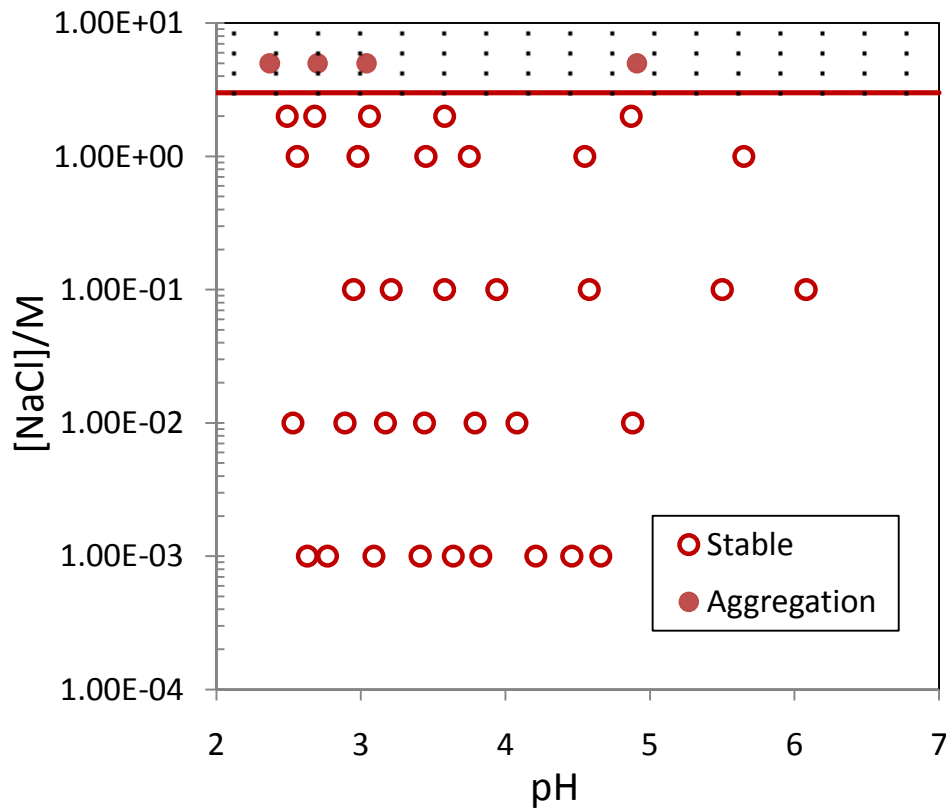


Figure 2.10. (continued on next page)

(b)

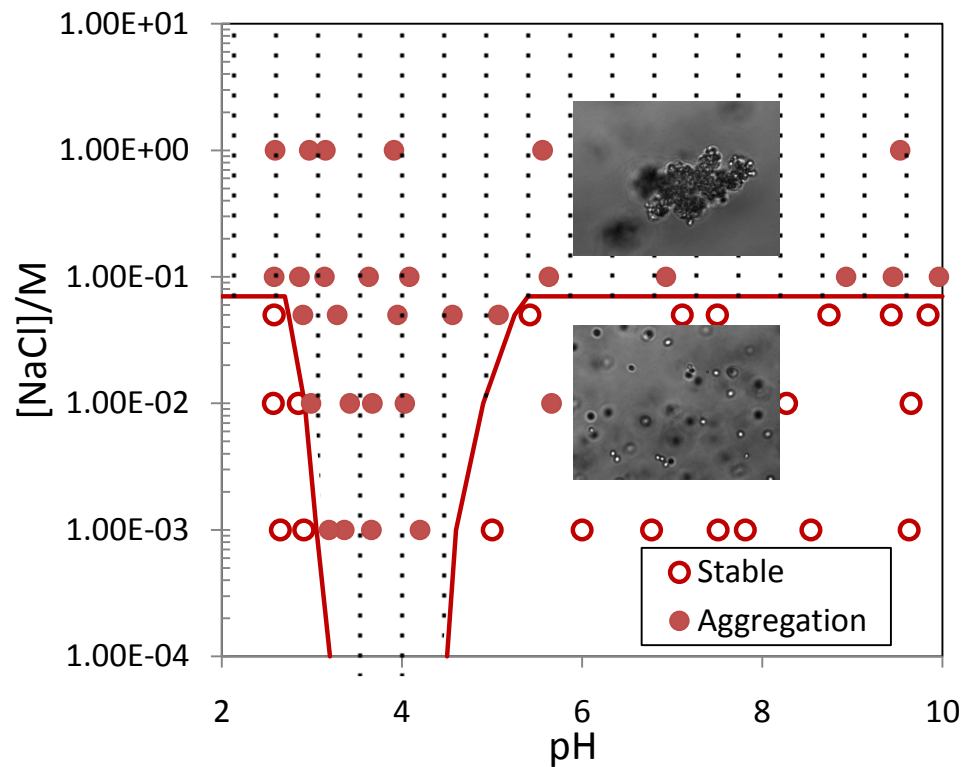


Figure 2.10. (continued on next page)

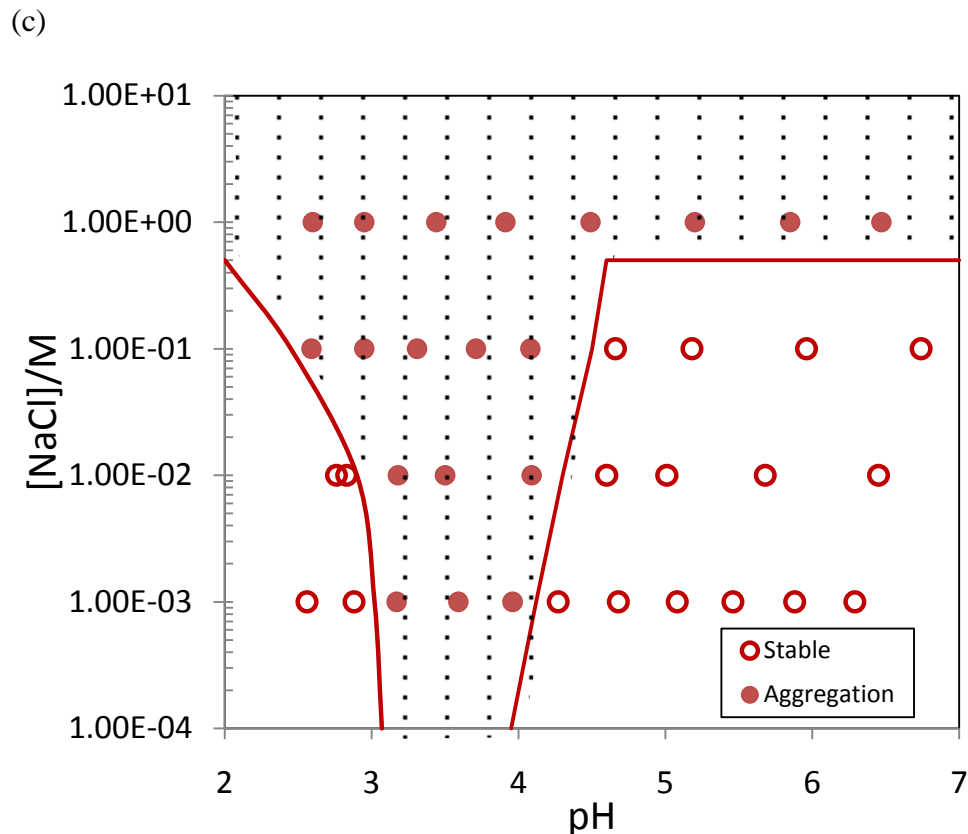


Figure 2.10. State diagram for dilute suspension of (a) HDC (b) CDC and (c) CSP, showing stable conditions (open circles) and conditions for aggregation (closed circles). Dotted domains stand for the domains for aggregation. Inset of part (b) shows the images of stable and unstable samples separately.

2.8 References

1. Sciortino, F.; Giacometti, A.; Pastore, G., *Physical Review Letters* **2009**, *103* (23).
2. Goyal, A.; Hall, C. K.; Velev, O. D., *Physical Review E* **2008**, *77* (3).
3. Goyal, A.; Hall, C. K.; Velev, O. D., *Soft Matter* **2010**, *6* (3), 480-484.
4. Miller, M. A.; Blaak, R.; Lumb, C. N.; Hansen, J. P., *Journal of Chemical Physics* **2009**, *130* (11).

5. Weis, J. J.; Levesque, D., *Physical Review Letters* **1993**, 71 (17), 2729-2732.
6. Ganzenmuller, G.; Camp, P. J., *Journal of Chemical Physics* **2007**, 126 (19).
7. Van Workum, K.; Douglas, J. F., *Physical Review E* **2006**, 73 (3).
8. Zhang, Z. L.; Glotzer, S. C., *Nano Letters* **2004**, 4 (8), 1407-1413.
9. Hong, L.; Jiang, S.; Granick, S., *Langmuir* **2006**, 22 (23), 9495-9499.
10. Jiang, S.; Granick, S., *Langmuir* **2008**, 24 (6), 2438-2445.
11. Pawar, A. B.; Kretzschmar, I., *Langmuir* **2008**, 24 (2), 355-358.
12. Snyder, C. E.; Yake, A. M.; Feick, J. D.; Velegol, D., *Langmuir* **2005**, 21 (11), 4813-4815.
13. Chen, C. H.; Shah, R. K.; Abate, A. R.; Weitz, D. A., *Langmuir* **2009**, 25 (8), 4320-4323.
14. Seiffert, S.; Romanowsky, M. B.; Weitz, D. A., *Langmuir* **2010**, 26 (18), 14842-14847.
15. Yuet, K. P.; Hwang, D. K.; Haghgooe, R.; Doyle, P. S., *Langmuir* **2010**, 26 (6), 4281-4287.
16. Hong, L.; Cacciuto, A.; Luijten, E.; Granick, S., *Nano Letters* **2006**, 6 (11), 2510-2514.
17. Hong, L.; Cacciuto, A.; Luijten, E.; Granick, S., *Langmuir* **2008**, 24 (3), 621-625.
18. Kim, J. W.; Larsen, R. J.; Weitz, D. A., *Journal of the American Chemical Society* **2006**, 128 (44), 14374-14377.
19. Sheu, H. R.; Elaasser, M. S.; Vanderhoff, J. W., *Journal of Polymer Science Part a-Polymer Chemistry* **1990**, 28 (3), 629-651.
20. Mock, E. B.; De Bruyn, H.; Hawket, B. S.; Gilbert, R. G.; Zukoski, C. F., *Langmuir* **2006**, 22 (9), 4037-4043.
21. Tang, C.; Zhang, C. L.; Liu, J. G.; Qu, X. Z.; Li, J. L.; Yang, Z. Z., *Macromolecules* **2010**, 43 (11), 5114-5120.

22. Mock, E. B.; Zukoski, C. F., *Langmuir* **2010**, *26* (17), 13747-13750.
23. Flory, P. J., *Principles of polymer chemistry*. Cornell University Press: Ithaca: New York, 1953.
24. Morton, M.; Kaizerman, S.; Altier, M. W., *Journal of Colloid Science* **1954**, *9* (4), 300-312.
25. Hiemenz, P. C.; Lodge, T. P., *Polymer chemistry*. Boca Raton: CRC Press: New York, 2007.
26. Homola, A. M.; Inoue, M.; Robertson, A. A., *Journal of Applied Polymer Science* **1975**, *19* (11), 3077-3086.
27. Dupin, D.; Fujii, S.; Armes, S. P.; Reeve, P.; Baxter, S. M., *Langmuir* **2006**, *22* (7), 3381-3387.
28. Kim, J. W.; Larsen, R. J.; Weitz, D. A., *Advanced Materials* **2007**, *19* (15), 2005-+.
29. Kramb, R. C.; Zukoski, C. F., *Langmuir* **2008**, *24* (14), 7565-7572.
30. Goodwin, J. W.; Hughes, R. W.; Partridge, S. J.; Zukoski, C. F., *Journal of Chemical Physics* **1986**, *85* (1), 559-566.

Chapter 3 Effect of PH-Response on Rheology of Shape Anisotropic Particles

3.1 Introduction

Densifying colloidal suspensions can result in a state where the particles are constrained by nearest neighbors and display slow relaxation times associated with a “glassy state”. This is accomplished by a quick concentration process or introducing some shape or size polydispersity to avoid crystallization. Most studies of the colloidal glass transition have focused on spherical particles experiencing uniform interaction potentials¹. With increasing interest in making non-spherical particles²⁻⁶, shape anisotropy has recently also been incorporated in theoretical work and simulations to study its effect on dynamics on glass formation and linear elasticity⁷⁻¹² in addition to searching for novel crystalline phases¹³⁻¹⁸.

Mode coupling theory (MCT), which was developed to describe the collective dynamics where nearest neighbors cage or blocking of long range diffusion, has been extended to study the kinetic arrest and shear elasticity of non-spherical particles^{7-9, 12}. For weakly shape anisotropic particles, the ideal glass transition volume fraction (ϕ_g) is found to be a nonmonotonic function of the degree of shape anisotropy. The maximum glass transition volume fraction is found to occur for weak anisotropy as experienced by hard dumbbells with length to diameter ratios of 1.4. A maximum in glass transition volume fraction is also predicted at different aspect ratios for triplets, spherocylinders and hard ellipsoids^{7, 10}. These studies suggest that elastic moduli of hard particle glasses have a universal behavior for different shape anisotropies when plotted as a function of volume fraction difference with the ideal glass transition volume fraction⁸.

One method suggested to characterize colloidal glasses and gels lies in the magnitude of yielding strain which is modeled as occurring when particles are displaced to a strain where they feel the maximum restoring force, M , imposed by nearest neighbors. For the glassy state, M

is found to depend on both ϕ and aspect ratio determined parameter C according to a power law

$$|M| \cong \frac{kT}{D} C \left[\left(\frac{\phi}{\phi_g} \right)^v - 1 \right],$$

where D is the diameter where the exponent is essentially constant with $v=8.7$, independent on shape anisotropy .

With large quantities of uniform shape anisotropic particles synthesized, experimental studies have confirmed many of the predictions for the volume fraction at the glass transition and the dynamics of the glassy state¹⁹. These studies support many of these results with hard shape anisotropic particles obtained by MCT including the increase of ϕ_g when increasing aspect ratio in a narrow region and universal behavior of shear elastic modulus when scaled on an aspect dependent glass transition volume fraction or shape dependent volume fraction at random close packing^{7, 8}.

Sluggish dynamics and high elasticities of colloidal suspensions can also be achieved by tuning the interaction potential to increase isotropic attractions. By increasing the strength of attraction, at volume fractions considerably below those where glasses are formed with hard particles, colloidal particles can be brought to a close contact distance and be localized. These systems form space filling networks and the system becomes solid-like. The volume fraction at the onset of the solid-like state will decrease with increasing strengths of attraction¹. MCT has also been applied to study the liquid-gel boundaries and the mechanical properties of the gel including elastic moduli in presence of attraction in thermal gels²⁰ and depletion gels²¹. In these systems, the gelation boundary is determined by the attractive potential at the point minimum particle separation, ϵ . At the gel point, $\epsilon_{gel} \sim B \phi_{gel}^{-x}$ ^{20, 21}. Specifically for strong attractive system ($K \rightarrow 0$) for low density ($\phi \rightarrow 0$), asymptotic limits are obtained with Hard Core Attractive Yukawa system by the relationship $K^2 \phi / b = \text{constant}$, where K and b are parameters in the attractive Yukawa potential denoting attraction strength and attractive range separately. Thus, for

many systems, $\alpha \sim 0.5$ while B is dependent on the range of interparticle attraction range²². In colloidal systems, the strength of attraction is the result of a solvent modified potential of mean force. As a result, ε can be controlled through changes in solvent conditions. For thermal gels the surface properties of the colloid are sensitive to temperature such that ε typically increases with T while in depletion gels ε is a function of polymer concentration.

Elastic moduli G' for the gel state are predicted to be strongly dependent on volume fraction ϕ and a characteristic localization length r_{loc} according to a power law $\frac{G'D^3}{kT} \sim \frac{\phi D^2}{r_{loc}^2}$, with r_{loc} determined by both volume fraction and attraction strength. At the same time, for a gel, absolute yield stress τ_{abs} is dependent on ϕ and ϕ_g which also denotes the magnitude of attraction by $\tau_{abs} \sim (\phi/\phi_g)^v - 1$ where v is a function of ϕ_g ²³.

Changing particle shape for hard interactions is a first step to understanding the role of anisotropic interactions in suspension behavior. A second step is to treat the shape anisotropic particles as being composed of spheres which interact with centro-symmetric pair potential potentials. This allows investigation of the impact of isotropic interactions between shape anisotropic particles. We emphasize that due to the shape anisotropy of the composite particles, the pair potentials introduced in this approach are indeed anisotropic but this anisotropy is tied solely to the underlying composite particle shape. Experimental studies of shape anisotropic particles composed of identical interpenetrating spheres have demonstrated universal volume fraction scaling for elastic moduli and yield stresses where ϕ_g is found to contain much of the shape and strength of attraction dependent information^{19,24}.

For the glassy state or gels formed by spherical particles and those with small shape anisotropies that experience isotropic interactions, stress sweep experiments have recently been carried out to understand a variety of constraints encountered in dynamical relaxation processes²⁴.

²⁵. In these experiments, the suspension is subjected to an oscillatory stress at a fixed frequency and the maximum stress is increased. For dense glasses formed by hard spheres, a single yield event is observed in a stress sweep where elastic modulus (G') drops below the zero strain or linear elastic modulus with a single monotonic decay while the viscous modulus (G'') shows a single local maximum value. This single yield event is associated with applying stresses sufficient to delocalize the particle's center of mass (CM) and enable long range self-diffusion. When shape anisotropy is integrated into hard particles, a double yield phenomenon is observed where, with increasing stress, a second shoulder in the decay of G' and two local maxima in G'' are observed. These two yielding events are associated with applying a stress sufficient to enable stress relaxation by rotation and by CM diffusion. Experimentally it has been shown that when the pair potential is altered through addition of nonadsorbing polymer for depletion gels or by increases in ionic strength for van der Waals gels, at high volume fractions ($>\sim 0.55$) even spheres show double yielding behavior. Under these conditions, the two constraints are associated with applying sufficient stress to release the particles first from bonding constraints and second from caging constraints. For anisotropic particles two yield events are also observed, the same assignments are made with the argument that under attractive conditions rotational and CM diffusion are strongly coupled^{24, 26}. For strongly attractive spheres, where gels are formed at low volume fraction, only single yield event is observed. This is associated with releasing bonding constraints. Simulations suggest there is a volume fraction below which only bonds constrain the particles. Again for shape anisotropic particles that are strongly attractive, experimentally only a single yield event is observed in low volume fraction gels indicating that attractions couple rotational and CM diffusion²⁴.

These experiments and simulations provide a strong foundation for understanding the onset of gelation and mechanical properties of gels composed of spherical and shape anisotropic particles experiencing short range, isotropic interactions. Recently interest has been triggered in studying patchy particles experiencing a variety of anisotropic interaction potentials. These studies suggest that depending on the number and configuration of attractive patches, particles will cluster into novel configurations²⁷⁻²⁹ with altered liquid-gas phase boundaries^{30, 31} and to crystallize into novel ordered structures.^{32, 33}

Gel formation in suspensions of particles experiencing anisotropic interactions as well as exploring the predictions of the Wertheim theory for particles experiencing limited valence interactions³⁴, have been developed. This approach makes a connection between colloidal gels and molecular gels where molecules experiencing a limited number of bonds aggregate to form gels. Experimental confirmation of these predictions is limited due to a lack of synthetic techniques that result in uniform particles experiencing valence limited interactions.

Probably the best studied experimental system is that of Janus particles with different chemical properties on two different halves of a spherical particle that give rise to anisotropic interactions. Experimental studies hint at a wonderful array of structures that spontaneously form when particles experience these anisotropic pair potentials. Limited simulation work^{33, 35-37} has been carried out on gels composed of particles of this type. However, there has been essentially no characterization of the mechanical properties of the observed structures. Nevertheless, the simulations provide insights on the potential of some novel features of colloidal gels formed by introducing anisotropic interactions.

Molecular simulation predicts dynamical arrest and gelation in suspensions of low density, composed of strongly attractive soft dipolar dumbbells. Gelation is triggered by the

tendency for branching occurs when the dipole is increased and/or the particles are elongated³⁵. Aggregation processes have also been investigated in a model gel formed by particles with directional LJ-like potentials. The ability to produce space filling percolating networks systems was studied as a function of the rate of cooling (increase in strength of attraction), demonstrating that quenching favors more connected but less space filling network structures.

For hard spheres with short range dipolar interactions, two significant steps are observed when crossing phase transition boundaries by increasing volume fraction and/or dipolar interaction strength. First strings of particles are formed and then the strings percolate to form a network³³. In the dense state, these structures can be considered to be experiencing two limitations to long range diffusion. First, the particles are bonded together by head to tail dipolar interactions. Secondly, the particles are caged within strands of multiple particle widths. These predictions suggest gels composed of particles experiencing anisotropic interactions may display novel rheological properties, including but not limited to low kinetic arrest volume fractions, greater sensitivity to arrest procedure (rate of turning on of attractions), and novel bonding or caging constraints.

Of particular interest to this thesis is the formation of space filling gels produced by increasing the strength of attraction between shape anisotropic particles. Synthesis methods are developed to introduce both shape and chemical anisotropy to the particles and here we explore the impact of these effects on the mechanical properties of the resulting gels. These systems remain poorly studied such that there are no predictions or experiments probing differences in mechanical properties of gels composed isotropically attractive shape anisotropic particles, and particles that are both shape and chemical anisotropy. Here we seek signatures of the combined effects of shape and chemical anisotropy.

To demonstrate how subtle these effects may be, the effects of introducing shape anisotropy is considered alone first. For hard and weakly attractive particles composed of identical interpenetrating spheres, shape anisotropy alters the volume fractions at the point of kinetic arrest but does not greatly alter volume fraction dependence of the modulus of the materials in glasses and gels. The major qualitative difference in the mechanical properties of these systems is observed not in the volume fraction dependence of the yielding but in the yielding constraints as observed in stress sweep experiments. These differences are observed only in volume exclusion glasses. Even here if the attraction is too strong, rotational and center of mass diffusion are strongly coupled and a single yield constraint is observed²⁴. The volume exclusion interactions introduce anisotropic interactions associated with the dependence of the pair interaction energy of two particles on the angle between their major axis.. While the anisotropy of these interactions can be enhanced by placing patches on particle surfaces or placing them in a dipolar state, the subtle differences in mechanics seen here suggest the mechanical signatures of gels composed of chemically anisotropic gels may not be dramatic.

Here attempts are made to understand the effect of both shape anisotropy and interaction anisotropy on dynamic localization by quantitatively working with particles that are expected to be chemically anisotropic and investigating the effects of this anisotropy on the kinetic arrest volume fraction, shear elasticity, yield stress, and the presence of multiple yielding events.

Specifically in our experiment, two different kinds of shape anisotropic particles are made and coated with $C_{12}E_6$ to limit van der Waals attractions at high ionic strengths. One set of particles are homopolymer dicolloids (HDC) formed by pure polystyrene which have seen extensive study and are expected to show isotropic interactions. The second particle type is copolymer dicolloids (CDC) composed of copolymer formed by styrene and 2 vinyl pyridine

(2VP). The synthesis results in HDC particles being coated with strong acid groups giving it a constant charge for $\text{pH} > 2$. The CDC particles are pH-responsive as confirmed by both surface potential measurement and state diagram mapping discussed in chapter 2. By tuning pH and ionic strength, interaction potential is changed for both particles. We explore differences detected in glass/gel transition volume fractions (ϕ_g), volume fraction dependence of linear elastic moduli (G_0'), absolute yield stress values (defined as the stress value τ_y where $G' = G''$ in a stress sweep experiment), and multiple yielding behaviors indicating different constrain mechanisms. With these experiments, key questions we probe are the qualitative and quantitative changes observed in gel rheology when chemical anisotropy is introduced into shape anisotropic particles.

In the following sections, details of the stress sweep experiment will be given. In Section 3.2, the process of preparing samples will be introduced, along with the instrument and experimental setup. In Section 3.3, the changes in flow properties as determined in stress sweep experiments will be discussed. Linear elastic behavior is discussed in Section 3.3.1, and yield behaviors in Section 3.3.2. In section 3.4, the results are summarized with general conclusions given.

3.2 Experimental

Soap-free emulsion polymerization and following seeded emulsion polymerization were used to make uniform seeds and the two different kinds of dicolloids separately, with synthesis details stated in Chapter 2. After synthesis, the shapes and sizes of both particles were characterized with SEM with the pictures given in Figure 2.1. By measuring the main size parameters with the image processing software ImageJ, it was found that final particles can be considered to be fused spheres of the same size with average diameters of $D \approx 850 \text{ nm}$. The length

of particle along the line connecting two centers of the overlapping spheres is $L \approx 1100 \text{ nm}$, resulting in an aspect ratio $L/D \sim 1.3$. These values vary slightly from batch to batch. However, the variation is small leading to essentially no variations the physical properties of the suspensions. Nevertheless, specific measurements were carried out and used for specific batch once these parameters were desired for following dimensionless parameter calculation.

The resulting suspension was cleaned by settling where the supernatant was first replaced with 10^{-3} M NaOH . After the particles settled for several times, it took more than 5 hours for the particles to settle. The suspension was then placed into SpectraPor 4 dialysis tubing (molecular weight cut-off 12,000-14,000) and underwent dialysis against 10^{-3} M NaOH solution for 2-3 days with the solution changed for about four times until conductivity of the solution outside the tubing became constant. This cleaning process eliminated undesired oligomers and electrolytes. Volume fraction were determined by weight loss after drying $\sim 0.5 \text{ mL}$ suspension based on a polymer density of $1.055 \text{ g} \cdot \text{cm}^{-3}$ for HDC particles and $1.066 \text{ g} \cdot \text{cm}^{-3}$ for CDC particles after the suspension was transferred out of the dialysis tubing. The volume fraction of the resulting suspension is about 5% in most cases, but differs slightly from batch to batch. The particles were then stabilized with a monolayer of nonionic surfactant C_{12}E_6 based on the adsorption isotherm results in Chapter 2. The critical micelle concentration (C_{cmc}) of C_{12}E_6 in pure aqueous solvent is $8 \times 10^{-5} \text{ M}$ and the saturated surface concentration of C_{12}E_6 for HDC particles is $1.5 \text{ molecules/nm}^2$, while the saturated surface concentration for CDC particles is $9.8 \text{ molecules/nm}^2$. The equation used here to calculate the total mass of surfactant added to the solutions is $m(\text{C}_{12}\text{E}_6) = M_s V_t (1 - \phi) C_{cmc} + M_s V_t \phi \Gamma A_p / (V_p A_v)$. Here molar weight for surfactant $M_s = 450 \text{ g/mol}$, V_t and ϕ are total volume and volume fraction of the suspension separately, C_{cmc} and Γ are the critical micelle concentration and surface concentration for full coverage given above separately,

$A_p = 6.02 \times 10^{23} \text{ molecule/mol}$ is Avogadro constant, and A_p and V_p are surface area and volume of a single particle separately calculated with $A_p = 2\pi DL$, $V_p = \frac{1}{2}\pi L^2 \left(D - \frac{L}{3}\right)$. The desired amount of surfactant was added into the suspension and the sample was kept in the $\sim 30^\circ\text{C}$ oven for about 1 hour. To make sure of full coverage, surface tension was checked before further processing.

The suspension of coated particles was transferred to a SpectraPor 4 dialysis tubing (molecular weight cut-off 12,000-14,000) and dialyzed against 3L aqueous solution containing 10^{-3}M NaOH, $8 \times 10^{-5}\text{M}$ C_{12}E_6 and $\sim 200\text{g}$ polyethylene glycol (PEG, Mn $\sim 20,000$, Sigma) for 2 days to increase the volume fraction to $\phi \sim 0.30$. Here PEG increases the osmotic pressure of the dialyses and serves to pull water from the suspension. The final concentrated suspensions remained liquid-like and had volume $V_t \sim 30\text{mL}$ and was transferred to a 50mL centrifuge tube. For low density gel/glass samples ($\phi < 0.30$) discussed below, concentrated 0.1M HCl solution containing 10^{-3}M NaCl was added to tune pH for gel/glass formation but still keeping ionic strength $\sim 10^{-3}\text{M}$, or concentrated NaCl ($> 1\text{M}$) to increase ionic strength for gel/glass formation considering a dilution consequence based on a measurement of volume fraction. The solutions used to tune ionic strength and pH all contained $8 \times 10^{-5}\text{M}$ C_{12}E_6 to ensure full coverage. To obtain gel/glass samples with higher volume fractions, the suspensions were centrifuged at a rate $\sim 3,000$ rpm with force $\sim 2000\text{g}$ achieved for ~ 30 minutes, and then the supernatant was taken off with the remaining $\sim 20\text{mL}$ transferred to a glass vial for further dilution purpose in rheology experiment.

Rheological measurements were carried out on a Bohlin C-VOR rheometer with a cup and bob geometry, with $\sim 3\text{mL}$ samples loaded each time. The bob is made of roughened titanium with a diameter $\sim 14\text{mm}$ and $\sim 0.7\text{mm}$ gap remained when fit into the cup. The temperature was

kept constant $\sim 20 \pm 0.2$ °C with a water bath. Samples were pre-sheared by rotating the bob carefully with hand to avoid shear thickening and to guarantee uniform mixing. A solvent trap was placed to minimize the evaporation during the experiment, but time for each running was still controlled within 20 minutes to guarantee no obvious change in volume fraction. Dynamical stress sweep experiment was carried out then to measure elastic modulus G' (Pa) and viscous modulus G'' (Pa) as a function of sweep stress τ (Pa) with an oscillating frequency ~ 1 Hz. Corresponding dimensionless parameters were obtained by multiplying these three parameters with a factor $L^2 D / kT$ according to theory⁸ and termed as G'^* , G''^* and τ^* . For sweep strain below ~ 0.001 , a linear plateau region was observed for both G'^* and G''^* , termed as $G_0'^*$ and $G_0''^*$ separately. After each experiment, ~ 0.5 mL sample was taken from the cup and placed into a 20mL glass vial and the vial was kept in a ~ 110 °C oven for ~ 12 hours to measure weight loss and calculate volume fraction with uncertainty < 0.005 based on a homopolymer density of $1.055 \text{g}\cdot\text{cm}^{-3}$ for HDC particles and copolymer density of $1.066 \text{g}\cdot\text{cm}^{-3}$ for CDC particles. Rest of the sample in the cup was put back to the original centrifuge tube for further dilution to save particles, residuals on the bob and cup was cleaned with DIW and toluene, and the bob and the cup were rinsed with DIW again before the next experiment. At each step, the samples were diluted with the supernatant extracted from the centrifugation step. Dilution continued until the instrument could no longer measure G' and G'' in the linear region.

Kinetic arrest volume fraction ϕ_g was determined by noting that $G_0'^*$ and $G_0''^*$ are exponential functions of volume fraction. ϕ_g is defined as the volume fraction where $G_0'^* = G_0''^*$. The dimensionless yield stress τ_y^* was at a strain frequency of 1Hz where with increasing stress $G'^* = G''^*$. This stress is taken as that required to lower the relaxation time to $2\pi\tau$. Example plots for determining $G_0'^*$, $G_0''^*$ and τ_y^* is given in Figure 3.1.

3.3 Results and Discussion

3.3.1 Phase Behaviors and Linear Elastic Moduli

Linear dimensionless moduli $G_0'^*$ and $G_0''^*$ were determined for each volume fraction with method shown in Figure 3.1 and are plotted as functions of ϕ in Figure 3.2-3.5 for different conditions. As with other colloidal glasses and gels^{19, 20}, both $G_0'^*$ and $G_0''^*$ are approximately exponential functions of ϕ . By fitting the data to trend lines according to exponential functions and extrapolating the trend lines, the kinetic arrest volume fraction ϕ_g was determined as the point where $G_0'^*=G_0''^*$. This method is based on a Maxwell model where the characteristic relaxation time, t_{relax} , is determined as the point where $G'=G''$, for $t > t_{relax}$ the suspension relaxes at a rate faster than the deformation frequency of 1Hz and is thus liquid-like. For $t < t_{relax}$ the suspension relaxes stress slower than the deformation frequency and thus is solid-like. Similarly, for a certain sweep frequency $f=1\text{Hz}$, $\phi > \phi_g$ sample is solid-like either gel or glass, and the dispersion relaxes and becomes liquid-like when $\phi < \phi_g$. This method defines a kinetic arrest where the suspension has a relaxation time of $\sim 2\pi\tau$.

For CDC particles at ionic strength of 10^{-3}M and a $\text{pH}=4$, $G' > G''$ until very low volume fractions. However, the suspensions lose the linear response region at 1Hz (with an example plot given in the inset of Figure 3.3). For this condition, the sample was diluted little by little until dispersion became liquid-like without the appearance of a convincing linear plateau. For this sample, ϕ_g was defined as the average value of ϕ of last sample showing linear plateau and ϕ of first sample without linear plateau appearing. However, G' is still larger than G'' for the samples showing no linear plateau, so such low moduli might still exist but the instrument cannot make sensible measurements. By extrapolating the trend line, ϕ_g is 0.08. But considering the absence of data in the ϕ range 0.08-0.16 and the fluid-like state of sample for $\phi \sim 0.14$, ϕ_g is determined as

the middle point in the transition region, with details described above. The results of ϕ_g for different particles at different conditions are summarized in Table 3.1.

For ionic strength $[I]=0.001\text{M}$, $\text{pH}=9.0$, both CDC particles and HDC particles have a high kinetic arrest volume fraction ϕ_g , with $\phi_g=0.528$ for CDC and $\phi_g=0.602$ for HDC, respectively. The dimensionless linear moduli for CDC particles and HDC particles at $[I]=0.001\text{M}$ and $\text{pH}\sim 4$ are plotted in Figure 3.3 with resulting ϕ_g values given in Table 3.1. The values for HDC particles are close to the kinetic glass transition point values recently reported with hard dumbbells with similar aspect ratio 1.3^{19} . From the zeta-potential data given in Table 2.1 and the resulting pair potential calculation result given in Figure 2.5, for $[I]=0.001\text{M}$ and $\text{pH}\sim 9.0$ determined by $[\text{NaOH}]=0.001\text{M}$ and $[\text{NaCl}]=0\text{M}$, both CDC and HDC had high surface potentials and, if the surface charge is uniformly distributed over the particle surfaces, we would expect the particles to be effectively hard (i.e., experiencing only volume exclusion interactions). The shapes of the particles are essentially identical. Thus if the particles were hard, we would expect them to have similar glass transition volume fractions. However, there is a significant difference in ϕ_g for HDC (0.602) and CDC (0.528) particles, confirmed in Figure 3.2, which can be attributed to two potential sources.

One reason the particles having different kinetic glass transitions may be because of charge distributions which results in CDC particles interacting as if composed of interpenetrating spheres with different sizes. Swelling the particles with 2VP and inducing a phase separation during polymerization results in chemical anisotropy between the seed and protrusion. With sulfate groups which are cross linked onto the surface of the seed we would not expect massive redistribution of these negatively charged groups away from the seed. Thus under conditions where the P2VP is not protonated, we expect the polystyrene seeds to carry a stronger negative

charge than the protrusion. In the presence of double layers, this will make the seed look larger than the protrusion (i.e., the distance of separation where the repulsive pair potential drops to 1kT will occur at a larger separation for the seeds than for the protrusion. Thus a distribution of charge can give rise to an effective shape anisotropy). While we expect hard dumbbells with a size ratio of 1.3 to have a kinetic glass transition near 0.61, asymmetric hard dicolloids (heterodicolloids) will have a lower kinetic glass transition because they cannot pack as efficiently as the symmetric dumbbells¹⁹.

Considering that the double layer thickness is much smaller than the size of the particle, we would expect that effective shape anisotropy will not contribute significantly to the large difference (~0.10) in the kinetic arrest volume fraction between CDC particles and HDC particles. At the same time, ϕ_g of HDC particles (L/D=1.3) was ~0.60 which was a reasonable value for hard particles with this aspect ratio confirmed by previous report. Based on these two facts, the significant decrease of ϕ_g for CDC particles at the same condition should be attributed to a second source, attractive interactions.

For HDC particles at I=0.5M where the electrostatic interaction was screened out and the truncated van der Waals attraction dominated, ϕ_g is 0.527 (Figure 3.5), essentially the same as ϕ_g of the CDC particles at I=0.001M and pH=9.0 (0.528). At this high ionic strength condition, the negative surface charge of HDC particles is almost fully screened out and a local minimum ~-13kT is obtained in interaction potential predicted in Figure 2.5(b). With this attraction, kinetic arrest volume fraction was decreased from ~0.60 to 0.527. By fitting the exponential function $G_0^{f*} \sim Ae^{b\phi}$ and comparing the two conditions for HDC (I=0.5M and I=0.001M), a lower sensitivity to volume fraction was found for higher ionic strength. As a result we attribute the lower value of $b \approx 29 \ll 100$ to the overwhelming effect of bonding. A high gel volume fraction of

0.527 and small $G_0'^*$ ($<3 \times 10^4$) even at $\phi=0.60$, indicate remarkably weak attractions. These dense suspension rheological results confirm weak attractions observed in the stability of dilute suspension at this pH and ionic strength as shown in state diagram of Figure 2.10 (a). Given that the particles have the same degree of shape anisotropy, by driving the particles to have the same gel volume fraction (HDC at $I=0.5M$ and CDC at $I=0.001M$ and $pH=9.0$), we posit that the particles experience the same strength of pair potential. This hypothesis is based on particle experiencing essentially the same separation dependence of pair potential. At this ionic strength the electrostatic pair potential is fully screened for HDC.

The HDC and CDC particles are considered as being composed of two interpenetrating spheres. For the HDC particles these spheres are identical in chemical composition. Previous studies²⁴ indicate that the HDC particles can be modeled as spheres interacting with their electrostatic surface potentials and a truncated van der Waals attraction indicating that if two particle approach, the spheres in each dicolloid will feel a contact pair potential with a sphere in the second dicolloid with a magnitude of $-13kT$. (See Figure 2.5 (b)). Our assumption is that if the CDC particles experience the same truncated van der Waals isotropic pair potentials, they will display the same gel volume fraction at the same strength of contact potential. Thus we might expect the pair potentials of the CDC particles at an ionic strength of 0.001 to be similar to the HDC particles at 0.5M. This contradicts calculations showing that if the particles have a surface potential of $-66mV$ at an ionic strength of 0.001M, no attractions are expected if the surface charge is uniformly distributed(Figure 2.5(a)). Thus based on expectations of isotropic pair potential we would expect hard interactions with $\phi_g \sim 0.62$ for the CDC particles while we see $\phi_g \sim 0.52$ which corresponds to an effectively isotropic attraction potential with a contact value of $-13kT$.

This contradiction can most easily be resolved if the CDC particles experience an anisotropic pair potential resulting from anisotropically distributed surface charge. This anisotropic charge distribution gives rise to directional attractive interactions for the CDC particles at pH=9.0 and I=0.001M. To understand the essence of this directional attraction, we can assume that charge is uniformly distributed on each of the fused spheres to simplify this problem. A dicolloidal particle with different amount or/and sign of charge on each of the fused spheres, can be treated as a dicolloidal particle with charge multiples located at the center of the particle. For example, a dicolloid composed of one neutral sphere fused with a negatively charge sphere, can be treated as a dicolloid with monopole and dipolar moments located at the particle center. Our hypothesis is that at pH=9, this is the situation for the CDC particles with the result being particle interacting with isotropic repulsion and a superimposed dipolar contribution. A larger degree of charge anisotropy results in a larger dipole moment. The contribution from the dipole can be tuned by changing ionic strength and pH and will be discussed below. If the charge is anisotropically distributed even within each sphere, a more complicated addition of multipolar interactions will be expected.

When the pH was decreased with HDC particles from 9.0 to 4.3 gradually, no obvious change was found in ϕ_g . (The small change from $\phi_g=0.6$ to $\phi_g=0.61$ and lies within experimental uncertainty.) This reflects the near constancy of the expected pair potential where the van der Waals forces will be independent of pH. The average charge on the HDC particles will be independent of pH as shown in the electrophoretic mobility vs. pH data in Figure 2.6. At low volume fraction, the HDC particles started to aggregate at the same ionic strength independent of pH. This confirms the lack of pH-sensitivity in pair potential that is indicated by the weak sensitivity of ϕ_g with result shown in Figure 2.10(a). By fitting the data to a function $G_0'^* \sim Ae^{b\phi}$

in the logarithm-linear panel, the slope $b=112$, also close to the value obtained at $[I]=0.001M$ and $pH\sim 9.0$, again supporting the concept that the HDC particles are not pH-sensitive. To search the universal volume fraction dependencies for elastic modulus with above three conditions with reasonably high ϕ_g , a dimensionless volume fraction $\phi^*=1/(\phi_{max}-\phi)$ is introduced²⁴. A correlation has been seen for hard objects where ϕ_{max} is the maximum volume fraction for random close packing and, as a result, is dependent of particle shape. This correlation has also been shown to collapse data for attractive particles when the attractions are weak (i.e., $\phi_g>0.50$). Based on previous analysis with barrier hopping theory³⁸, elastic moduli are found scale as $G' \propto (\phi_{max} - \phi)^{-4}$. Here ϕ_{max} were determined based on this dependency with fixed exponent at 4 and to obtain best collapse of data for these three low ionic strength conditions, which are 0.663 for HDC at $pH=9$ and 0.665 for HDC at $pH=4.3$ and 0.595 for CDC at $pH=9$ separately. The collapse of the data is shown in Figure 3.6.

At this lower pH the CDC particles show a much stronger tendency to enter a solid-like state with $\phi_g\sim 0.15$. For all the $\phi>0.148$, a space filling percolating network were formed. For $\phi<\phi_g$, the aggregates formed and settled instead of forming space filling network. This behavior indicates that the samples form a cluster phase. This cluster phase is first observed at volume fractions less than 0.001 and clusters remain discrete up to volume fraction near 0.15 where the clusters percolate to form a space filling gel. As a result we conclude that attractions are sufficiently strong to localize particles at much lower volume fractions but that the resulting structures are dense non-percolating aggregates. As seen in the phase diagram in Fig 2.10(b), clusters were seen at $\phi\sim 0.001$.

There are three reasons which might explain the formation of a cluster phase and gelation at a low volume fraction. First, lowering the pH will result in protonation of the P2VP. As a

result, one might expect the p2VP to become hydrophilic and to swell resulting in a volume expansion. This would result in an effective volume fraction that is substantially larger than the core particles resulting in glass formation by crowding at a much lower mass fraction of polymer that would be expected for the particles remain unswollen. This mechanism is the basic principle to produce microgels³⁹. We discount this mechanism because as the pH was decreased further, at $\phi \sim 0.30$, the suspensions reentered a fluid-like state. Thus, even though the 2VP will have a larger degree of protonation and thus swelling at this lower pH, aggregates enhanced rheological properties are not observed. By measuring hydrodynamic diameters of the particles with DLS, this possibility was excluded further by finding out that $D \approx 1040\text{nm}$ for $\text{pH}=7$ where particles are stable with negative surface charge and $D \approx 1116\text{nm}$ for $\text{pH}=3$ where particles are stable with a positive surface charge. The changes in diameter are within the experimental uncertainty. Finally, the observation of cluster phases at low volume fractions indicates the particles feel attractions. As a result we conclude that gels seen at a volume fraction above 0.15 are the result of strong attractions.

The second reason the particles aggregate is then that we are working near the point of zero charge for the particles and the attractions arise from van der Waals interactions. If the charge were uniformly distributed over the particle surface, we would expect an isotropic van der Waals attraction that is truncated due the absorption of the surfactant. With the surface fully coated with C_{12}E_6 , truncated van der Waals attraction could only reach a minimum $\sim -15kT$.

If the CDC particles experience an isotropic truncated van der Waals attraction, we expect the gels formed to be similar to those produced from fully screened particles as would be expected for HDC particle at $\text{pH}=9$ at a high ionic strength. As indicated in Table 3.1 and Figures 3.5, this expectation is not met. If the particles experience interactions with a similar

degree of anisotropy as the CDC particles at pH=9 we would anticipate a ϕ_g to be similar to CDC particles at pH=9 at high ionic strength. In both cases at pH~9, and an ionic strength of 0.5M, both CDC and HDC particles had gel volume fractions substantially above that seen for the CDC particles at pH~4.6. In addition, neither of these suspensions showed the existence of a cluster phase- i.e., below the gel volume fraction, the particles settled essentially as individual particles while below the ϕ_g for the CDC particles at pH=4.6 clusters settled rapidly.

A third explanation for the cluster phase and the strong attractions giving rise to a low gel volume fraction for the CDC particles at pH=4.3 is anisotropy in particle interaction energy. We envision two different mechanisms for producing that anisotropy. First, due to changes in polarity of the P2VP rich regions, the particles may not be fully coated with surfactant. It is difficult to exclude this possibility even though we fully coated the particles at high pH. However, at low pH, hydrophilicity of the surface might vary between the polystyrene and P2VP rich regions resulting in surfactant dissociation from the 2VP rich protrusion. Partially coated particles may aggregate from but anisotropic van der Waals attractions. One might expect this mechanism to be observed at lower pH. However at pH=3.7, the average particle charge is sufficiently positive to restabilize the particles and this anisotropy in attractions cannot be probed.

A second potential source of anisotropy lies in dipolar interactions. Strong electrostatic attraction ($W_{\min} < -100kT$) could be achieved with anisotropic charge distribution which was shown in Figure 2.7, resulting in a low density gel, as predicted with simulation³⁵. Although we cannot exclude the second possibility or confirm the third explanation with only linear elasticity results, the presence of a strong attractions, the existence of a cluster phase at low volume fractions, and gels whose mechanical properties are different from those seen with fully screened electrostatic interactions as indicated by the large values of G_0^* (up to 10^6) at volume fractions

of 0.3, suggested the particles experienced substantially different pair potentials than do the HDC particles.

This potential might be the result of an effective dipole moment and an effective monopole located in the center of the particle as discussed above for CDC at $I=0.001M$ and $pH=9.0$. At this medium pH near i.e.p., this effective monopole is near zero supplying no electrostatic repulsion but the dipolar interaction is enhanced significantly, decreasing ϕ_g in a large degree. By applying function $G_0'^* \sim Ae^{b\phi}$, b is $\sim 44 \ll 100$, the value for HDC particles at $[I]=0.001M$, denoting this bonding effect, although little theory has been developed to enable us to understand this volume fraction dependence.

To understand better the gelation process due to truncated van der Waals attraction, results for dimensionless linear moduli of both particles at high ionic strength $[I]=0.5M$ was given in Figure 3.4 with ϕ_g summarized in Table 3.1. Here pH for CDC particles was controlled strictly to ~ 9.0 due to the pH-sensitivity, but not for HDC particles which were proved to be weakly dependent on pH. As discussed above, at this high ionic strength condition, the negative surface charge is almost fully screened out and a local minimum $\sim -13kT$ is obtained in interaction potential predicted in Figure 2.5(b) for HDC particles which can be treated as shape anisotropic particles with isotropic attraction.

By working at the same high ionic strength condition $[I]=0.5M$, with $pH \sim 9.0$, we ensured that on the CDC particles the pyridine groups are not protonated but the high ionic strengths ensured electrostatic forces are fully screened and van der Waals attractions would dominate particle interactions. A much larger decrease of ϕ_g (from 0.528 to 0.205) was observed than that of HDC particles (from 0.614 to 0.527), together with large $G_0'^* = 8 \times 10^5$ at $\phi = 0.292$. The low kinetic arrest volume fraction and large elastic moduli for gel states denote an underlying strong

attraction already proved by the stability of dilute sample shown in state diagram Figure 2.10 (b). Nevertheless, compared to the low density gel formed by tuning pH to the range of i.e.p other than increasing ionic strength discussed above, this low density gel still had a larger gel volume fraction 0.205 (>0.148), and obviously smaller $G_0'^*$ for samples with $\phi \sim 0.20$. In another aspect, by fitting the function $G_0'^* \sim Ae^{b\phi}$ and comparing these two conditions with ϕ_g slightly different, $b=58$ (>44 for $[I]=0.001M$ and $pH=4.6$), meaning a larger volume fraction sensitivity of elastic modulus. This is understood as arising from a slightly weaker effect of bonding, possibly a less enhanced dipolar interaction introduced by a smaller effective dipole moment for the CDC particles at $pH=9$ and $I=0.5M$ compared to $I=0.001M$ and $pH=4.6$ condition. As discussed above, CDC particles are treated as dicolloids with an effective dipole moment and an effective point charge in the center. So changing pH to i.e.p. is more efficient to introduce strong directional attraction as this can change the magnitude of the dipolar interaction efficiently, but increasing ionic strength is less efficient because it controls the isotropic pair potential part rather than changing dipolar interaction significantly.

In another aspect, substantial difference have been obtained with HDC and CDC particles at this high ionic strength, including gel volume fraction, elastic moduli and the multiple yielding behaviors which will be discussed in the next subsection. Previous theoretical study²² has predicted that minor change in strength of attraction might result in a prominent change in gel volume fraction. Based on this argument, difference in surface potential vs. ionic strength for CDC and HDC particles reported in Chapter 2 denoted that chemical composition difference would result in different interaction and different gelation conditions. One significant thing to notice with the chemical composition is that P2VP was not only a main composition in the protrusion but also incorporated into the seed part. So although the seed part of the particles is

negatively charged at high pH with sulfate group bonded to the network, poly-2VP could make the particles less stable and more sensitive to ionic strength change at high pH due to smaller amount of negative charge. This was confirmed by a re-entrance into fluid state by decreasing pH from 4.6 to 3.7 for CDC particles at $\phi \sim 0.30$ discussed below. These results can be understood as an increase in magnitude of the directional attractions seen at pH=9 and I=0.001M with increasing ionic strength.

In decreasing the pH from 4.6 to 3.7 CDC particles became positively charged with ϕ_g increasing to a ~ 0.512 and $G_0'^*$ decreased to a much smaller order again, shown in table 3.1 and Figure 3.5 separately. At pH=3.7 the sulfate groups cross linked into the seed particle retain their negative charge. The average charge on the particles at this pH indicates that the P2VP is sufficiently charged to counteract these negative charges. If the P2VP is only contained in the protrusion, the particle dipole moment would be larger at pH=3.7 than at pH= 4.6 and even greater aggregation would be expected. Instead the particle gelation behavior is similar to that observed at pH=9 where the CDC particles have a large ϕ_g . As a result, we conclude that the P2VP is distributed over the entire particle surface and at pH=3.7 is sufficiently charged to render the seed part neutral or positive thus greatly reducing the dipolar character of the pair potential. As a direct consequence, the gel volume fraction is dramatically increased over that seen at pH=4.6

These results demonstrate that the CDC particles are amphoteric-they change sign of their charge with varying pH. The distribution of the charge is more difficult to determine. There are, as yet, no chemical measures of P2VP or sulfate group distribution over the particle surfaces. Never-the-less, it is only near the isoelectric point that the particles show signs of strong attraction as would be expected for van der Waals interactions in the classical DLVO theory of

colloid stability. We suggest this picture is incomplete. There are two major pieces of evidence for this suggestion. First, if the attractions at pH=4.6 were due to van der Waals interactions, the gels should behave in a similar manner when fully charged but at high ionic strength. As seen for both CDC and HDC particles at pH=9 and I=0.5M, this is not the case. The surfactant coating on the particle surfaces has a sufficient extent to limit the strength of attraction such that gel volume fractions are greatly increased over that seen at pH=4.6. Secondly, for these high ionic strengths, and at low ionic strength at pH=3.7 and pH=9, the suspensions gel without prior clumping. The clumping seen at pH=4.6 indicates qualitatively different pair potentials are acting under these conditions. Finally at pH=9 at I=0.5M, CDC particle gels are produced at a volume fraction substantially lower than that observed for HDC particles. This, in and of itself, might reflect subtle differences in magnitude of the electrostatic potential. However, at this ionic strength these effects are sufficiently screened that we consider the stronger attractions seen in the CDC particles under these conditions than in the HDC particles to arise from differences in surfactant coating, or differences in Hamaker constant due to chemical difference in composition of seed and protrusion parts of the CDC particles. In addition these added attractions may arise from weak variations in charge distribution between the seed and protrusion portions of the CDC particles that can be viewed as the source of an effective dipolar interaction and an effective isotropic interaction among those dicolloids tunable by changing pH or ionic strength.

3.3.2 Yield Stresses and Multiple Yielding Events

The results of dimensionless yield stresses τ_y^* were plotted as functions of ϕ in Figures 3.7-3.9 for different conditions described above. Considering the complex multiple yielding events discussed below, τ_y^* was determined with the stress sweep experiment data to locate the stress where $G'^*=G''^*$ similar in previous study⁴⁰ to obtain a single value. With data fit to a

exponential equation $\tau_y^* \sim Ae^{b\phi}$, similar volume fraction dependence as $G_0'^*$ was found for all the conditions. Generally the parameter A tracks the location of ϕ_g , and for samples with reasonably close ϕ_g , the relative volume fraction sensitive of τ_y^* is displayed in b. From these data we conclude that the volume fraction dependencies of τ_y^* do not offer great insight above that carried by G_0' and G_0'' into the nature of the interaction potentials of the particles.

On the other hand, the results of dynamic stress sweep experiments are shown in Figures 3.10-3.12 provide insights. As mentioned in the introduction, previous studies suggest single yielding is observed for shape anisotropic particles experiencing isotropic interactions in plastic glasses (centers of mass are localized but the particles continue to rotationally diffuse) and when rotational and center of mass diffusion are strongly coupled. This happens at high volume fraction for volume exclusion interactions, and when the particles are strongly attractive. This behavior is repeated here where we see the HDC particles had double yielding at pH=9 (Figure 3.10 (a) (b)) and pH~4 (Figure 3.11(a) (b)) for I=0.001M. The shoulder in the decay of G'^* and the double maxima in G''^* are characteristics of two yielding events. The loss of multiple constraints is seen for pH=9 at I=0.5M (Figure 3.12 (a) (b)). Here a single decay in G'^* and the loss of a maximum in G''^* indicate rotational and center of mass diffusion are strongly coupled.

Yielding in suspensions of CDC particles is qualitatively different than that seen in the HDC particles. Double yielding is seen under all ionic strength and pH conditions. This is expected at pH=9 at I=0.001M where the particles experience bonding due to weak attraction and coupled rotational and center of mass diffusion (Figure 3.10 (c) (d)). At pH=4.6 and I=0.001 (Figure 3.11 (c) (d)), the gel volume fraction is well below that where caging constrains give rise to double yielding in suspensions of volume exclusion attractive particles. Never-the-less, double yielding is clearly evident up to the highest volume fraction where it may be lost. This

behavior is not understood in terms of rotational and center of mass diffusion for particles experiencing isotropic interactions. The same is true at $\text{pH}=9$ and $I=0.5\text{M}$ (Figure 3.12(c) (d)). Again double yielding is observed from the gel point up to the highest volume fractions where it may be lost. In contrast the HDC particles do not show double yielding as the attractions are sufficiently strong so as to couple rotational and center of mass diffusion. The lower gel volume fraction indicates and even stronger attraction between the CDC particles under these conditions and yet double yielding is observed (stress sweep experiment results with parameters not scaled for represented volume fractions are shown in Figure 3.13). On the basis of this evidence, we conclude that the pair potentials felt by the CDC particles are qualitatively different from those experienced by the HDC particles.

The origin of double yielding under conditions where the CDC particles are strongly attractive is uncertain. We hypothesize that it arises from two types of interactions, the first is stretching of clumps of particles that are aggregated roughly in side to side and head to tail configurations. At a sufficient stress these bonds will unravel and particles will tend to declump and form strings where the particles are still bonded through directional interactions. At a sufficiently large stress the remaining directional interactions will yield. In this hypothesis, the particles are in bonded states-short range interactions hold the particles together. However, these bonds have a dipolar character at $\text{pH}\sim 4$ and $I=0.001\text{M}$ or at $\text{pH}\sim 9$ and $I=0.5\text{M}$, such that yielding requires stretching and then yielding of clumps. However coupling of double yields for $\text{pH}\sim 4$ and $I=0.001\text{M}$ at high volume fractions which was absent for $\text{pH}=9$ and $I=0.5\text{M}$ condition denotes the difference in the magnitude of directional attraction for these two conditions.

3.4 Conclusion

Here the rheological properties have been explored with both HDC particles and CDC particles. By studying volume fraction dependence of linear moduli and kinetic arrest volume fraction at different pH and ionic strength conditions, HDC particles were proved to be non pH-sensitive at $[I]=0.001M$ with a high glass transition volume fraction, and weakly attractive at high ionic strength $[I]=0.5M$. This was confirmed with volume fraction dependence of dimensionless yield stress and multiple yielding behavior. At $[I]=0.001M$, HDC showed double yielding as hard shape anisotropic particles undergoing breakage of rotational confinement and CM caging effect. But for $[I]=0.5M$, loss of this double yielding denoted strong coupling of different constrains due to attraction or loss of some constrains due to lowering volume fraction.

For CDC particles, were proved to be directional weakly attractive at $pH=9.0$ and $[I]=0.001M$, with slightly anisotropic charge distribution. At $[I]=0.001M$. ϕ_g was found to be nonmonotonic function of pH with a very small value at medium pH but much larger values for high pH and low pH, showing behavior expected for their amphoteric nature as observed with electrophoresis. Two different kinds of strong flocculated gel could be made by increasing ionic strength at a high pH and tuning pH to a medium value at low ionic strength. The resulting gel volume fractions, volume fraction dependencies of $G_0'^*$ and τ_y^* , and multiple yielding behaviors all indicate that the attractions giving rise to the gels are not due to deep van der Waals attractions but arise from anisotropic attractions.

One of the essential conclusions of this work lies in the similarity of gels formed from particles experiencing isotropic interaction potentials and those experiencing anisotropic interaction potentials. The gel points will depend on the average strength of attraction. The volume fraction dependencies of the yield stresses and elastic moduli in the gelled state are largely dependent on the average strength of attraction. It is only in the low volume fraction

clumping and in the yielding of these clumps that the presence of anisotropy may be clearly visible. Further work is clearly needed to confirm these preliminary studies.

3.5 Tables and Figures

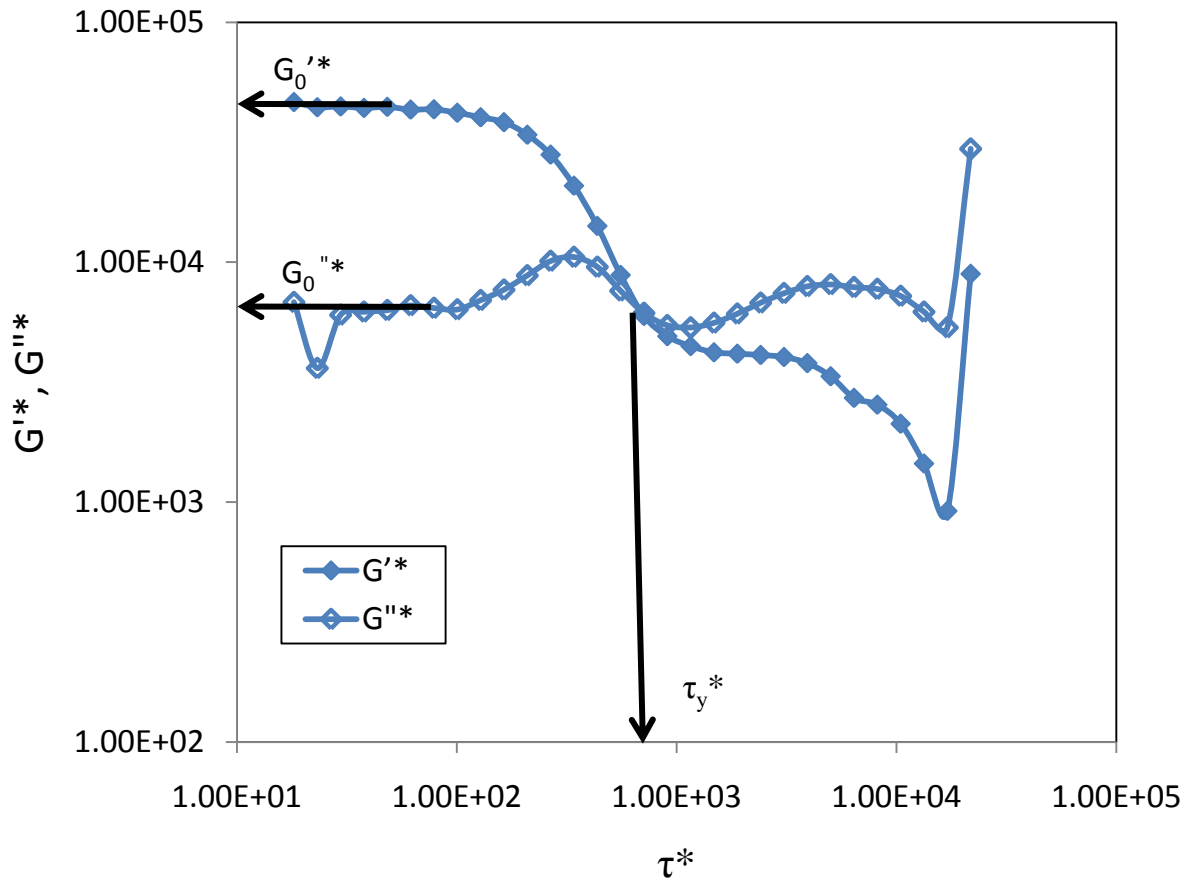


Figure 3.1. Example plot for showing the method to determine $G_0'^*$, $G_0''^*$ and τ_y^* .

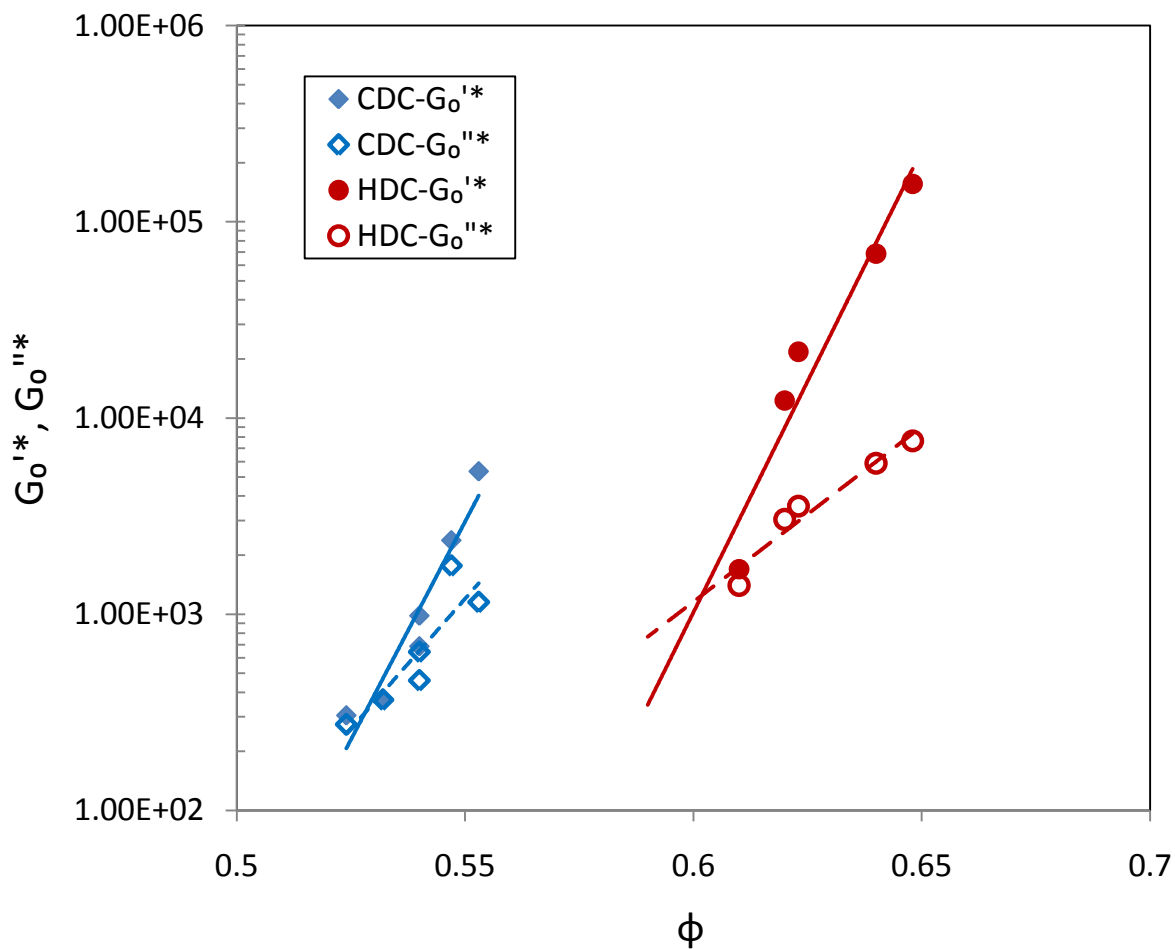


Figure 3.2. Dimensionless linear elastic modulus $G_0'^*$ (closed) and viscous modulus $G_0''^*$ (open) as functions of volume fraction for CDC particles (diamonds) and HDC particles (circles) at pH=9, I=0.001M. And trend lines according to exponential functions were used to fit the data of $G_0'^*$ (solid line) and $G_0''^*$ (dashed line).

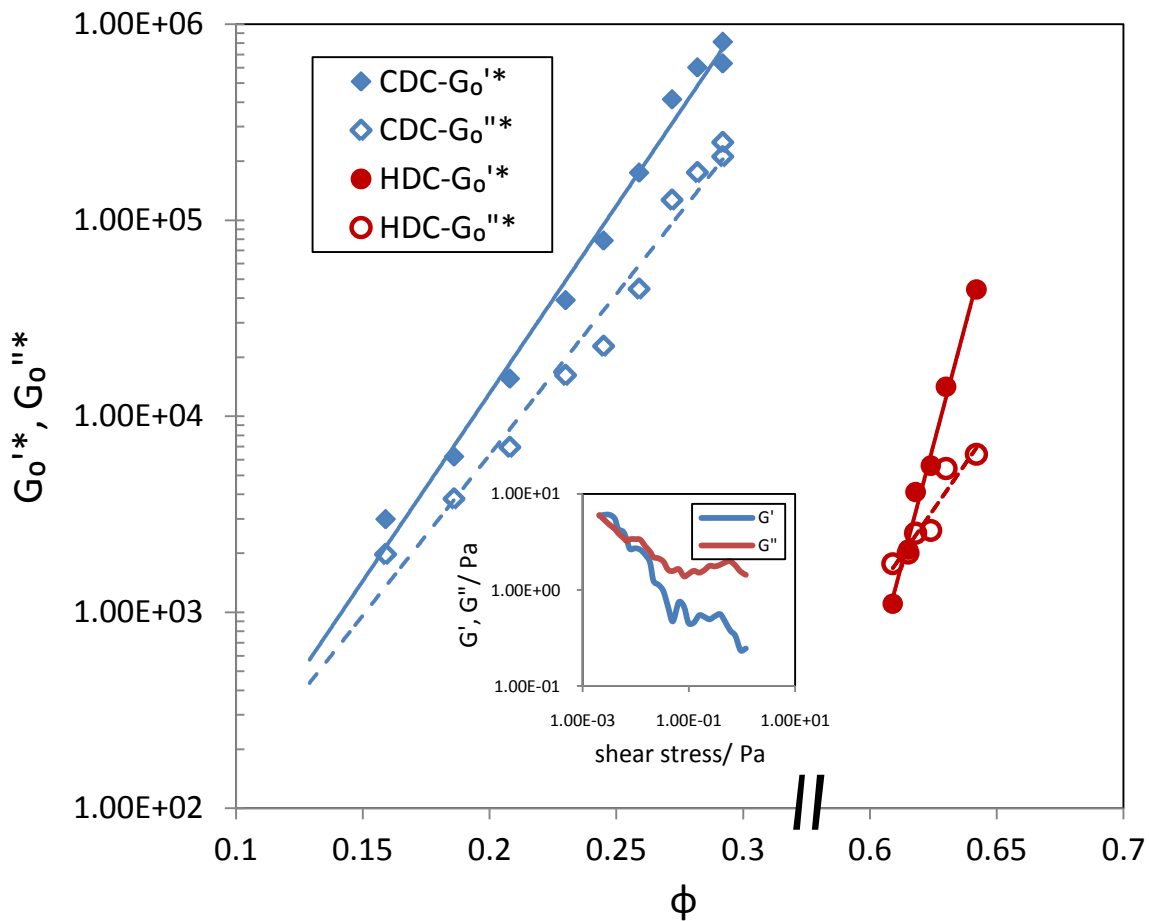


Figure 3.3. Dimensionless linear elastic modulus $G_0'*$ (closed) and viscous modulus $G_0''*$ (open) as a function of volume fraction for CDC particles (diamonds) and HDC particles (circles) at medium pH (near 4), $I=0.001M$. And trend lines according to exponential functions were used to fit the data of $G_0'*$ (solid line) and $G_0''*$ (dashed line). Inset is the example of stress sweep experiment for CDC particles in the transition volume fraction range between gel and fluid state with $\phi=0.136$.

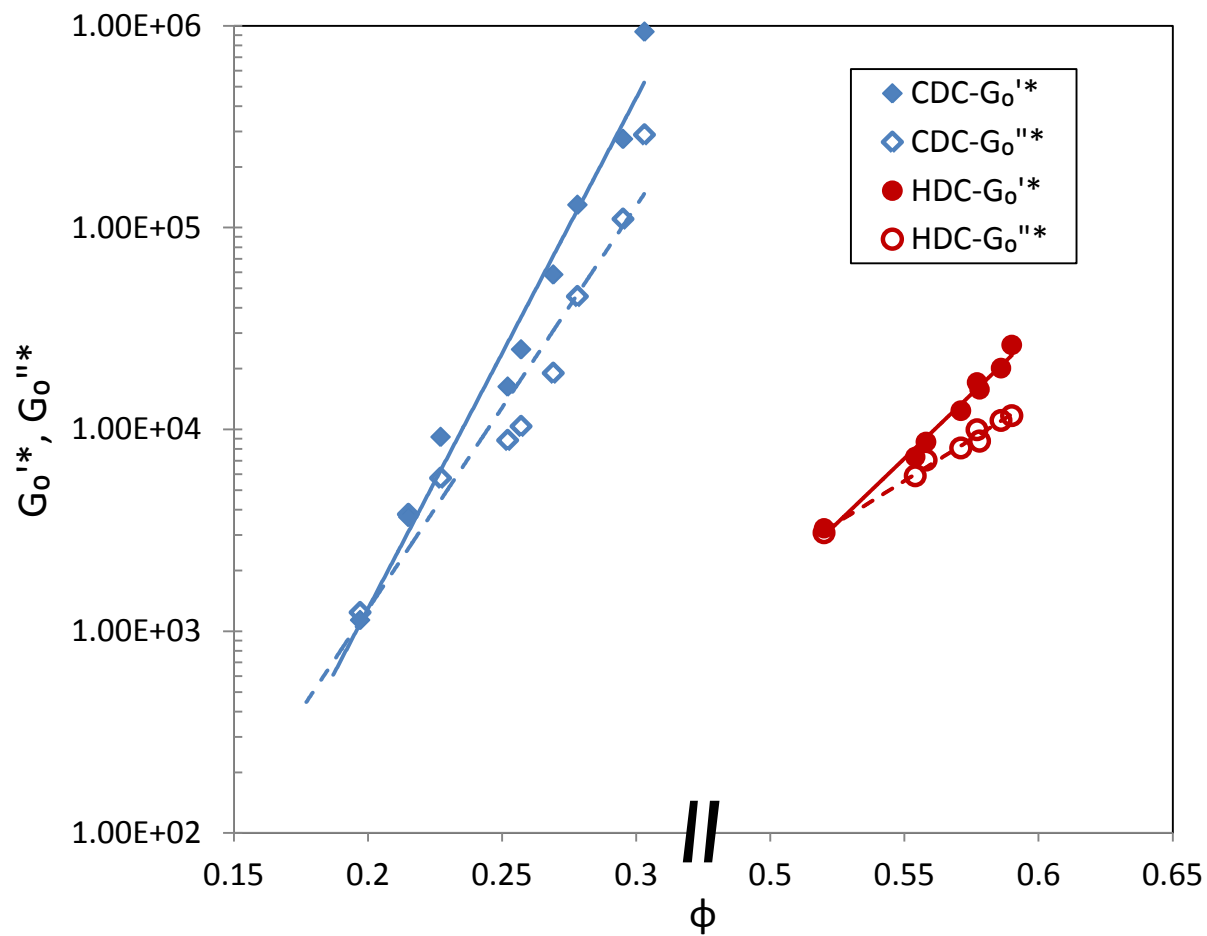


Figure 3.4. Dimensionless linear elastic modulus G_0' (closed) and viscous modulus G_0'' (open) as a function of volume fraction for CDC particles (diamonds) and HDC particles (circles) at high salt concentration $I=0.5M$, with high pH (near 9) guaranteed CDC particles. And trend lines according to exponential functions were used to fit the data of G_0' (solid line) and G_0'' (dashed line).

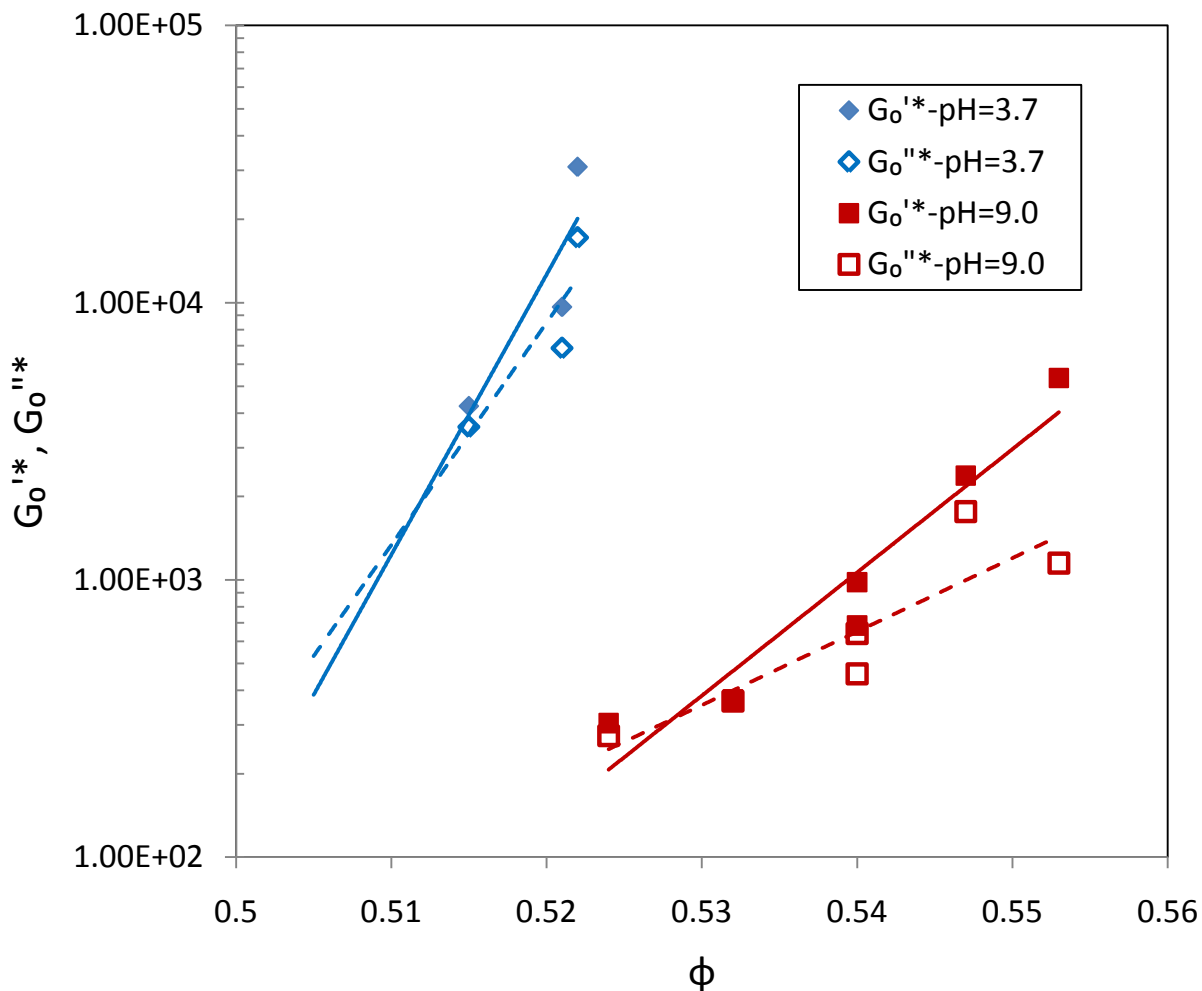


Figure 3.5. Dimensionless elastic modulus (closed) and viscous modulus (open) as a function of volume fraction for positively charged CDC particles at pH=3.7 (diamonds) and negatively charged CDC particles at pH=9 (squares). And trend lines according to exponential functions were used to fit the data of $G_0'^*$ (solid line) and $G_0''^*$ (dashed line). Similarity in high gel volume fractions at high pH and low pH and aggregation at medium pH prove that the particles are amphoteric when varying pH.

Table 3.1 Kinetic arrest volume fractions ϕ_g for different particles at different conditions

Particle Type	Surface charge type	pH	[I]/M	ϕ_g
CDC	Negative	~9.0	0.001	0.528
CDC	Neutral	~4.6	0.001	0.148
CDC	Negative	~9.0	0.5	0.202
CDC	Positive	~3.7	0.001	0.512
HDC	Negative	~9.0	0.001	0.602
HDC	Negative	~4.3	0.001	0.614
HDC	Negative	~9.0	0.5	0.527

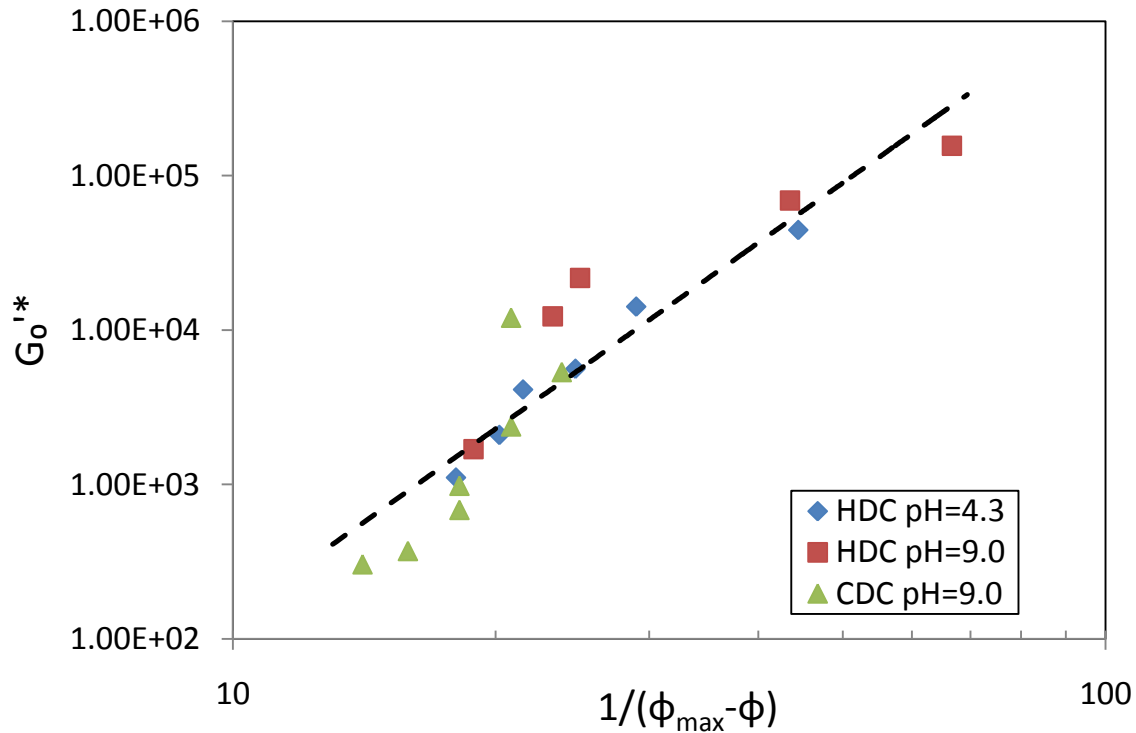


Figure 3.6. Collapse of $G_0'^*$ for three conditions at $I=0.001M$ based on a dimensionless volume fraction $\phi^*=1/(\phi_{max}-\phi)$. The data are fitted to dotted line showing $G_0'^* \propto (\phi_{max} - \phi)^{-4}$.

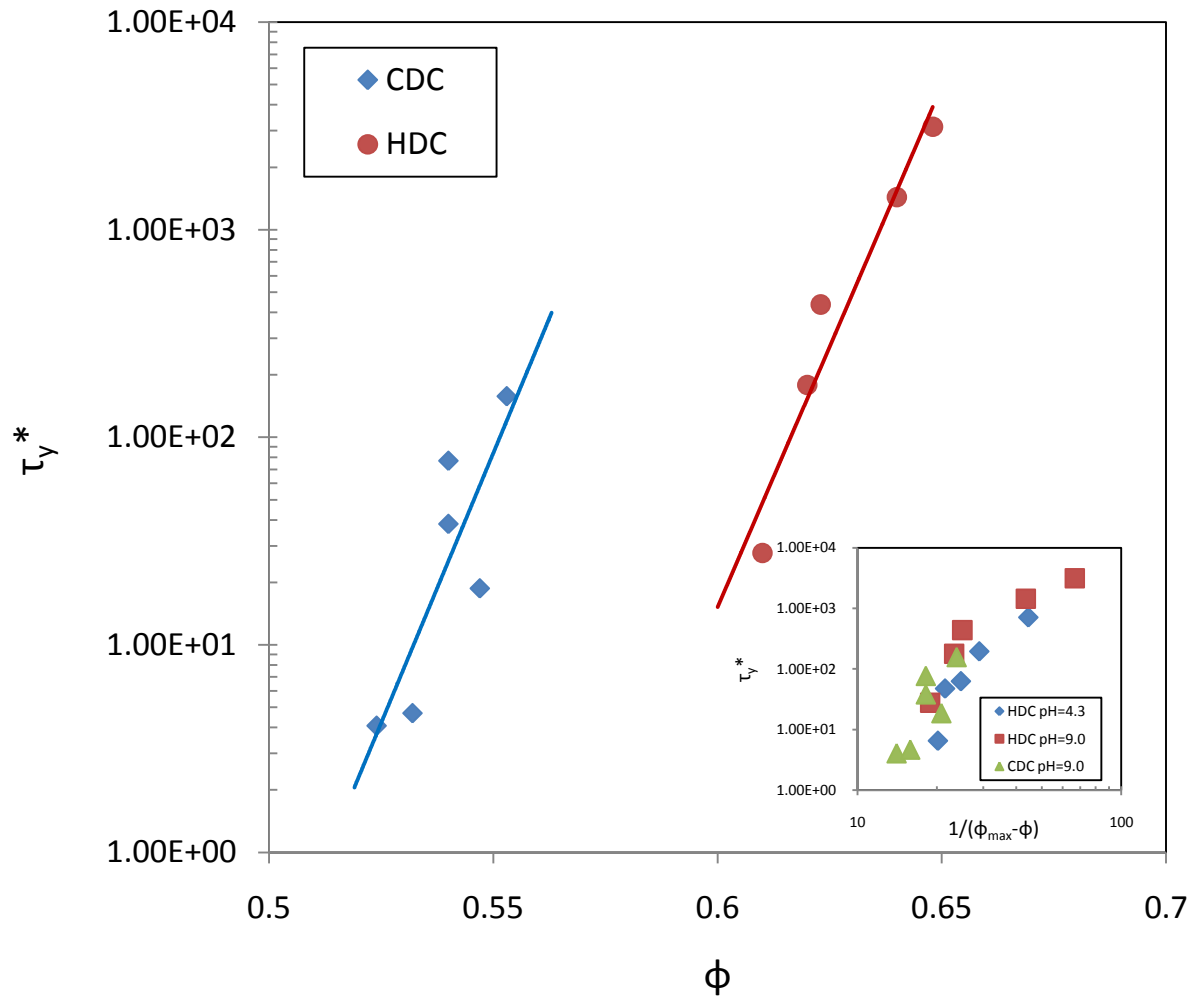


Figure 3.7. Dimensionless yield stress τ_y^* as a function of volume fraction for CDC particles (diamonds) and HDC particles (circles) at pH=9 and I=0.001M. And trend lines according to exponential functions were used to fit the data. Inset is collapse of τ_y^* for three conditions at I=0.001M based on a dimensionless volume fraction $\phi^*=1/(\phi_{max}-\phi)$ with same parameters ϕ_{max} used as in Figure 3.6.

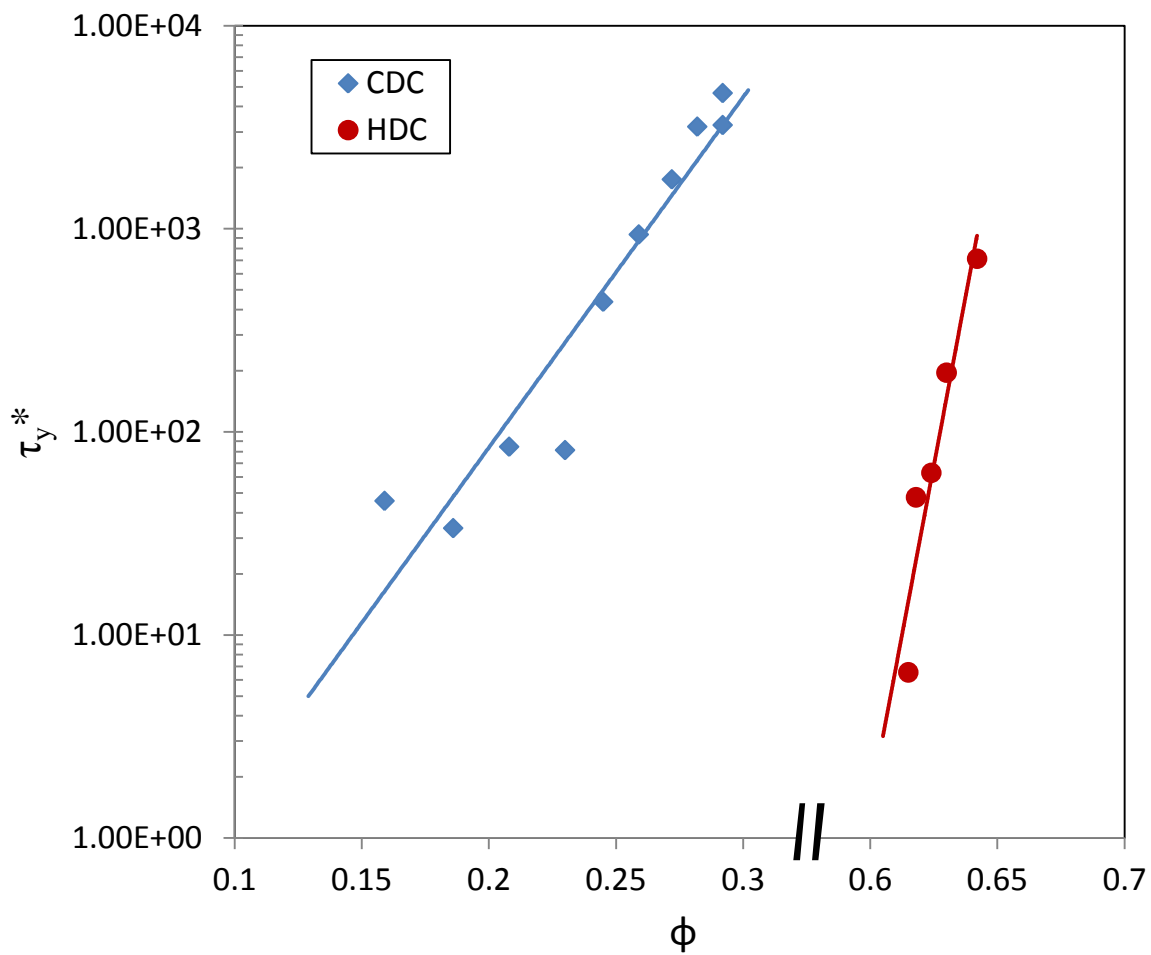


Figure 3.8. Dimensionless yield stress τ_y^* as a function of volume fraction for CDC particles (diamonds) and HDC particles (circles) at medium pH (near 4), $I=0.001M$. And trend lines according to exponential functions were used to fit the data.

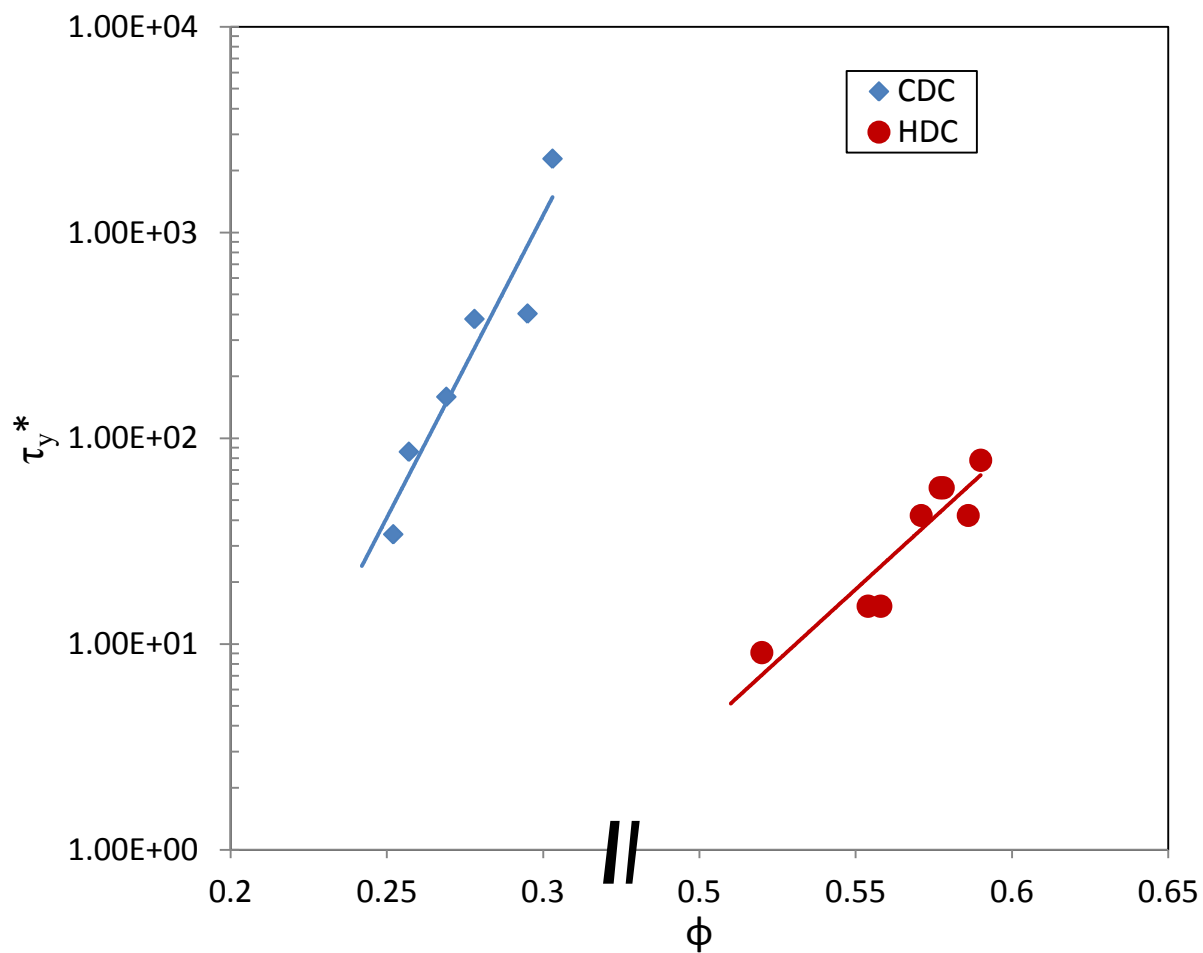


Figure 3.9. Dimensionless yield stress τ_y^* as a function of volume fraction for CDC particles (diamonds) and HDC particles (circles) at high salt concentration $I=0.5M$, with high pH (near 9) guaranteed CDC particles. And trend lines according to exponential functions were used to fit the data.

(a)

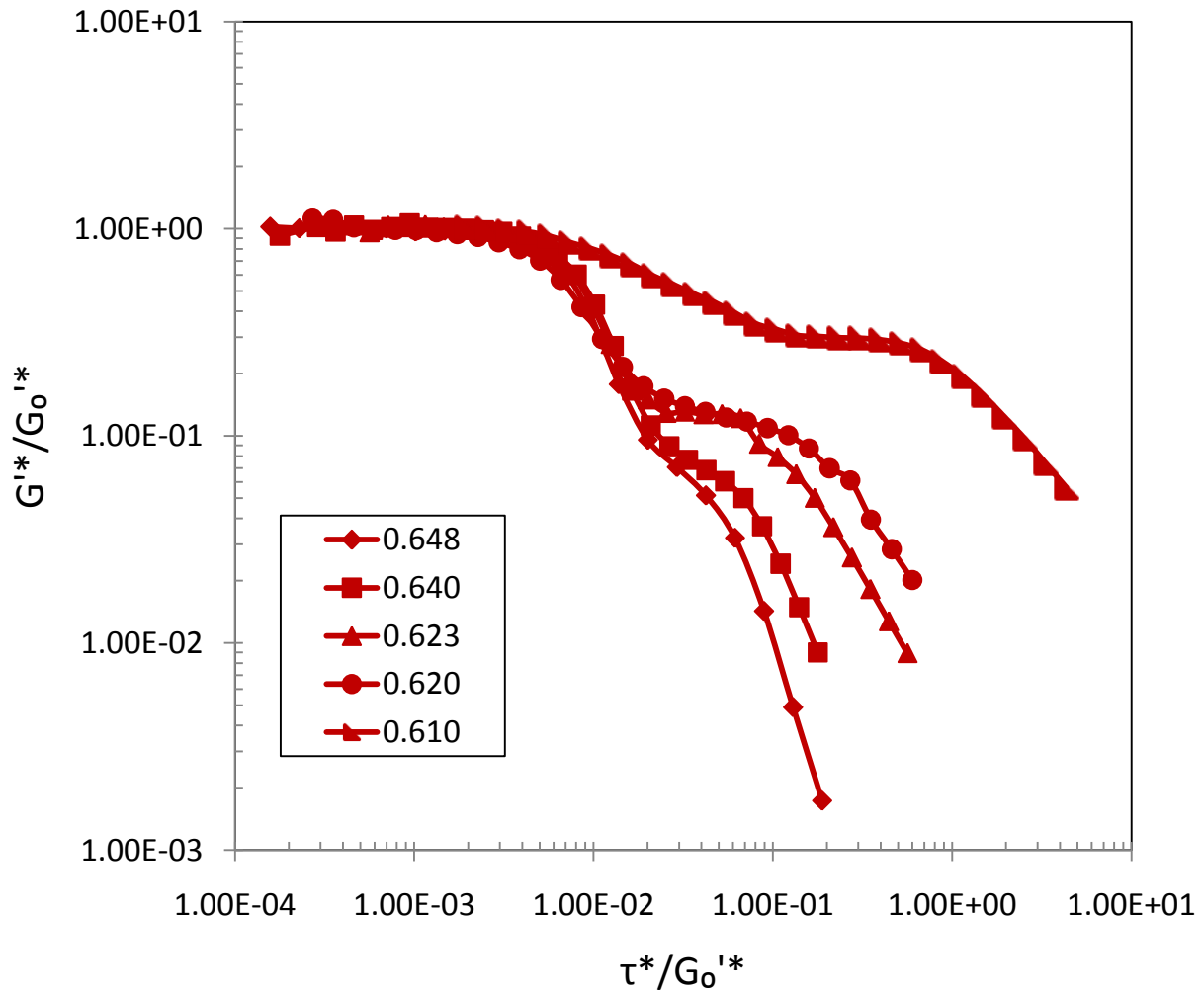


Figure 3.10. (continued on next page)

(b)

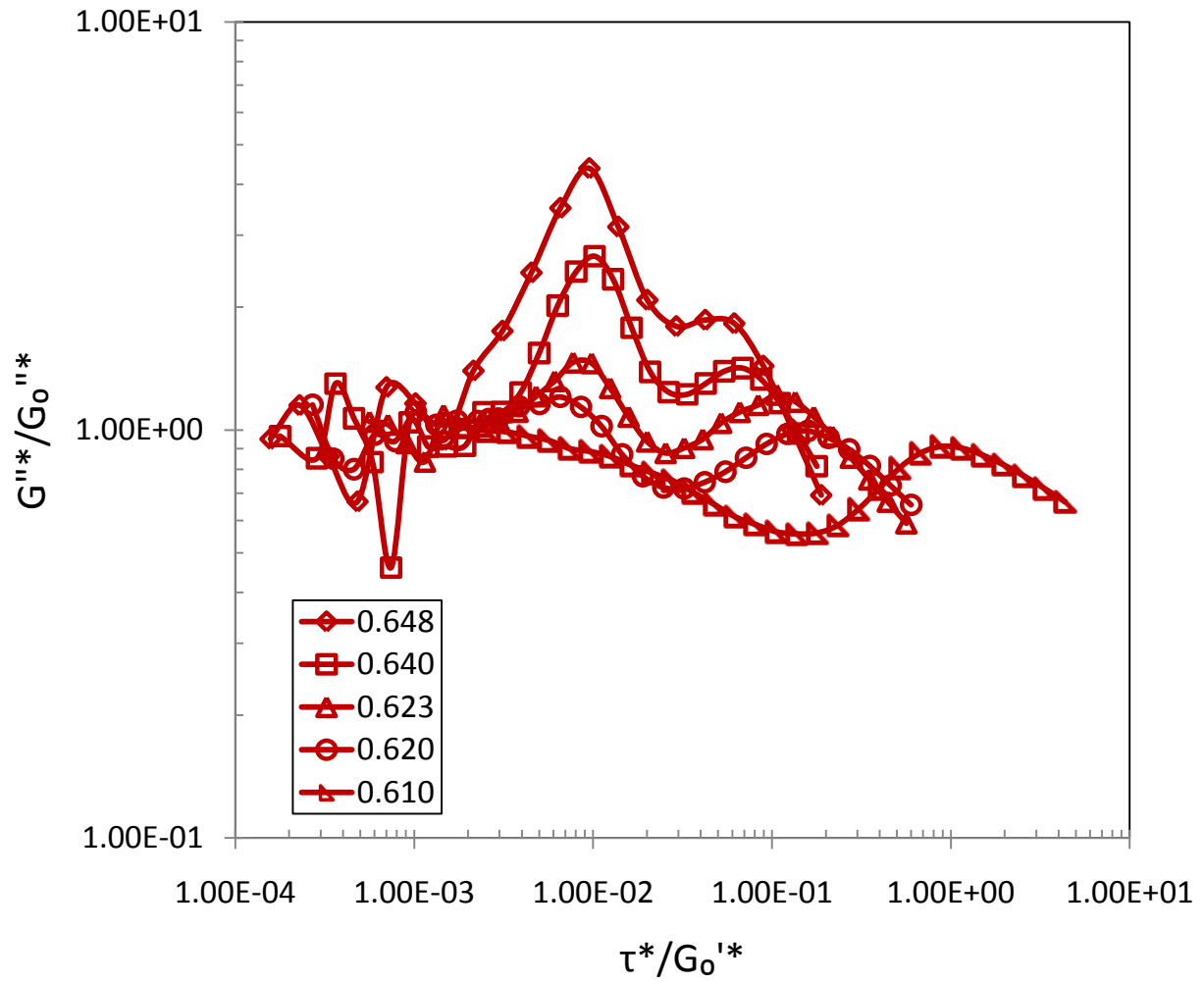


Figure 3.10. (continued on next page)

(c)

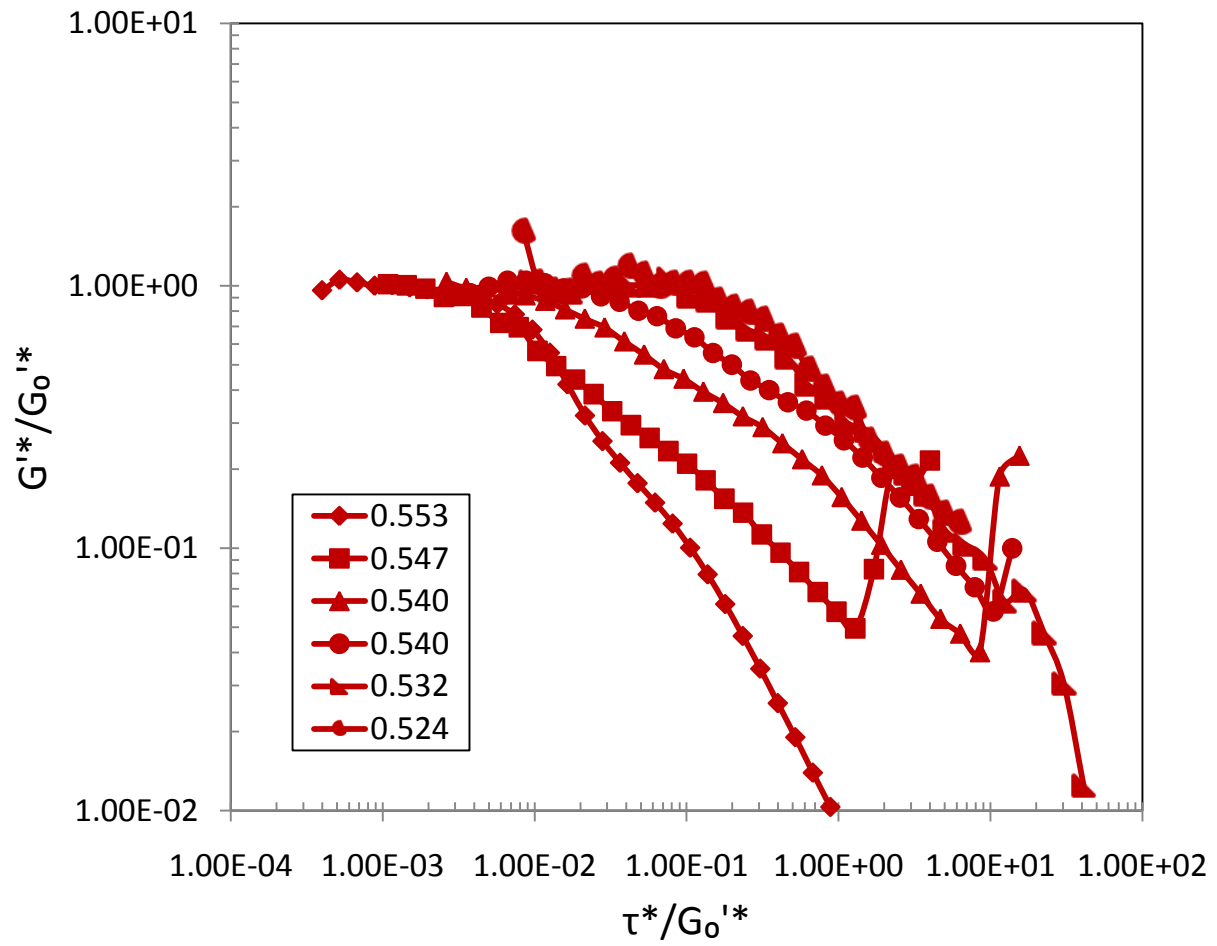


Figure 3.10. (continued on next page)

(d)

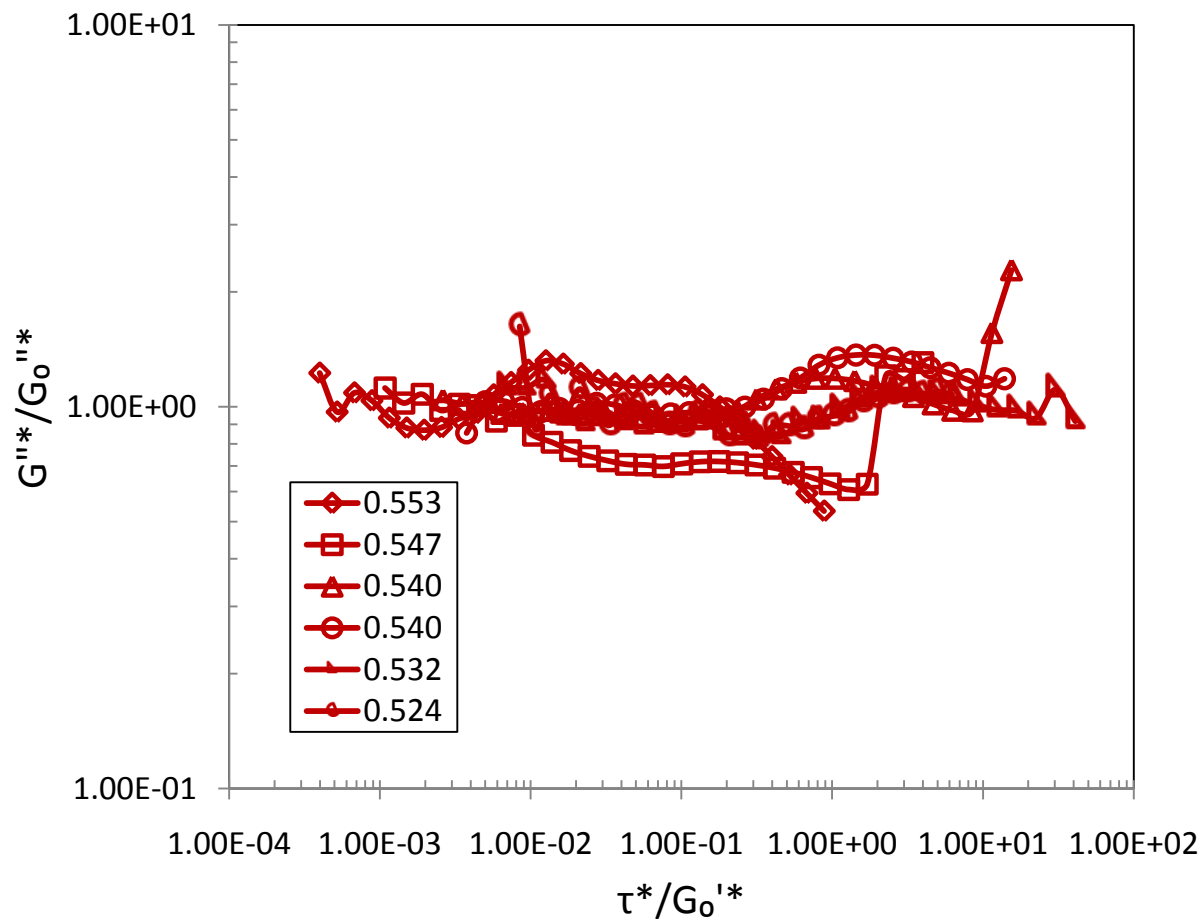


Figure 3.10. Dynamic stress sweeps for different volume fractions at pH=9, I=0.001M for HDC particles (a) (b) and CDC particles (c) (d). G'^* have been scaled on the plateau values $G_0'^*$ (a) (c) (closed), and G''^* have been scaled on the plateau values $G_0''^*$ (b) (d) (open). Dimensionless stress τ^* have been scaled on the plateau values $G_0'^*$. All the samples show double yield behavior.

(a)

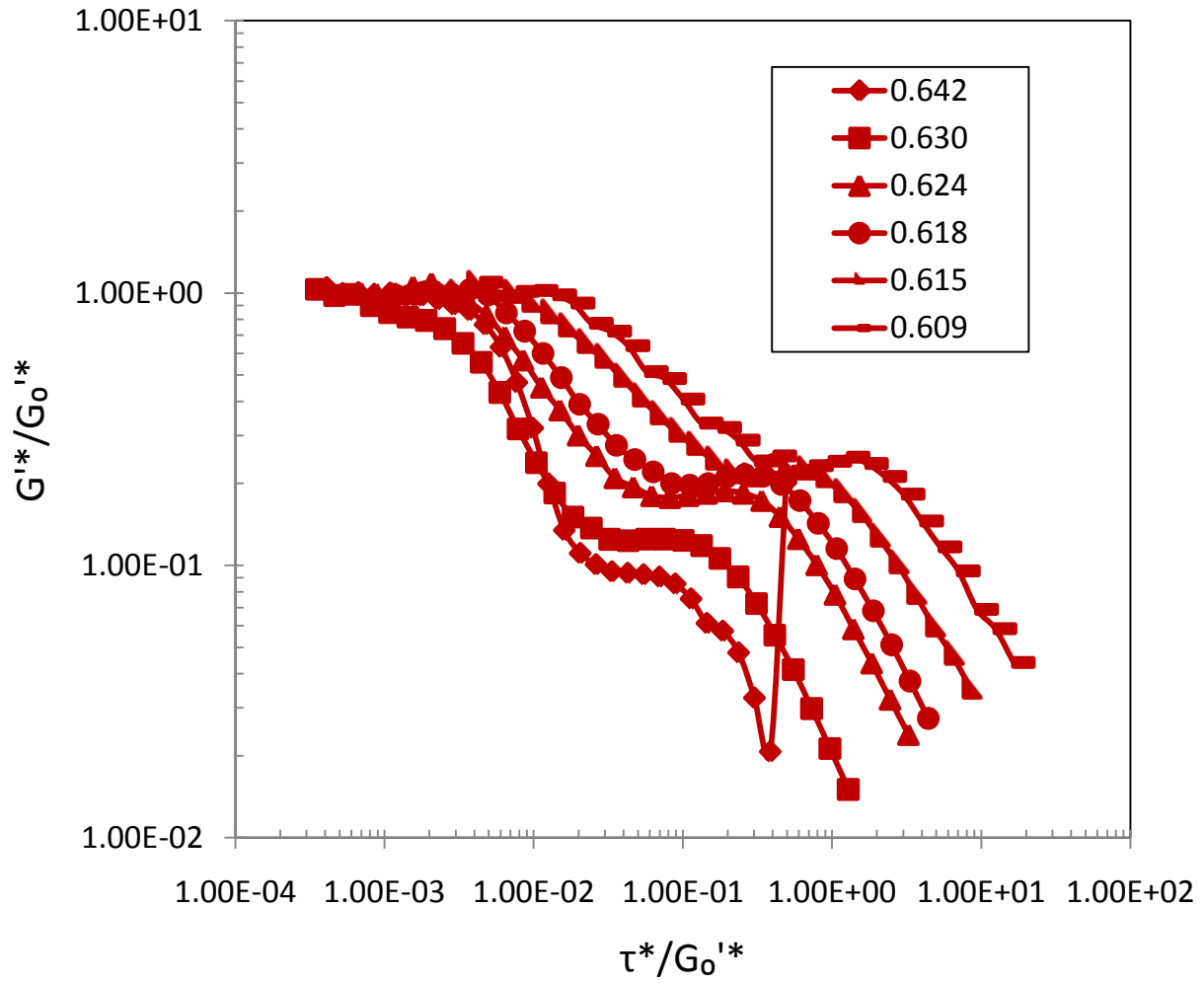


Figure 3.11. (continued on next page)

(b)

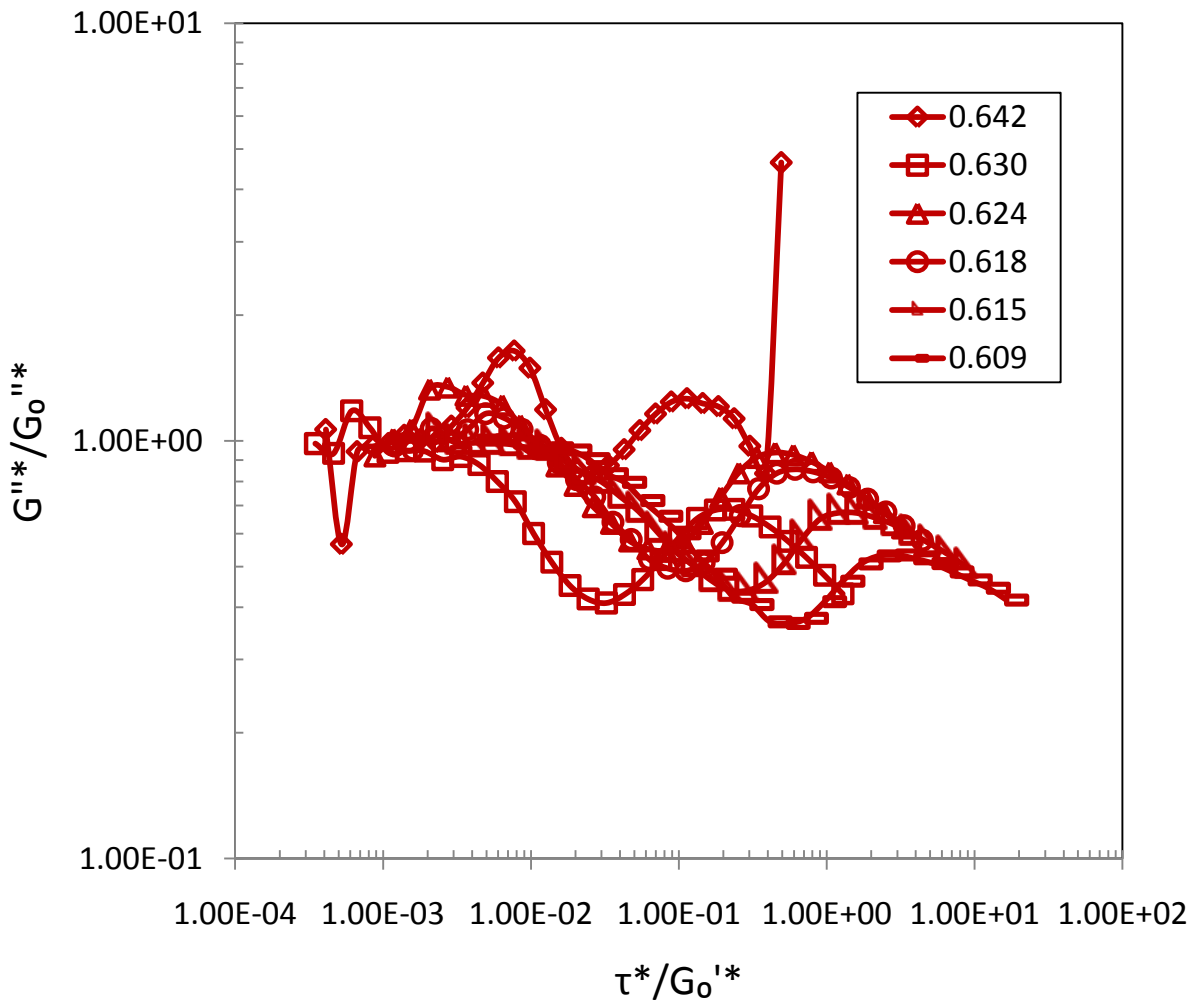


Figure 3.11. (continued on next page)

(c)

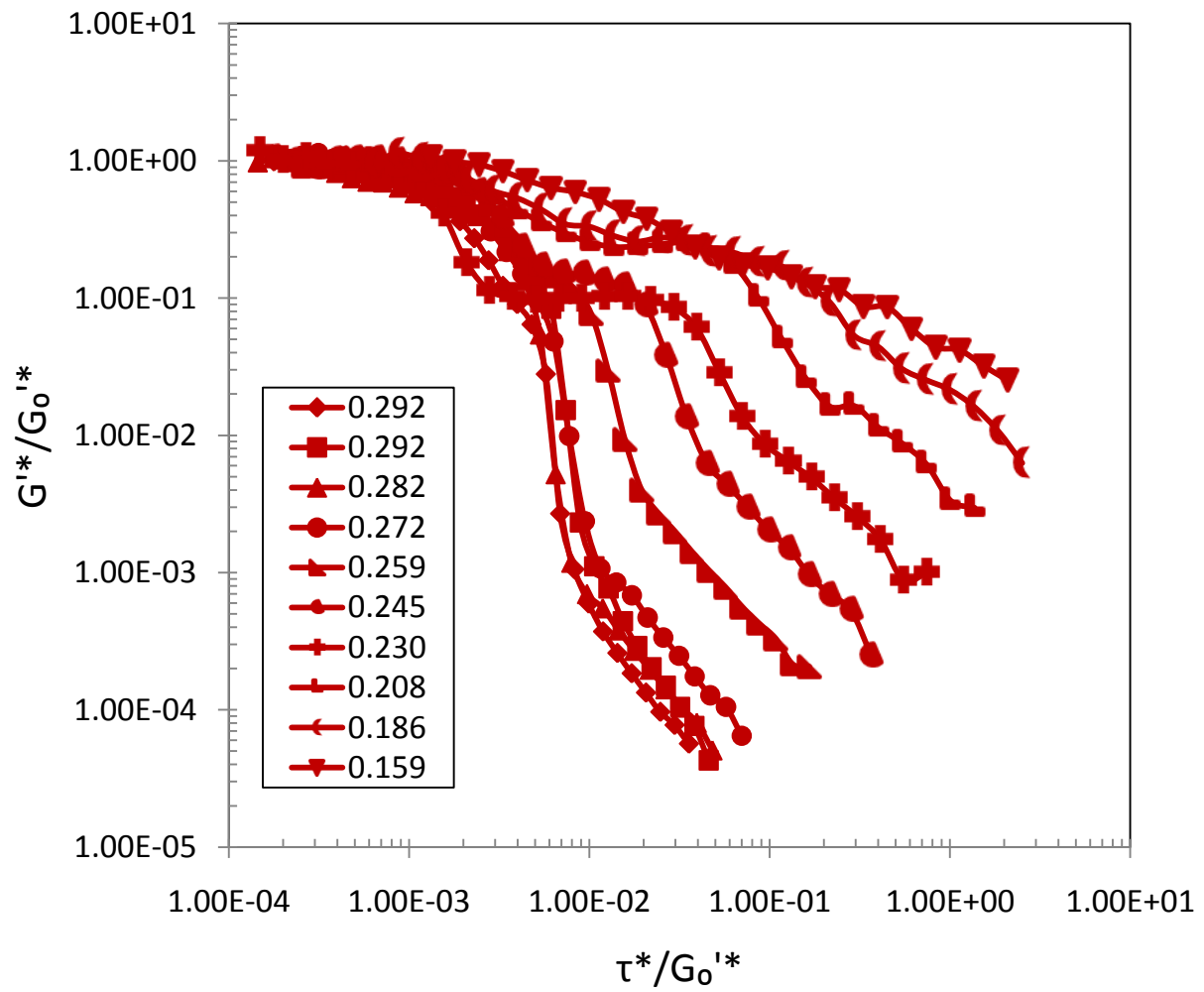


Figure 3.11. (continued on next page)

(d)

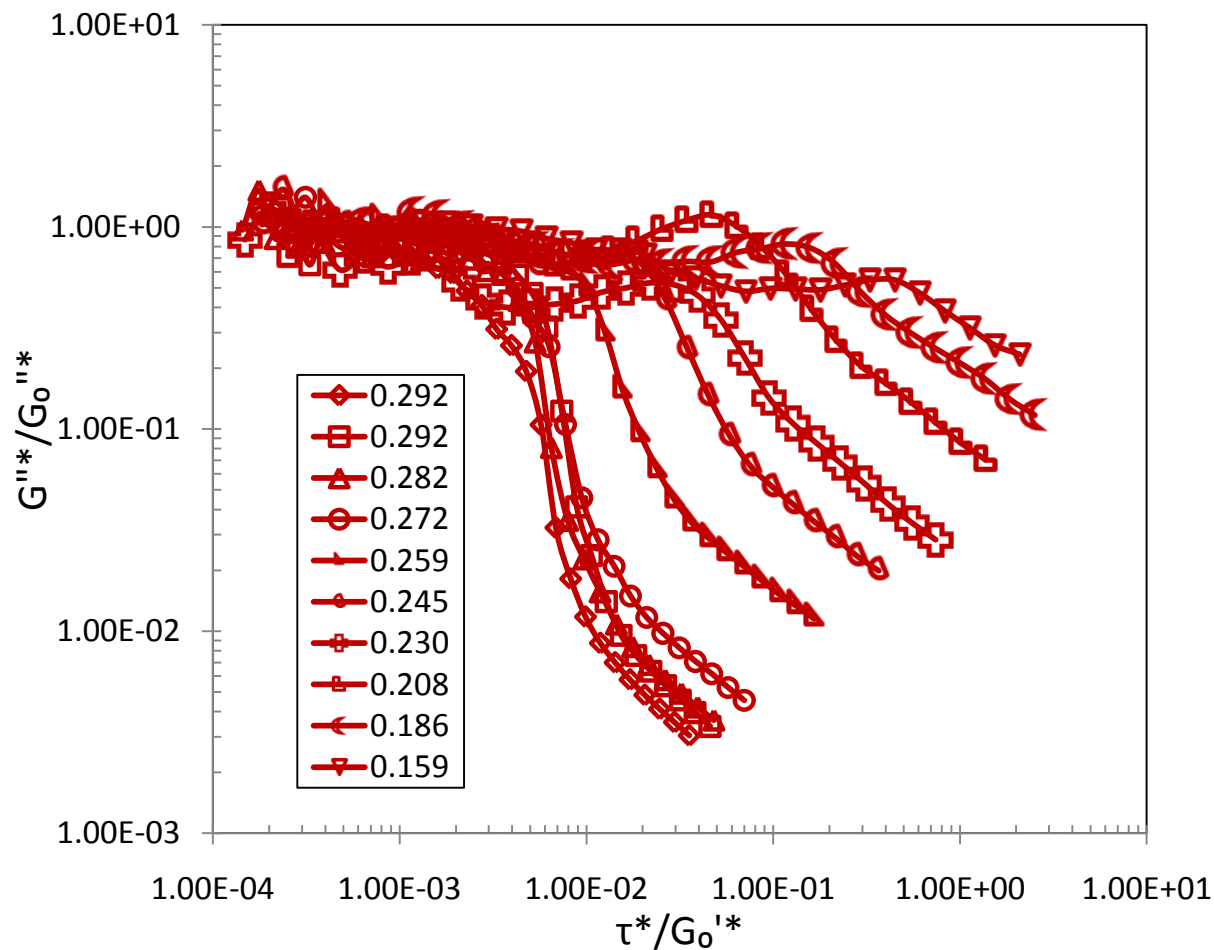


Figure 3.11. Dynamic stress sweeps for different volume fractions at medium pH (near 4), $I=0.001M$ for HDC particles (a) (b) and CDC particles (c) (d). G''^* have been scaled on the plateau values $G_0''^*$ (a) (c) (closed), and G''^* have been scaled on the plateau values $G_0''^*$ (b) (d) (open). Dimensionless stress τ^* have been scaled on the plateau values $G_0''^*$. All the HDC samples show double yield behavior. CDC particles show double yielding behavior at low volume fractions (≤ 0.259) and single yielding at high volume fractions (≥ 0.272)

(a)

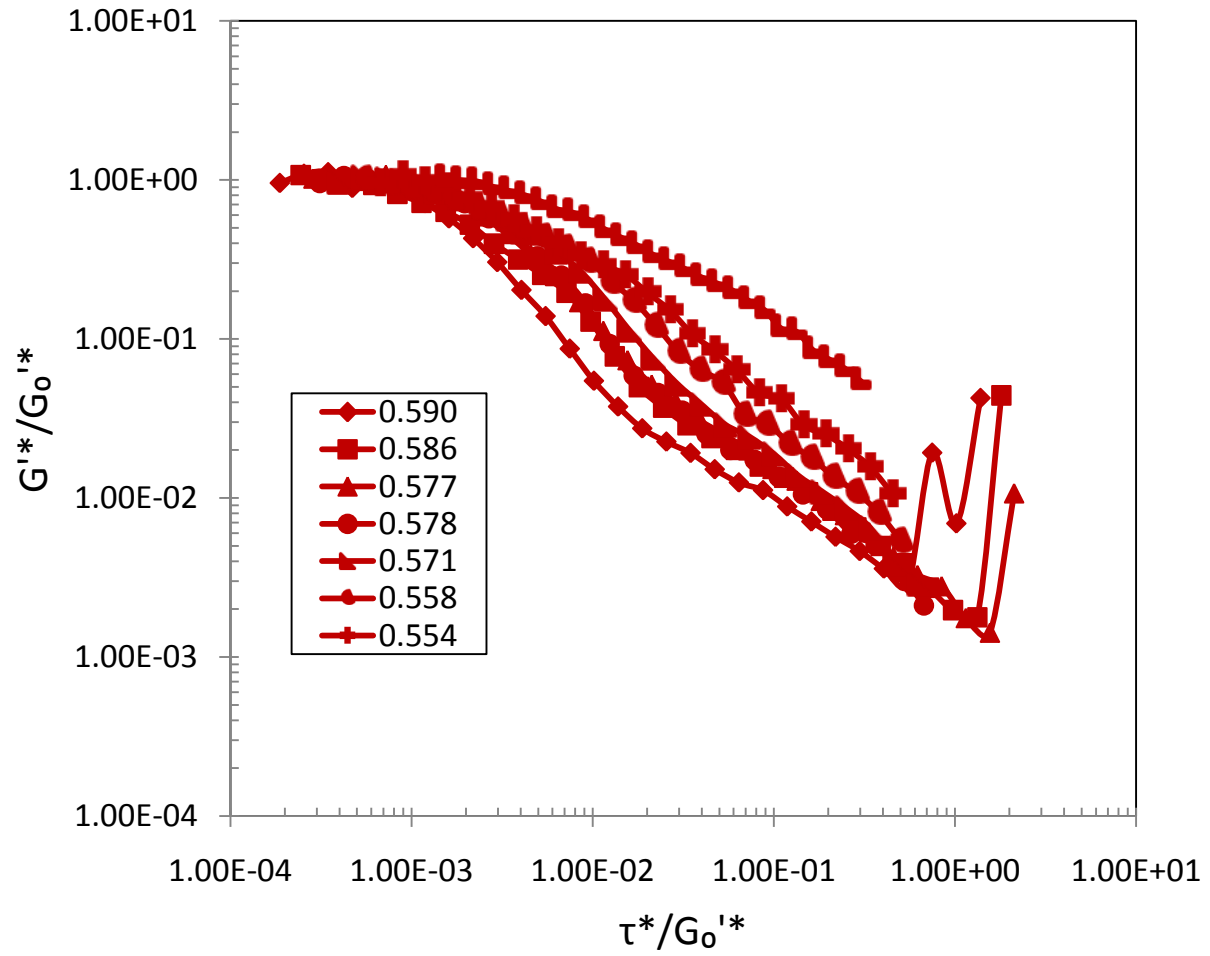


Figure 3.12. (continued on next page)

(b)

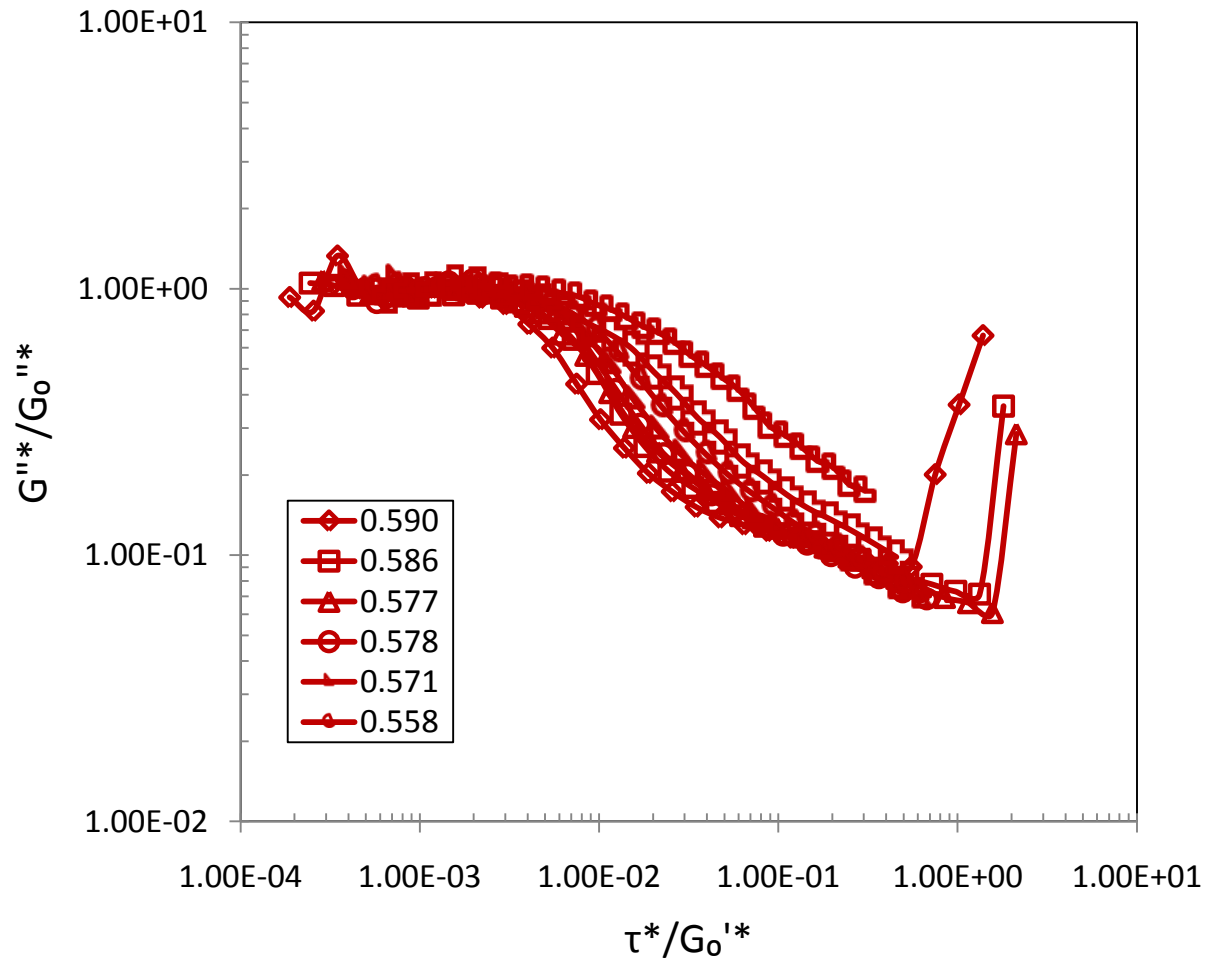


Figure 3.12. (continued on next page)

(c)

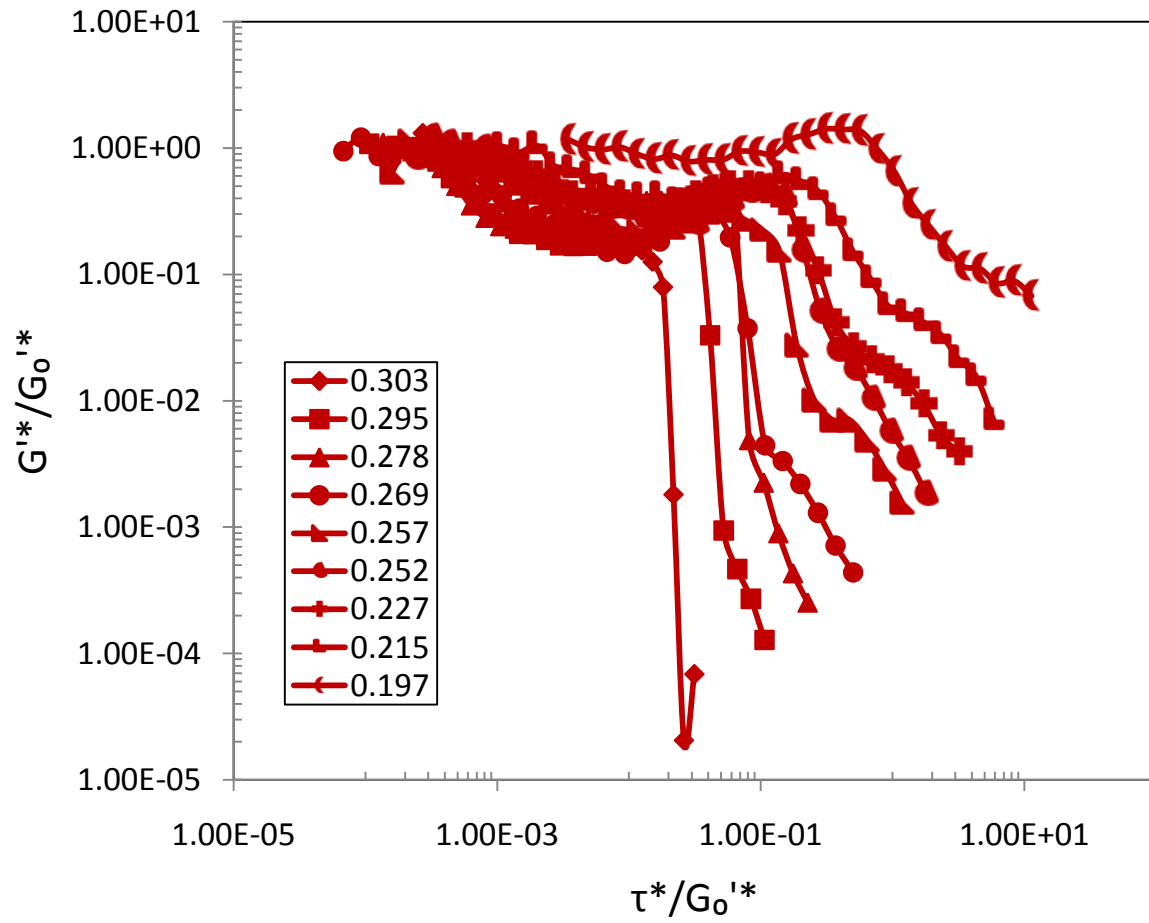


Figure 3.12. (continued on next page)

(d)

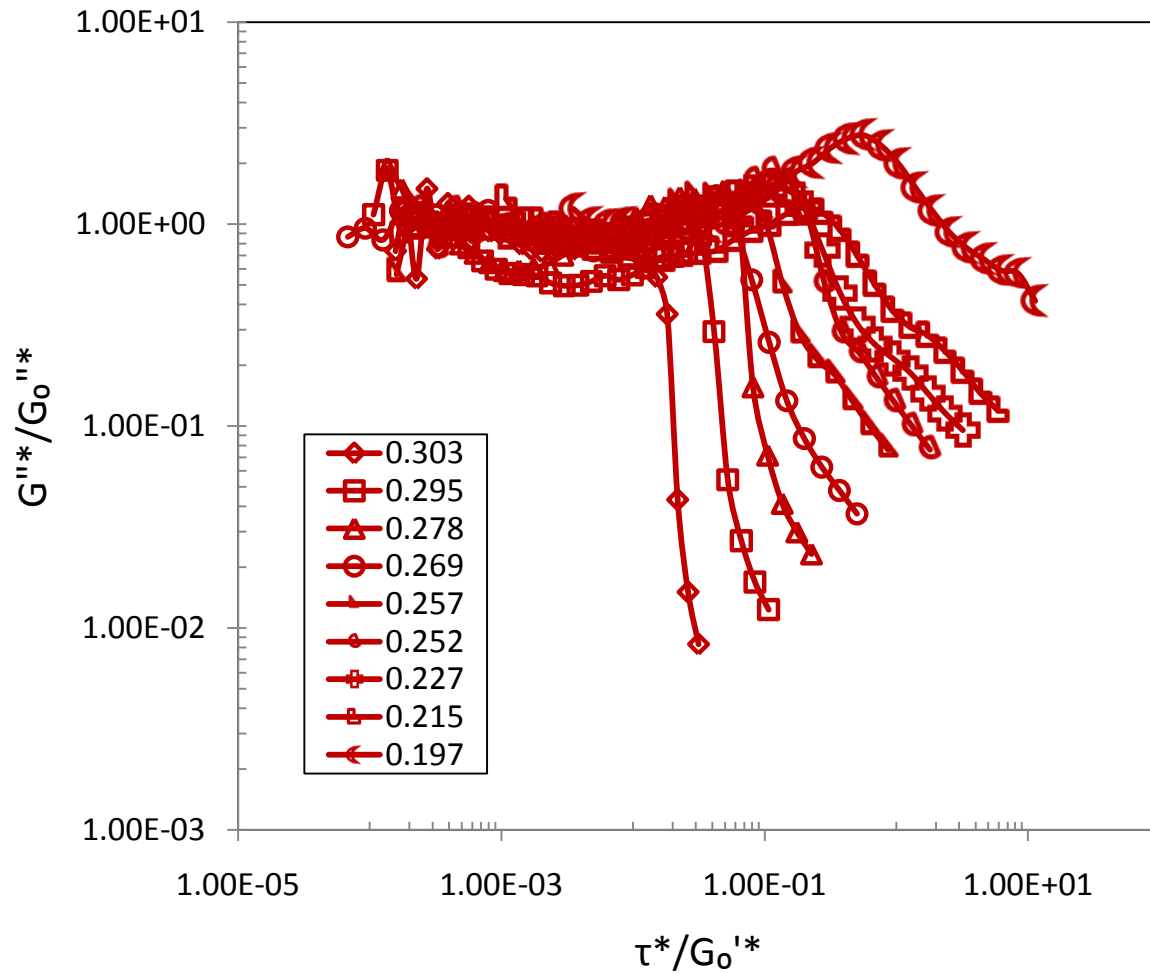


Figure 3.12. Dynamic stress sweeps for different volume fractions at high ionic strength, $I=0.5M$ for HDC particles (a) (b) and CDC particles (c) (d). G''^* have been scaled on the plateau values $G_0''^*$ (a) (c) (closed), and G''^* have been scaled on the plateau values $G_0''^*$ (b) (d) (open). Dimensionless stress τ^* have been scaled on the plateau values $G_0'^*$. All the HDC samples show no double yielding behavior. CDC particles show double yielding behavior at higher volume fractions (≥ 0.227) and single yielding at lower volume fractions (≤ 0.215).

(a)

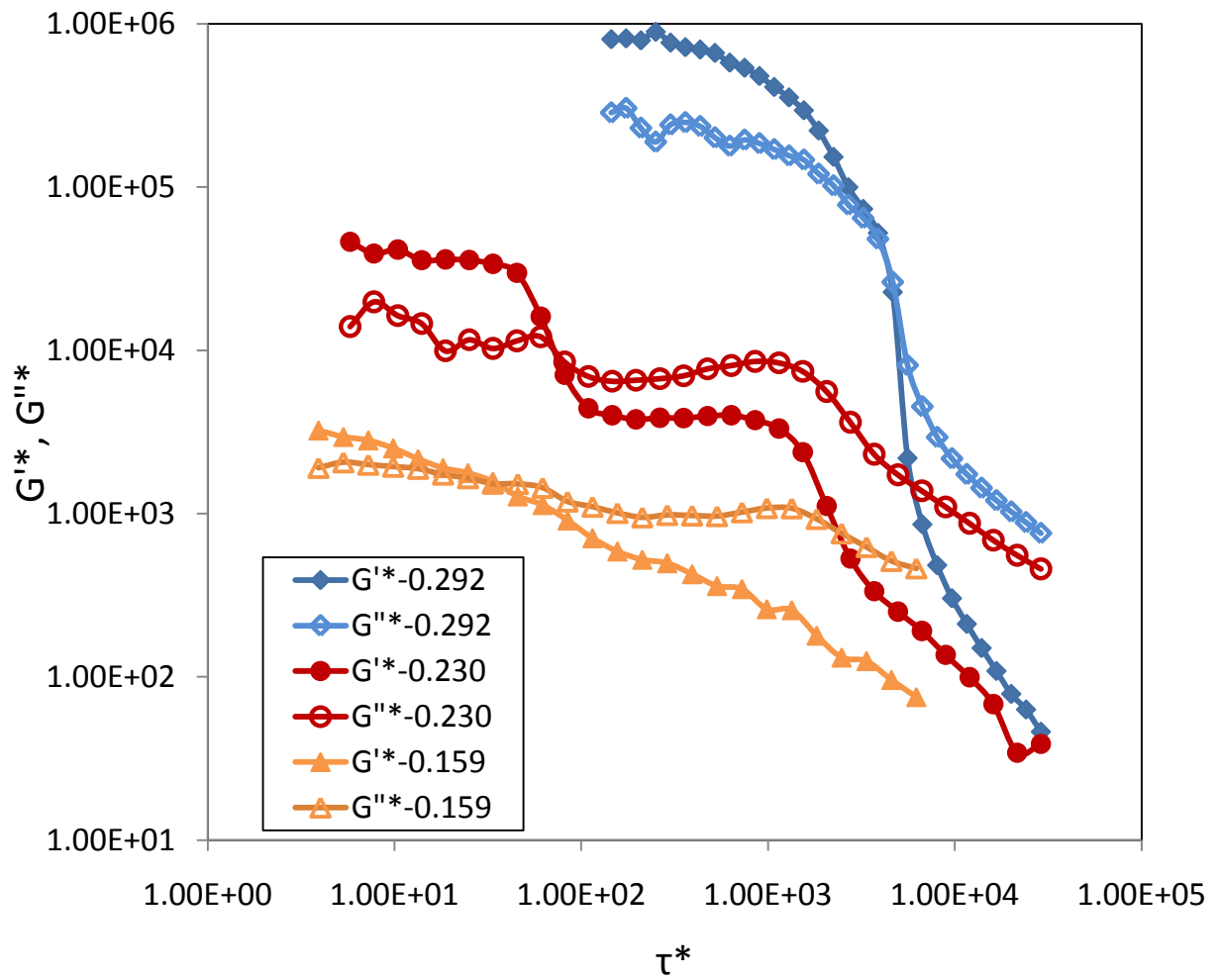


Figure 3.13. (continued on next page)

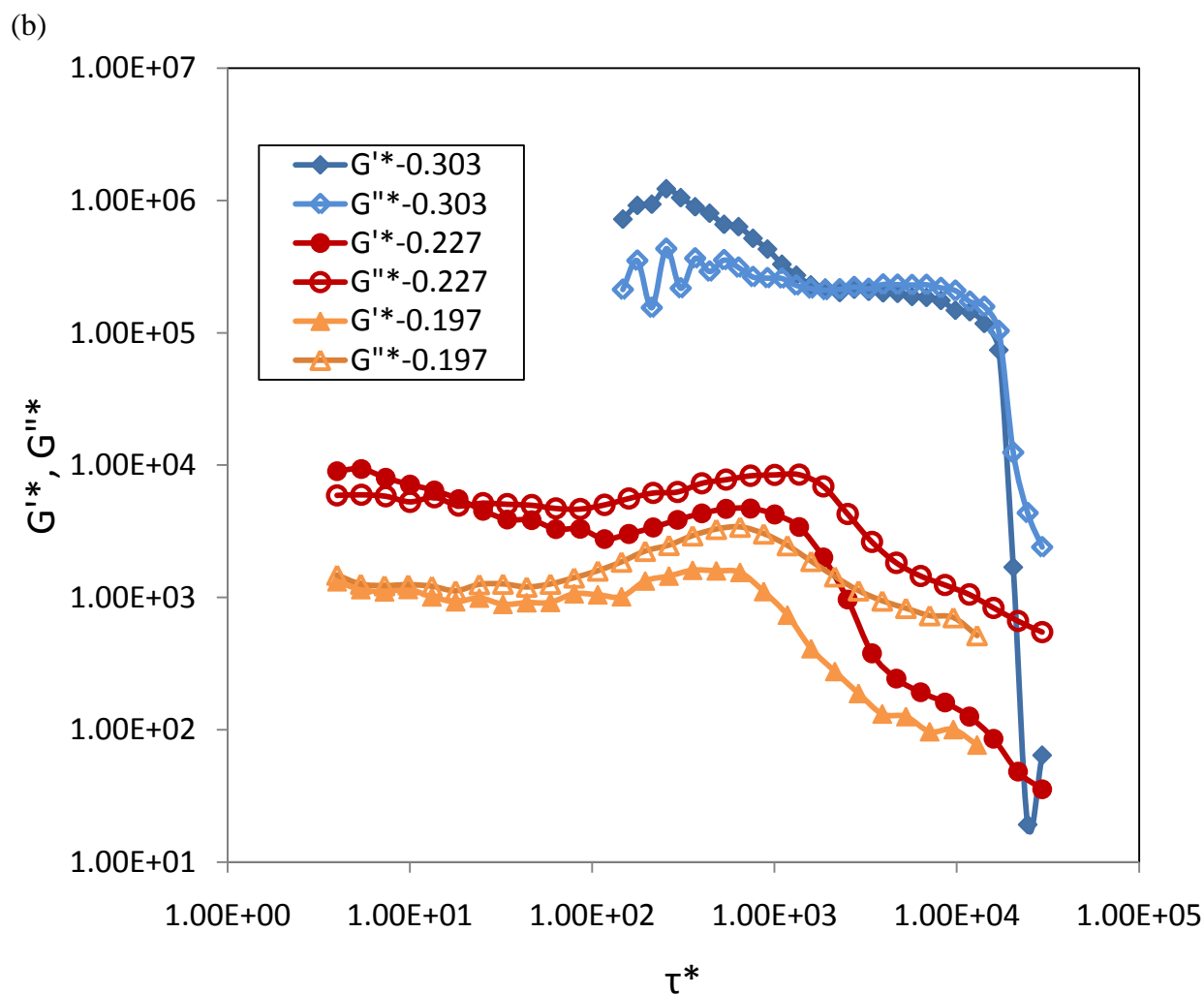


Figure 3.13. Dynamic stress sweeps for CDC particles of three representative volume fractions at pH=4.6 and I=0.001M (a) and pH=9.0, I=0.5M (b).

3.6 References

1. Zaccarelli, E., *Journal of Physics-Condensed Matter* **2007**, *19* (32).
2. Manoharan, V. N.; Elsesser, M. T.; Pine, D. J., *Science* **2003**, *301* (5632), 483-487.
3. Mock, E. B.; De Bruyn, H.; Hawket, B. S.; Gilbert, R. G.; Zukoski, C. F., *Langmuir* **2006**, *22* (9), 4037-4043.

4. Sheu, H. R.; Elaasser, M. S.; Vanderhoff, J. W., *Journal of Polymer Science Part a-Polymer Chemistry* **1990**, 28 (3), 629-651.
5. Sung, K. E.; Vanapalli, S. A.; Mukhija, D.; McKay, H. A.; Millunchick, J. M.; Burns, M. A.; Solomon, M. J., *Journal of the American Chemical Society* **2008**, 130 (4), 1335-1340.
6. Park, J. G.; Forster, J. D.; Dufresne, E. R., *Journal of the American Chemical Society* **2010**, 132 (17), 5960-+.
7. Yatsenko, G.; Schweizer, K. S., *Physical Review E* **2007**, 76 (4).
8. Yatsenko, G.; Schweizer, K. S., *Journal of Chemical Physics* **2007**, 126 (1).
9. Letz, M.; Schilling, R.; Latz, A., *Physical Review E* **2000**, 62 (4), 5173-5178.
10. Man, W. N.; Donev, A.; Stillinger, F. H.; Sullivan, M. T.; Russel, W. B.; Heeger, D.; Inati, S.; Torquato, S.; Chaikin, P. M., *Physical Review Letters* **2005**, 94 (19).
11. Tripathy, M.; Schweizer, K. S., *Journal of Chemical Physics* **2009**, 130 (24).
12. Zhang, R.; Schweizer, K. S., *Physical Review E* **2009**, 80 (1).
13. Vega, C.; Monson, P. A., *Journal of Chemical Physics* **1997**, 107 (7), 2696-2697.
14. Pfleiderer, P.; Schilling, T., *Physical Review E* **2007**, 75 (2).
15. De Michele, C.; Schilling, R.; Sciortino, F., *Physical Review Letters* **2007**, 98 (26).
16. McGrother, S. C.; Williamson, D. C.; Jackson, G., *Journal of Chemical Physics* **1996**, 104 (17), 6755-6771.
17. Bolhuis, P.; Frenkel, D., *Journal of Chemical Physics* **1997**, 106 (2), 666-687.
18. Radu, M.; Pfleiderer, P.; Schilling, T., *Journal of Chemical Physics* **2009**, 131 (16).
19. Kramb, R. C.; Zhang, R.; Schweizer, K. S.; Zukoski, C. F., *Physical Review Letters* **2010**, 105 (5).
20. Ramakrishnan, S.; Zukoski, C. F., *Langmuir* **2006**, 22 (18), 7833-7842.

21. Chen, Y. L.; Schweizer, K. S., *Journal of Chemical Physics* **2004**, *120* (15), 7212-7222.
22. Bergenholtz, J.; Fuchs, M., *Journal of Physics-Condensed Matter* **1999**, *11* (50), 10171-10182.
23. Kobelev, V.; Schweizer, K. S., *Journal of Chemical Physics* **2005**, *123* (16).
24. Kramb, R. C. The effects of particle shape, size, and interaction on colloidal glasses and gels. University of Illinois at Urbana-Champaign, Urbana, IL, 2010.
25. Pham, K. N.; Petekidis, G.; Vlassopoulos, D.; Egelhaaf, S. U.; Pusey, P. N.; Poon, W. C. K., *Europhysics Letters* **2006**, *75* (4), 624-630.
26. Pham, K. N.; Petekidis, G.; Vlassopoulos, D.; Egelhaaf, S. U.; Poon, W. C. K.; Pusey, P. N., *Journal of Rheology* **2008**, *52* (2), 649-676.
27. Zhang, Z. L.; Keys, A. S.; Chen, T.; Glotzer, S. C., *Langmuir* **2005**, *21* (25), 11547-11551.
28. Zhang, Z. L.; Glotzer, S. C., *Nano Letters* **2004**, *4* (8), 1407-1413.
29. Wilber, A. W.; Doye, J. P. K.; Louis, A. A., *Journal of Chemical Physics* **2009**, *131* (17).
30. Sciortino, F.; Giacometti, A.; Pastore, G., *Physical Review Letters* **2009**, *103* (23).
31. Ganzenmuller, G.; Camp, P. J., *Journal of Chemical Physics* **2007**, *126* (19).
32. Goyal, A.; Hall, C. K.; Velev, O. D., *Soft Matter* **2010**, *6* (3), 480-484.
33. Goyal, A.; Hall, C. K.; Velev, O. D., *Physical Review E* **2008**, *77* (3).
34. Russo, J.; Tartaglia, P.; Sciortino, F., *Journal of Chemical Physics* **2009**, *131* (1).
35. Miller, M. A.; Blaak, R.; Lumb, C. N.; Hansen, J. P., *Journal of Chemical Physics* **2009**, *130* (11).
36. Del Gado, E., *Journal of Physics-Condensed Matter* **2010**, *22* (10).
37. Blaak, R.; Miller, M. A.; Hansen, J. P., *Epl* **2007**, *78* (2).

38. Schweizer, K. S.; Yatsenko, G., *Journal of Chemical Physics* **2007**, *127* (16).
39. Dupin, D.; Fujii, S.; Armes, S. P.; Reeve, P.; Baxter, S. M., *Langmuir* **2006**, *22* (7), 3381-3387.
40. Anderson, B. J.; Zukoski, C. F., *Journal of Physics-Condensed Matter* **2009**, *21* (28).

Chapter 4 Conclusion

4.1 Summary

In this thesis, a seeded emulsion polymerization method was used to make a novel kind of polymer colloids with both shape anisotropy and pH-responsive behavior. Scanning electron microscopy (SEM) was used to characterize the size and shape anisotropy of the particles, and with these particles coated with a nonionic surfactant to minimize contact van der Waals interactions. The particles can be considered as fused spheres with a diameter of 850nm and a length of 1100nm yielding an aspect ratio of 1.3. Changes in the electrostatic properties of the particles was explored by measuring the particle surface potential as a function of pH-response and ionic strength. The colloidal stability of dilute suspensions was determined by visual inspection as a function of pH and ionic strength establishing conditions giving rise to aggregation. These suspensions form glasses or gels as volume fraction is increased at fixed ionic strength and pH. The elasticity and yielding of gels and glasses of these particles was characterized.

In the synthesis process, ~800nm negatively charged cross-linked polystyrene seed particles were synthesized. Two types of particles were made from these seeds. The first were made following previously published methods where the seeds are swollen with styrene¹. When this styrene is polymerized, it phase separates from the cross linked seed particle producing a dicolloid. Under these conditions both the seed and the protrusion have the same chemical composition and the particles are referred to as homopolymer dicolloids, HDC particles.

The second set of particles are synthesized by swelling the seeds with a mixture of styrene and 2-vinyl pyridine (2VP) including 1wt% cross-linker divinyl benzene. With increasing increasing temperature at high pH, the monomer and seed particles undergo phase

separation from the crosslinked polystyrene network and a secondary polymerization results in a protrusion on the surface of seed. These copolymer dicolloids (CDC) were designed to be both amphoteric and to result in non uniform electrostatic charge distribution between the seed and protrusion. The pyridine groups from poly-2VP (P2VP) are expected to be concentrated on the protrusion and will be protonated at low pH while the negative surface groups produced during the synthesis of the seeds will remain primarily on the seed as they are cross linked into place. The resulting particles can be considered of fused spheres of different chemical composition.

These CDC particles have similar size and shape anisotropy to the HDC particles thus enabling the HDC particles to be used as control particles to understand the effects of moving from isotropic to anisotropic interactions of shape anisotropic particles.

A nonionic surfactant $C_{12}E_6$ was chosen as the stabilizer to truncate strong van der Waals attraction but still keep CDC particles pH-responsive. Further studies in characterization were based on these fully coated CDC particles and HDC particles guaranteed at high pH. Electrophoretic mobility dependence on pH was also studied, proving that CDC particles were negatively charged at high pH and positively charged at low pH with an iso-electric point (i.e.p.) near 4.0, while HDC particles were negatively charged in a wide pH range above 3.0. Considering the anisotropic charge distribution introduced by concentrated negative charge on seed surface and positive charge on protrusion, calculation of surface potential showed that the attractive potential minimum for CDC particles at i.e.p. could be as deep as $-190kT$. In another aspect, CDC particles had a smaller total negative surface charge than HDC particles at high pH according to zeta-potential measurements for $[NaCl]=0M$ to $0.5M$, showing less stability when screening out surface charge by increasing ionic strength ($[I]$). If the particle surface charge were uniformly distributed on the particle surfaces, for both fully coated particles the strength of the

van der Waals attractive minimum at contact was estimated to saturate near $-15kT$ as ionic strength is raised.

State diagrams of dilute suspensions of the CDC particles and HDC particles were mapped in a $[\text{NaCl}]$ -pH panel. In the results, HDC showed no pH-sensitivity, with particles very stable and dispersed into suspension in a wide ionic strength range. Aggregation was observed only when $[\text{NaCl}]=5\text{M}$, proving that only weak attraction were presented with HDC particles. For CDC particles, particles aggregated in a narrow pH range around i.e.p. at low $[\text{NaCl}]$ proving that CDC particles were amphoteric pH-responsive. Aggregation was also observed at high $[\text{NaCl}]$ ($\geq 0.1\text{M}$) throughout the whole pH range, denoting less stability compared to the HDC particles. Nevertheless, the serious aggregation of CDC particles either at medium pH range with low $[\text{I}]$ or for $[\text{NaCl}]\geq 0.1\text{M}$, indicated strong attractions. These attractions can be explained by electrostatic attractions, and/or detaching of surfactant and chemistry variation at different conditions.

Rheological properties of dense dispersions were also studied with CDC particles and HDC particles based on different conditions varied by pH and ionic strength. With small dimensionless linear elastic moduli ($G_0'^*$) measured and kinetic arrest volume fraction (ϕ_g) derived, HDC particles were proved to be softly repulsive with $\phi_g\sim 0.60$ at $[\text{I}]=0.001\text{M}$ and weakly attractive with $\phi_g\sim 0.50$ at $[\text{I}]=0.5\text{M}$. For CDC particles, similar high density glassy state ($\phi_g > 0.5$) with small $G_0'^*$ was obtained for high pH or low pH with $[\text{I}]=0.001\text{M}$, but strong flocculated gel was formed at medium pH range with low density ($\phi_g < 0.20$) and large $G_0'^*$, showing the amphoteric behavior when varying pH and a strong attraction at medium pH. This strong attraction was slightly different from that obtain with CDC at high pH and $[\text{I}]=0.5\text{M}$ for which gel also formed with kinetic arrest point a little higher ($\phi_g\sim 0.20$). Nevertheless for all these

conditions CDC particles behave as a dicolloid with some dipolar character to their interactions, resulting in directional attraction to undergo kinetic arrest at a lower ϕ_g than hard particles with similar shape anisotropy.

Yielding behaviors were also studied and understood in terms of pH and ionic strength dependent interaction potentials. At $[I]=0.001M$, HDC particles showed double yielding as hard shape anisotropic particles undergoing breakage of rotational confinement and center of mass (CM) caging effect. But for $[I]=0.5M$, loss of this double yielding denoted strong coupling of different constrains due to attraction or loss of some constrains due to lowering volume fraction. CDC particles showed double yielding at high pH and $[I]=0.001M$, a sign of shape anisotropic particles successively overcoming bonding constrains due to directional attraction and translational and rotational confinement. At medium pH and $[I]=0.001M$ or high pH and $[I]=0.5M$, low density double yielding gels were obtained indicating breaking the bonding in forming percolated network in two steps. This yielding behavior can be explained as resulting from the nature of the aggregation of particles experiencing directional attractions with an essence of dipolar interactions enhanced compared to $[I]=0.001M$ and $pH=9.0$. Further study is necessary to understand the origin of this anisotropic interaction.

4.2 Future Studies

In the future, understanding of this pH-responsive particles with shape anisotropy can be improved by selecting a more effective stabilizer and searching efficient characterization method to study the interaction potential. $C_{12}E_6$ could be used to truncate van der Waals attraction and keeping particles pH-responsive but not useful in stabilizing particles against strong electrostatic attraction. Low ensity grafting of polymer might be a good choice allowing ions to pass through the stabilizer layer and truncating potential electrostatic attraction. This effect of stability has

been proved, but more refined modification technique is desired to apply only limited amount of a certain polymer hair to keep particles still pH-responsive.

In another aspect, to prove the presence of charge anisotropy and measure the interaction potential, some experimental techniques can be developed. Rotational electrophoresis² is a potential technique to characterize the anisotropic charge distribution. In principle, the interaction potential in dipolar particle system can be understood by obtaining second virial coefficient B_2 which has been studied theoretically³. And experimentally, B_2 can be obtained by studying osmotic compressibility dependence on volume fraction⁴.

In addition, as the Debye length in the searched ionic strength range is too small compared to the particle size and the shape anisotropy makes side-to-side configuration more favorable, we have no novel structure including string gel and complex crystal with current large particles. It is possible in the future to make large quantities of monodispersed small particles with same pH-responsive properties but smaller shape anisotropy. With these particles, we can study the novel microstructures in addition to the dynamics in dense dispersions.

4.3 References

1. Mock, E. B.; De Bruyn, H.; Hawket, B. S.; Gilbert, R. G.; Zukoski, C. F., *Langmuir* **2006**, *22* (9), 4037-4043.
2. Feick, J. D.; Velegol, D., *Langmuir* **2000**, *16* (26), 10315-10321.
3. Philipse, A. P.; Kuipers, B. W. M., *Journal of Physics-Condensed Matter* **2010**, *22* (32).
4. Ramakrishnan, S.; Zukoski, C. F., *Journal of Chemical Physics* **2000**, *113* (3), 1237-1248.